Title

The Evolution of the Human Pelvis: 3D Geometric Morphometric and Virtual Solutions to an Incomplete Fossil Record

Permalink

https://escholarship.org/uc/item/8cb842mn

Author

Adegboyega, Mayowa Titilope

Publication Date

2022

Peer reviewed|Thesis/dissertation

The Evolution of the Human Pelvis:
3D Geometric Morphometric and Virtual Solutions to an Incomplete Fossil Record

By

MAYOWA TITILOPE ADEGBOYEGA
DISSERTATION

Submitted in partial satisfaction of the requirements for the degree of
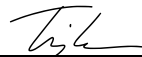
DOCTOR OF PHILOSOPHY

in

Anthropology

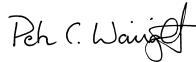in the

OFFICE OF GRADUATE STUDIES

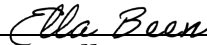of the

UNIVERSITY OF CALIFORNIA

DAVIS

Approved:

_____
Timothy D. Weaver, Chair

_____
Peter C. Wainwright

_____
Ella Been

Committee in Charge

2022

To Kunle, Sola, and Olumide Adegboyega
for your unending support.

The Evolution of the Human Pelvis:
3D Geometric Morphometric and Virtual Solutions to an Incomplete Fossil Record

Mayowa Titilope Adegboyega

Department of Anthropology

University of California, Davis

July, 2022

ABSTRACT

The human pelvis plays a significant role in many critical biological processes. The angle of pelvic tilt impacts the curvature of the vertebral column which influences posture, the articulation of the pelvis with the femur affects locomotor ability, the width of the pelvis impacts thermoregulation, and the size and shape of the birth canal influence the mechanism and difficulty with which childbirth occurs. The relationship between individual pelvic bones to the femur, the vertebral column, and even to infant head size has been well documented, but due to the paucity of complete fossils, a robust analysis of the evolution of the shape and size of the pelvic girdle and the dimensions of the birth canal throughout hominin evolution is yet to be firmly established.

Here, I seek to contribute to our understanding of the evolution of the human pelvis by confronting issues of bone fragmentation and the absence of soft tissue in the fossil record using virtual anthropology techniques including three-dimensional (3D) visualization and geometric morphometrics. I achieve this through three studies that focus on different challenges to paleoanthropological analysis created by the typically poor preservation of pelvic remains.

In the pages that follow, the Introduction provides a review of the research that has contributed to the present understanding of hominin pelvic morphology and the methods that have previously been employed to elucidate patterns of pelvic variation.

In Chapter 1, my co-authors and I present two new reconstructions of the Kebara 2 Neanderthal (KMH 2) pelvis using both virtual and physical techniques. The reconstruction process involved correcting the positions of misaligned fragments of the right hip bone and the sacrum, mirror imaging the right half of the sacrum and the right hip bone to create a new left side, articulating 3D printouts of the reconstructed elements, and using the physical articulations to align virtual renderings of the bones. Measurements taken on the new reconstructions were then compared to measurements taken from a previous reconstruction by Yoel Rak to assess interobserver reconstruction variation. In general, these new reconstructions tend to accentuate features noted previously in Kebara 2 and other Neanderthals, for example, they both present a long superior pubic ramus and an anteriorly positioned pelvic inlet; however, we also detect reconstructor interobserver error in the shape and size of the outlet. Relative to the previous reconstruction, in the first reconstruction, the outlet is small and has a smaller pelvic index (i.e., is more circular), while in the second reconstruction, the outlet is larger and retains the same shape (i.e., the same pelvic index). These two reconstructions not only help to improve our understanding of Neanderthal pelvic anatomy but also highlight the subjectivity inherent in fossil reconstructions.

Chapter 2 examines the shape, size, and spacing of the adult human pubic symphysis. The goals of this study are to identify a statistical model that best predicts pubic symphysis morphology, and to assess the relationships between the

anthropometric variables used to train the model and symphyseal shape. My co-authors and I trained several simple linear regressions and 2-stage linear regression models on a dataset of biometric data and landmark and semilandmark coordinate data for the purpose of identifying the best model to predict symphysis shape. The data were collected from recent CT scans taken from patients in the University of California health system. This study shows that linear regression modeling can be used to quantitatively estimate the shape of an individual's pubic symphysis, and we propose that it can be used in addition to other reconstruction techniques to improve fossil pelvic reconstructions by more accurately estimating the shape of this joint and reducing the effects of researcher bias in the process.

In Chapter 3, my co-authors and I trained another linear regression model to predict the translation and rotation matrix values that would transform a human right hip bone onto its left pair to create a new left side without referring to the sacrum. We trained the model on landmark and semilandmark coordinate data collected from the human dataset used in Chapter 2. We then applied this model to the 2 new reconstructions of the Kebara 2 pelvis presented in Chapter 1 to predict their left hip bones, and finally we assessed how well the model predictions corresponded with the human left sides and Kebara's reconstructed left side. Our results showed that regression modelling can be used to reliably predict 'missing' human hip bones and Kebara 2's left hip bones using a human training sample. We believe that this method can be employed in conjunction with researcher's anatomical expertise and other techniques including the technique to predict the shape of the pubic symphysis which

we present in Chapter 2, to reduce subjectivity in the fossil pelvic reconstructions and to elucidate more of hominin pelvic morphology.

The Conclusion provides closing remarks, as well as some future directions we wish to pursue on this topic.

ACKNOWLEDGEMENTS

The best metaphor for my experience completing this PhD is a rollercoaster ride; there were times when everything clicked so well together that I could not wait to get to the lab every day, and there were times I was so frustrated that I wanted to quit. This completed dissertation is a testament to the amazing mentors, colleagues, friends, and family who supported me through this journey.

My sincerest gratitude goes to my dissertation advisor Tim Weaver who took a chance on me. Before graduate school, I had almost no experience in the field of Anthropology and yet Tim saw enough of something to offer to guide me through this world and all the wonders therein, and what a journey it has been. I am also indebted to Mark Grote, the Anthropology department's Senior Statistician who helped me make sense of my data. Mark was so very generous with his knowledge about R language, statistics, and life, and he somehow managed to make a competent even enthusiastic data analyst out of me.

I am also grateful to the UC Davis Paleoanthropology group who taught me almost everything I know about human evolution. Special mention to Peter Stamos who took time out of his already busy schedule to help me with my first project and to David Katz and Laura Buck for sharing their knowledge about shape analysis with me. I also want to thank Sara Jhanjar, my undergraduate assistant who went above and beyond to help with data processing, analysis, and writing.

My sincerest thanks are extended to Damien Caillaud and Teresa Steele who served on my qualifying exam committee and to Ella Been and Peter Wainwright who served on both my qualifying exam committee and my dissertation committee. I also

the most trying parts of graduate school bearable. Mia Setka, Matt Lee, Jouke Peutz, and Ken Tam are the friend I never knew I needed, but I cannot imagine my life without, and I could not have asked for better housemates to help a girl get through her dissertation. My angel Bola Olusanya, you are always in my heart. To the Koinonia group, thank you for the spiritual support and for always reminding what is most important. Let us never stop doing this thing called life together.

Last but definitely not least, I would like to say a very big thank you to my parents Kunle and Sola Adegboyega who taught me that the even the sky is not the limit. There are no words sufficient enough to express my pride in being your daughter. I am doubly lucky to have grown up with the best siblings; my brother Olumide Adegboyega, and sister Adeola Akinsemoyin who have made every day an adventure. To the Adegboyega, Olowu, and Abina clans I want you to know that I feel incredibly lucky to be one of you.

Ẹ seun.

TABLE OF CONTENTS

INTRODUCTION

Functions of the Human Pelvis

The human pelvic girdle is an anatomical complex that consists of a left and right hip bone, also known as the *os coxa* or innominates; a sacrum; and a coccyx, commonly referred to as a tailbone and composed of multiple coccygeal vertebrae. The hip bones articulate anteriorly at the pubic symphysis and posteriorly with the sacrum at the sacroiliac joints. Superiorly, the sacrum articulates with the inferior surface of the last lumbar vertebra (usually L5 but can vary) and inferiorly it articulates with the first coccygeal vertebra. The acetabulum - a concave surface facing laterally from each hip bone - articulates with the head of the femur, forming the hip joint, i.e., the acetabulofemoral joint.

At different phases of human evolutionary history, conflicting selective pressures have acted on the shape of the pelvis to favor a suite of adaptations to different functions, including locomotion, thermoregulation, and, in females, childbirth (Gruss & Schmitt, 2015). Energetically efficient bipedalism requires a shape that maximizes muscle lever arms and minimizes load (Lovejoy et al., 1973; Rak, 1991). The dimensions of the pelvis influence the body's surface area-to-mass ratio, which thus affect the rate of heat loss from the body's surface (Ruff, 1991), and from a fitness standpoint, the shape of the pelvis must allow for the safe delivery of healthy infants (Rosenberg & Trevathan, 2005). Pelvic morphology is directly linked to the shift from arboreal to terrestrial habitation as walking upright in an energetically efficient manner requires that the pelvis has a shape that maximizes muscle lever arms and minimizes load (Lovejoy et al., 1973; Rak, 1991; Saunders et al., 1953). Obligate bipedalism is also linked to tool production as it freed up the hands and allowed for the development of increasingly advanced technocomplexes

(Hill & Heinemann, 1954; Shapiro, 1956; Washburn, 1959). Brain size is linked to cognitive function and intelligence (Luders et al., 2009) and much of the regulation of cranial size has been the result of changes in size of the birth canal to accommodate efficient bipedal locomotive and increasing fetal cranial encephalization (Wells et al., 2012).

Hominin Pelvic Evolution

In the earliest hominins – *Ardipithecus ramidus, Australopithecus afarensis, Au. africanus, Au. sediba* – the evolution of the pelvis seems to have been largely driven by the biomechanical requirements for bipedal locomotion (Lovejoy, 1988; Lovejoy et al., 2009; Ruff, 1998; Ward, 2002). Many studies conducted on the available pelvic remains belonging to these early members of our lineage argue that the nature of their locomotion while bipedal was unlike that of our species (Berge, 1991; Cartmill & Schmitt, 1996; Rak, 1991; Rosenberg, 1998; Ruff, 1998; Schmitt et al., 1999; Stern & Susman, 1983; Susman et al., 1984; García-Martínez et al., 2014). Ruff (1995, 1998) proposed that in *Australopithecus*, the vertically reduced and widely flared iliac blades coupled with a relatively wide biacetabular breadth and long femoral necks would have increased the mediolateral (ML) loading of the femur beyond the range of *Homo sapiens* (to be referred to from this point on simply as humans) thereby resulting in a non-human-like gait. Alternatively, Lovejoy and others have proposed that these features, which are also noted in *Ardipithecus,* produce human-like hip abduction and joint motion (Lovejoy et al., 1973; Lovejoy, 2005; Lovejoy et al., 2009; Lovejoy & McCollum, 2010). These early hominins also retained features in their pelvises related to climbing (e.g., long ischiums). So, their pelvises show evidence of being shaped by selection for bipedalism while also retaining the ability to be good climbers (Lovejoy et al., 2009).

There is much more agreement that by the emergence of *Homo erectus* (~2 Ma, Herries et al., 2020), the biomechanics of bipedalism had moved much closer to its modern state. While the *Homo erectus* pelvis is ML wider than in humans, it is relatively narrow when compared to *Australopithecus* (Ruff, 1995, 2010). This change combined with their longer lower limbs (Walker & Leakey, 1993) would have allowed this taxon to be more energetically efficient during bipedal locomotion (Gruss & Schmitt, 2015; but see Wall-Scheffler & Myers, 2013) and might have even enabled the emergences of endurance running in our lineage (Bramble & Lieberman, 2004). From this period on, fetal encephalization is believed to have played an increasingly larger role in the morphology of the birth canal and consequently, the entire pelvis (Arsuaga et al., 1999; Ponce de León et al., 2008; Rak & Arensburg, 1987; Tague, 1992; Trinkaus, 2011; Weaver & Hublin, 2009; Wells et al., 2012). The ancestral platypelloid birth canal shape was still retained in these hominins, however there was significant increase in the AP inlet and in the overall size of the pelvis (Ruff, 1995; Simpson et al., 2008). Thermoregulation, also became increasingly important selective pressure during this period (Antón et al., 2016; Collard & Cross, 2017; Ruff, 1994, 2010). Many early African *Homo,* like many fossil hominins and humans from warmer climates, have smaller pelvic breadths than those from colder climates (Ruff, 1994, 1998, 2010; but see Simpson et al., 2008; 2014). These adaptations highlight how different selective pressures began to conflict with one another. While wider pelvises provide more room for fetuses to pass more easily through the birth canal, narrower pelvises are more efficient for regulating body temperature in warm climates and for bipedal locomotion (Gruss & Schmitt, 2015).

By the Middle Pleistocene (~780–130 ka), the size of the pelvis was comparable to in humans. This conclusion has also been supported by studies on

Homo neanderthalensis (to be referred to from this point on as Neanderthals) infant crania, which are similar in size to their human counterparts (Ponce de León et al., 2008; Rosenberg, 1992; Weaver & Hublin, 2009; Wells et al., 2012). There however remains some disagreement about the nature of the changes that happened in these later *Homo* to accommodate these larger offspring. Some researchers have proposed that the shapes of the birth canal in most Middle Pleistocene *Homo* retained the ancestral platypelloid shape relative to humans, which implies that both *Homo heidelbergensis* and Neanderthal fetuses would not have had to perform an extra turn that human fetuses make at the midplane while exiting the birth canal (Ruff, 2010; Weaver & Hublin, 2009). Other researchers suggest that the human pattern of fetal rotation likely began appearing earlier on (Rosenberg & Trevathan, 2001) from the moment when cranial encephalization and shoulder dystocia would have made it difficult for fetuses to pass through the birth canal (Rosenberg & Trevathan, 2002; Ponce de León et al., 2008). Arsuaga et al. (1999) describes a reconstructed pelvis with a sagittally long midplane that would suggest rotational birth was possible up to 400 ka (though this pelvis is believed to have belonged to a male so the female pelvises of the same species would probably have been wider).

Male and female humans experience different developmental changes to the pelvis at the onset of puberty. Females in particular require these developments to be able to allow for childbirth . These changes include the eversion of the sacrum and the ischiopubic region, the inversion of the iliac blades, and the widening of the subpubic angle, which give rise to an increase in the anteroposterior AP and ML dimensions of the pelvic midplane and outlet as well as the ML dimensions of the inlet (Arsuaga & Carretero, 1994; Huseynov et al., 2016). These changes result in the high degree of sexually dimorphism that has been well documented (Fischer &

Mitteroecker, 2015, 2017; Kurki, 2011; Tague, 1992). It should be noted that Huseynov et al. (2016) state that around the age of 40–45 years of age, the female pelvis resumes a mode of shape change similar to those of males whereby the ischiopubic region is inverted, the midplane and outlet AP lengths become relatively shorter, the iliac blades become more everted, and the subpubic angle narrows amongst other changes. The presence or absence of these differential adaptations are much harder to evaluate in the fossil record because very rarely do we recover pelvic remains of males and females of the same species that can be clearly analyzed. Amongst the early hominins, *Au. sediba* provides us one of the few instances to observe pelvic sexual dimorphism (Kibii et al., 2011) though we cannot draw strong conclusions drawn from these remains as the male individual is a juvenile and the remains have been heavily reconstructed. Nevertheless, Kibii et al. (2011) state that *Au. sediba* might not possess the sexually dimorphic traits seen in humans. In an attempt to glean any information about the sexual dimorphism in early *Homo,* Häusler & Schmid (1995) compared the pelvises of Sts 14 (*Au. africanus*) and AL288-1 (*Au. afarensis*) – which are commonly believed to have belonged to females – and concluded that the differences between them could reflect sexual dimorphism; however, they admitted that the differences could also just be the result of species differences. The small body size estimated for the Gona pelvis suggests a high degree of sexual dimorphism in *H. erectus* ((Simpson et al., 2008); however, this individual falls outside the range of most other *H. erectus* fossils whose body sizes are closer to those of humans (Ruff, 2010). Neanderthals present us with the first opportunity to clearly evaluate hominin sexual dimorphism. As expected, their birth canals are larger in females than males; however, this may have more to do with the external rotation of the pubic bone (Rak & Arensburg, 1987) rather than its lengthening as in humans. In fact, based what we know from the available specimens, Neanderthal

pubic rami are longer in males than in females (Ponce de León et al., 2008; Rosenberg et al., 1988; Ruff, 1998; Tague, 1992; Weaver & Hublin, 2009).

Kebara 2 Neanderthal Pelvis

During the 1983 excavation at the Kebara Cave, Mount Carmel, Israel, a skeleton of an adult male individual known as the Kebara 2 (KMH 2) Neanderthal was found within Mousterian layers (Bar-Yosef et al., 1986) dated by thermoluminescence to 61 – 59 ka (Valladas et al., 1987) and by electron spin resonance to 60 – 60 ka (Schwarcz et al., 1989). The skeleton is in relatively good condition, although it is missing the cranium and much of the lower limbs. The pelvis boasts a nearly complete right hip bone and sacrum, along with a badly damaged left hip bone (Rak & Arensburg, 1987). Further evaluation of the right hip bone, reveals that it possesses an almost symmetrically anterior and posteriorly flared iliac blade, which contrasts with the more posteriorly flared ilium in humans. The ischiopubic region is also considerably different from the morphology found in humans. The pubic angle is very long and low forming a sub pubic concavity that resembles the human female pelvis. Much of the ischiopubic ramus and anterior most part of the pubis is eroded. Additionally, Chris Ruff (1995) noted that what is left of the ischiopubic ramus appears to be misaligned and is unnaturally projects anterolaterally from the body causing the outlet to have a shorter straight length between the pubic symphysis and the ischial tuberosity than it would have had in life. The pubic symphysis wad reconstructed by Yoel Rak (1991) to obtain the length of the superior pubic ramus and the inlet length, but the ischiopubic ramus was largely left unaltered. Examination of the ventral aspect of the sacrum reveals that the first sacral vertebra shifted posteriorly and is not fully fused with the rest of the sacrum. The articulation between the third and fourth sacral vertebrae is also unfused and

has rotated slightly downwards creating an anteriorly diverging gap between the sacral vertebrae. Mirroring of the right innominate and sacrum by Rak and Arensburg (1987) gave us the first look of a virtually complete Neanderthal pelvis and even now, it remains the only Neanderthal pelvis found with a relatively complete hip bone and sacrum. The excellent state of preservation of the Kebara 2 specimen has enabled us to evaluate so called Neanderthal morphological features and to challenge some of the assumptions and interpretations surrounding them.

Pubic Symphysis Morphology

The pubic symphysis is a rigid joint that forms the anterior arch of the skeletal pelvis and connects both pubic bones at the midline. Several attempts have been made to investigate the width of the pubic symphysis in humans (Becker et al., 2010, see Table 2; Björklund et al., 1996; Gamble et al., 1986; Loeschcke, 1912; Testus & Latarjet, 1928; Vix & Ryu, 1971), but many of these studies have methodological flaws and poorly described dissection and measurement protocols. They are also missing information such as the precise age of the individuals, their height and weight, and history of childbirth in women, which are important factors that affect the shape of the symphysis. Vix & Ryu (1971) and Nejad et al. (2012) both identified degenerative changes that cause the space between the pubic bones to narrow with age. Unfortunately, most of these studies are not directly comparable as the pubic symphysis was measured at different sites in different planes with different degrees of accuracy. Further analysis is therefore needed to better describe pubic symphysis shape variation in humans. Additionally, this information could be employed to create better reconstructions of fossil specimens. As there is already so much that is unknown about hominin pelvic shape and so much that is left to individual reconstructors to decide upon based on their subjective expertise, developing

systematic means of inferring pelvic dimensions such as the pubic symphysis could thereby contributing to more accurate fossil reconstructions.

Pelvic Bone Orientation

An important aspect of hominin pelvic variation is the orientation of the hip bones within the pelvic girdle. As previously described, early hominins possessed more laterally flared iliac blades and a more constricted outlet in part due to the angle at which the ilium articulates with the sacrum. This is noticeably different from the orientation of the hip bones in later hominins, which display more vertically oriented iliac blades and a wider outlet (Kibii et al., 2011; Simpson et al., 2008; Vansickle, 2017). These differences have been linked to changes to locomotive adaptations (Lovejoy et al., 1973; Lovejoy, 2005) as well as parturition requirements in females at different points in our evolution that necessitate a wider midplane and outlet to accommodate increasing hominin encephalization (Kibii et al., 2011; Lovejoy et al., 1973; Lovejoy, 2005; Tague & Lovejoy, 1986; Trevathan, 2015; Trevathan, 2017). It is crucial that we understand this aspect of pelvic shape variation when creating pelvic reconstructions because slight changes to the orientation of the pelvic bones can greatly impact not only the shape of the birth canal but the body dimensions of the individual as well. Great care must be taken to ensure that hip bones are placed in the correct position so that the analysis that is conducted and the inferences that are drawn from these reconstructions accurately reflect the evolutionary trajectory and variation of the human pelvis.

Virtual Anthropology

In recent years, the preferred way to conduct hominin fossil reconstructions and to analyze morphological characteristics has been withing the realm of virtual anthropology. Virtual anthropology can best be described as a multidisciplinary

approach that combines expertise from the fields of anthropology, primatology, medicine, and paleontology with technological innovations in the fields of mathematics, statistics, computer science, design, and engineering to offer new opportunities for morphological and functional analyses (Weber, 2015; Weber & Bookstein, 2011). It is no surprise that the innovations within this space have become popular in biological anthropology as they offer a myriad of tools specifically tailored to address many of the hindrances to comprehensive analyses within this field. For example, by creating 3D renderings of fossil elements, we can create infinite virtual copies of the specimens that are permanently available and can be manipulated without damaging rare and unique physical objects. These virtual renderings also allows for multiple reconstructions, so the robustness of the conclusions and reconstruction uncertainty can be assessed. We can also conduct large scale comparative analyses using statistical methods to quantify morphological variation and to assess complex anatomical regions which is particularly important in paleoanthropology, where the scarcity of fossils requires us to extract as much information as possible from fragmentary remains. Finally, VA has helped to promote data sharing because rare specimens can easily be copied and shared to researchers who are interested in using them in their analyses (Weber, 2015; Weber & Bookstein, 2011). Many of these techniques were utilized in this work to clarify patterns of pelvic morphology and to predict the shape of morphological data.

Study Objectives

Because of the scarcity of complete pelvic fossils, much is still unknown or uncertain about the evolution of the human pelvis. In the following 3 chapters, I describe three studies that my co-authors and I undertook to address some of the issues faced by biological anthropologists who seek to study hominin pelvic evolution and pelvic

variation. My goal was to employ existing virtual reconstruction techniques, and to develop new ones, to estimate the shape of missing pelvic elements so to help us more systematically fill in gaps in the fossil record. In Chapter 1, my co-authors and I present two new reconstructions of the Kebara 2 pelvis. We employed both virtual and physical techniques to realign fragments of the right hip bone and the sacrum, mirror image the reconstructed right to the left side and articulate the individual pelvic elements. Afterwards, we assessed the dimensions of the new reconstructions, and compared them to the dimensions collected on a previously reconstruction to assess interobserver reconstruction variation. In Chapter 2, we trained several linear regression models on anthropometric variables collected from recent humans to predict their pubic symphysis morphology, and we identified the one that performed best. We then evaluated the relationships between these variables and symphyseal shape. We propose that this method can be used to estimate missing pubic symphysis morphological data. In Chapter 3, my co-authors and I trained another linear regression model to predict the translation and rotation matrix values that would transform a human right hip bone onto its left pair to create a new left side. We trained the model on landmark and semilandmark coordinate data collected from the human dataset used in Chapter 2 and then we applied this model to the 2 new reconstructions of the Kebara 2 pelvis presented in Chapter 1 to predict their left hip bones. Finally, we assessed how well the model predictions corresponded with the human left sides and Kebara's reconstructed left side. These studies each propose new approaches to reconstructing fossil pelvises, and I believe that they have the potential to elucidate more details about patterns of pelvic morphological variation specifically, and human evolution in general.

CHAPTER 1: VIRTUAL RECONSTRUCTION OF THE KEBARA 2 NEANDERTAL PELVIS

Authors: Mayowa T. Adegboyega, Peter A. Stamos, Jean-Jacques Hublin, Timothy D. Weaver

ABSTRACT

The paucity of well-preserved pelvises in the hominin fossil record has hindered robust analyses of shifts in critical biological processes throughout human evolution. The Kebara 2 pelvis remains one of the best-preserved hominin pelvises, providing a rare opportunity to assess Neandertal pelvic morphology and function. Here, we present two new reconstructions of the Kebara 2 pelvis created from CT scans of the right hipbone and sacrum. For both reconstructions we proceeded as follows. First, we virtually reconstructed the right hipbone and the sacrum by repositioning the fragments of the hipbone and sacrum. Then, we created a mirrored copy of the right hipbone to act as the left hipbone. Next, we 3D printed the three bones and physically articulated them. Finally, we used fiducial points collected from the physically articulated models to articulate the hipbones and sacrum in virtual space. Our objectives were to: (1) reposition misaligned fragments, particularly of the ischiopubic ramus; (2) create a 3D model of a complete pelvis; (3) assess interobserver reconstruction variation. These new reconstructions show that, in comparison with previous measurements, Kebara 2 possessed a higher shape index (maximum anteroposterior length/maximum mediolateral width) for the pelvic inlet and perhaps the outlet, and a more anteriorly positioned sacral promontory and pubic symphysis relative to the acetabula. The latter differences result in a lower ratio between the distances anterior and posterior to the anterior margins of the

acetabula. Generally, the new reconstructions tend to accentuate features of the Kebara 2 pelvis––the long superior pubic ramus and anteriorly positioned pelvic inlet––that have already been discussed for Kebara 2 and other Neandertals.

INTRODUCTION

The human pelvis plays a significant role in many aspects of human biology that have been critical for survival and reproduction. For instance, the angle of pelvic incidence, along with the curvature of the vertebral column, influences posture and locomotion (Abitbol, 1987; Duval-Beaupère et al., 1992; Lovejoy, 2005; Tardieu et al., 2006; Been et al., 2013; 2017); the hip joint connects the lower limbs to the rest of the body and transfers load from the upper body to the hindlimbs during bipedal locomotion (Paul, 1966; Crowninshield et al., 1978; Stern and Susman, 1983; Ruff, 1995; Lovejoy, 2009); the width of the pelvis impacts thermoregulation (Ruff, 1991; 1994; 2010; Holiday, 1997; Weaver and Hublin, 2009); and the dimensions of the birth canal influence the ease and mechanism by which childbirth occurs (Trinkaus, 1984; Tague and Lovejoy, 1986; Rosenberg, 1992; Rosenberg and Trevathan, 1995; Ruff, 1995; Kappelman, 1996; Arsuaga et al., 1999; Simpson et al., 2008; Weaver and Hublin, 2009; Ruff, 2010; Gruss and Schmitt, 2015). The size and shape of the pelvis that is optimal for each of these aspects of biology may differ (Rosenberg and Trevathan, 1995; Wells et al., 2012; Grabowski, 2013). Consequently, the variation in pelvic morphology in the hominin fossil record reflects shifting selective pressures related to these functions as well as neutral evolutionary processes (Rosenberg, 1992; McHenry and Coffing, 2000; Gruss and Schmitt, 2015; Betti and Manica, 2018).

Although the particularly fragmentary nature of the hominin pelvic fossil record has made it difficult to reconstruct the evolution of the hominin pelvis, many studies have documented evolutionary changes through time and differences across hominin taxa in pelvic anatomy and their potential functional implications, from the emergence of early hominins (Stern and Susman, 1983; Simpson et al., 2008; Lovejoy et al., 2009, Berge and Goularas, 2010), the transition from *Australopithecus* to *Homo* (Ruff, 1995; Rosenberg et al., 2006; Simpson et al.,

2008), and the diversification of *Homo* (Arsuaga et al., 1999; Rosenberg, 1998; Weaver and Hublin, 2009; Bonmatí et al., 2010). The Kebara 2 pelvis remains one of the best-preserved pelvises in the hominin fossil record (Rak and Arensburg, 1987; Rak, 1991), providing a rare opportunity to assess Neandertal pelvic morphology and function. Additionally, due to its completeness, this pelvis has played an important role in discussions about multiple topics in human evolution, including the phylogenetic relationships between Neandertals and humans (Stewart, 1960; Rak and Arensburg, 1987; Rosenberg et al., 1988; Rak, 1993), hominin sexual dimorphism (Tague, 1992; Rosenberg et al., 1988; Weaver and Hublin, 2009), the effect of climate on hominin morphology (Ruff, 1991; Tague, 1992; Weaver and Hublin, 2009; Gruss and Schmitt, 2015), the evolution of hominin childbirth (Rosenberg, 1992; Rosenberg and Trevathan, 1995; DeSilva and Lesnik, 2008; Ponce de León et al., 2008; Weaver and Hublin, 2009), and differences in locomotion between Neandertals and humans (Rosenberg, 1992; Rak, 1993).

The Kebara 2 pelvis preserves the left hipbone (os coxae), right hipbone (Fig. 1.1), and sacrum (Rak and Arensburg, 1987). The left hipbone is missing the pubis as far back as the root of the superior pubic ramus and the entire ischiopubic ramus, and it shows extensive signs of plastic deformation and fragmentation. The right hipbone, on the other hand, is relatively well preserved. Further examination reveals that it is composed of many fragments that appear to be held together by sedimentary matrix (Fig. 1.2). Other than some superficial cracks along the iliac fossa, the ilium seems to have retained its original anatomical shape. The right pubic body presents the most fragmentation and loss of bone; however, much of the pubic symphysis is preserved, making it possible to locate the mid-sagittal plane (Rak, 1991), which is important for creating a mirror image to reconstruct the left half of the pelvis.

The Kebara 2 sacrum, although essentially complete, exhibits some developmental anomalies and postmortem damage (Duday and Arensburg, 1991; Trinkaus, 2018). The left and right superior articular processes are unequal in size and orientation; the right process is larger and more coronally oriented, while the left one is smaller and more sagittally oriented (Rak, 1991; Duday and Arensburg, 1991). The right side, particularly at the inferolateral end, exhibits more taphonomic bone loss than the left side, but the damage does not extend up to the margins of the auricular surface, which is important for articulating the hipbone and sacrum. The first sacral vertebra (S1)— which shows signs of lumbarization—is completely unfused to the second sacral (S2) vertebra, and the neural arches of these vertebrae exhibit some developmental anomalies, which may have produced minor spondylolisthesis of the S1 on the S2 (Duday and Arensburg, 1991; Trinkaus, 2018). Additionally, the third and fourth sacral vertebrae (S3 and S4) are not completely fused (Trinkaus, 2018).

The Kebara 2 pelvis was first described and reconstructed by Rak and Arensburg (1987). Visualizing the complete pelvis required manually mirroring a cast of the right half, and bilateral analysis required measurements taken on the right half to be doubled. The most significant limitation of this reconstruction was the inability to realign fragments without posing further damage to the fossil. For example, the fragments of the ischiopubic ramus of the right hipbone are misaligned such that the pubic body is rotated posteroinferiorly (Fig. 1.3A; Ruff, 1991). These misalignments clearly affect the morphology of this region, but it is not clear how much they impact the overall shape of the pelvis, and the conclusions drawn.

Here, we apply virtual and physical reconstruction techniques to produce two new reconstructions of the Kebara 2 pelvis. By presenting more than one reconstruction, we are able to assess, at least in part, interobserver reconstruction variation and the extent to which the choices made affect the end results, highlighting the decisions

that are an inevitable part of reconstructing a fragmentary fossil. Implicit in a single reconstruction is an inflated sense of accuracy that is diminished by the inevitable differences that arise in the process of producing multiple reconstructions. From our reconstructions, we collected measurements of the hipbone, sacrum, and the complete pelvis and compared them with the data collected on the original reconstruction by Rak (1991), allowing us to quantify the changes these new reconstructions made to the size and shape of the pelvis, and to reassess Neandertal pelvic anatomy.

MATERIALS AND METHODS

Fossil Data

The Kebara 2 pelvis is part of an adult male Neandertal skeleton discovered in the Mousterian layers of Kebara cave, Mount Carmel, Israel (Rak and Arensburg, 1987; Bar-Yosef et al., 1991). It has been dated by thermoluminescence and electron spin resonance to about 59–64 ka (Valladas et al.,1987; Schwarcz et al.,1989). The pelvis consists of right and left hipbones and the sacrum (see discussion above). Because the left hipbone is more poorly preserved than the right, we created our models using only the right hipbone. CT scans of the right hipbone and sacrum (Fig. 1.2A–C) were generated with a Bio Imaging Research (BIR) ACTIS 225/300 industrial CT scanner from the Max Planck Institute for Evolutionary Anthropology (Leipzig, Germany). The CT data have a resolution of 0.09 mm and 0.08 mm for all dimensions for the hipbone and sacrum respectively. The data were imported as tagged image files (TIFF) into Avizo Lite 9 (Thermo Fisher Scientific, Waltham). A cast of the right hemipelvis of the original reconstruction of Kebara 2—created by Rak and Arensburg (1987)—was used to generate a virtual model for comparison with the new

reconstructions. This was accomplished by using fiducial points collected on the cast to align the virtual models of the hipbones to the sacrum.

Reconstruction Procedures

Virtual reconstruction of the hipbones

In Avizo, we digitally separated the bone from the sedimentary matrix, and bone fragment from bone fragment by manually segmenting each fragment into individual surface renderings, which resulted in the identification of 39 fragments in total for the right hipbone (Fig. 1.2D, E). Transformation tools in Avizo were used to realign the identified fragments by matching anatomical features according to the two different reconstruction protocols that we followed (see Supplement S1.1 for more details). These steps resulted in the creation of two different reconstructions (Fig. 1.3). Finally, the newly reconstructed right hipbones were mirrored to create two new left hipbones that could be used to create two new reconstructions of the complete pelvis.

Virtual reconstruction of the sacrum

Similar to the process we applied to the right hipbone, the sacrum was manually segmented into surface renderings (Fig. 1.2F). We identified 4 main pieces demarcated by the unfused joints between the first and second (S1/S2) and the third and fourth (S3/S4) sacral vertebrae, and between a fragment of the left ala and the rest of the sacrum. The sacrum was not segmented into more individual fragments because crushing of the dorsal side of the sacrum made this impractical. The S1 fragment and left ala fragment were realigned relative to the margins of S2, and the S4 was realigned relative to the margins of S3. The sacrum was then mirrored along its sagittal midline (Fig. 1.4B), and the half that was originally from the left side in both the original sacrum (Fig. 1.4A) and the reflected sacrum were removed (Fig.

1.4C). We mirrored the right side of the sacrum because the left side was significantly distorted and for smooth articulation of the left side of the sacrum with the mirrored right hipbone.

<u>Physical articulation of the pelvis</u>

The virtually reconstructed hipbones and sacrum were 3D printed with a Zortrax M200 3D printer at 0.12 mm layer thickness. Afterwards, the three bones were physically articulated following criteria described in Bonneau et al. (2012). The articulation of the hipbones and sacrum was done on the physical models because the lack of haptic feedback in the virtual space increases the opportunities for the virtual renderings to overlap one another. The well-preserved anterior borders of the auricular surfaces on the S2 served as the main guide for the sacroiliac articulations. Sacroiliac cartilage—which was estimated to be approximately 3 mm thick based on studies that have characterized its shape and size in adult recent humans (Schunke, 1938; Lawson et al., 1982; McLauchlan and Gardner, 2002; Bonneau et al., 2012)— was mimicked using modeling clay, because it has been shown that representing the cartilage between bones results in reconstructions that more closely approximate the original pelvic shape than is achieved by directly connecting the bones (Li, 2002; Claxton et al., 2016). Priority was given to the alignment of the ventral margin of the sacroiliac joint, which was very well preserved on both the hipbone and sacrum. The dorsal ends of the auricular surfaces were not as well preserved, so modeling clay was used to support the joint in this region. Modeling clay was also used to estimate the missing parts of the pubis by following the curvature of the pectineal line and the preserved part of the pubic symphysis. Linear measurements were then collected on the articulated physical models using various calipers, and angles were collected using a goniometer (Table 1.4).

Virtual articulation of the pelvis

After the physical reassembly, five fiducial points were collected on each of the pelvic elements (15 in total for each reconstruction) using a Microscribe 3DX digitizer (Table 1.3). Then, in Avizo these points and image warping tools were used to align the virtual elements to the same coordinates as the physical pelvises (Fig. 1.5) thereby creating virtual replicas of the physically articulated reconstructions.

Assessing reconstruction uncertainty

All of the reconstruction steps described above were completed by the first author (M.T.A.). Subsequently, a second reconstruction was made to address the uncertainty involved in the reconstruction process (see Claxton et al., 2016). A coauthor (P.A.S.) who had not participated at any previous point in the study was tasked with conducting the second reconstruction. P.A.S. was provided with the segmented surface renderings of the right hipbone and sacrum as well as basic instructions. The instructions explained the observed damages and suggested in broad terms the possible steps and tools in Avizo that could be applied to align anatomical features and conduct the mirror imaging. No quantitative data (e.g., translation metrics) were provided, and P.A.S. was encouraged to deviate from the possible steps outlined in the instructions as needed (see Supplement S1.1 for more details).

RESULTS

Here we describe the morphological differences between the original reconstruction of Kebara 2 (designated hereafter as RA) and the new reconstructions (designated hereafter as NR1 and NR2, and NRhip and NRsacrum when discussing the specific bones). The new measurements we present were taken on the 3D printed

models of NR1 and NR2. This allowed us to use similar osteometric tools as those used by Rak (1991), to avoid introducing error that could result of comparing physically collected data to virtually collected data. We did however collect a subset of the measurements on the virtual models to check our alignments with the physical models and because they were very similar, we only present the measurements collected on the physical models. All measurements taken on NR1 and NR2 were collected by the first author (M.T.A.). The measurements are presented in Table 1.1 (disarticulated right innominate), Table 1.2 (sacrum), and Table 1.4 (articulated pelvis).

Hip Bone

Rak (1991) estimated the length of the superior pubic ramus to be about 89 mm. This measurement is longer in both NRhip1 (92 mm) and NRhip2 (91 mm; estimated in NRhip1 and NRhip2 by reconstructing the upper part of the pubic body with modeling clay). The arcuate chord—the straight-line distance between the most posterior point of the arcuate line at the sacroiliac joint and the most anterior point of the arcuate line at the pubic symphysis—also shows an increase from RA (128 mm) to NRhip1 (130 mm) but is shorter in NRhip2 (127 mm). A similar pattern is found for the arcuate arc, which in comparison with RAhip (149 mm) is longer in NRhip1 (151 mm) but shorter in NRhip2 (148 mm).

Sacrum

The repositioning of S1 in relation to S2, and S4 in relation to S3 resulted in an increased ventral curvature of the sacrum. Because of this increase in curvature, the ventral height—measured from the midline of the promontory to the apex—showed a reduction from 115 mm in RA to 109 mm (NRsacrum1) and 108 mm (NRsacrum2). The sacral widths of NRsacrum1 (119 mm) and NRsacrum2(117 mm) were less than

in RAsacrum (122 mm). A by-product of mirroring the right half of the sacrum was the replacement of the sagittally-oriented left superior articular facet with a more coronally-oriented facet. While this change does not affect the measurements taken in this study, future attempts to articulate the Kebara 2 lumbar vertebrae to either of the newly reconstructed sacra (NRsacrum1 and NRsacrum2) will have to rely solely on the right side.

Complete Pelvis

The measurements collected on the new reconstructions are compared to those collected by Rak (1991)—and one measurement from Tague (1992)—in Table 1.4. Shape indices calculated from these data are also presented in Table 1.4.

In both new reconstructions, the pubic symphysis is more anteriorly positioned (more prominently in NR1) creating a more anteroposteriorly (AP) elongated pelvic canal. As a result, the maximum AP length of the inlet is 8 mm (NR1) and 2 mm (NR2) longer than in RA. The maximum mediolateral (ML) width of the inlet is also 2 mm (NR1) and 4 mm (NR2) narrower than in RA. For the outlet the differences are less pronounced; the maximum AP length is 1 mm longer (NR1) and 2 mm shorter (NR2) than in RA; however, there are larger alterations to the maximum ML width, which is 8 mm narrower (NR1) and 2 mm wider (NR2) than in RA. The RA inlet shape index (maximum AP length/maximum ML width) is 0.83 while the inlet shape indices of the new reconstructions are 0.90 (NR1) and 0.87 (NR2), respectively. The outlet shape index is higher in NR1 (0.91) than in RA (0.85), and it is the same in NR2.

The distance between the anterior superior iliac spines is longer in the new reconstructions (237 mm in NR1 and 231 mm in NR2) than in RA (224 mm). The distance between the anterior margin of the acetabula is also longer in the new

reconstructions (165 mm in NR1 and 168 mm in NR2) than in RA (156 mm in RA). This distance in RA is 79.5% of the distance between the posterior margins (Rak, 1991). In NR1 and NR2, the percentages are 83.2% and 83.8% respectively. As a result, the angle between the plane of the acetabular rim and the sagittal plane in RA as measured by Rak and Arensburg (1987) is 18°. This angle is 20° in NR1 and 24° in NR2.

Another difference is in the position of the inlet within the pelvis relative to the anterior edge of the acetabular rim. Rak and Arensburg (1987) assessed that 75.2% of the maximum length of the inlet is found posterior to an imaginary line stretching between the anterior margins of the acetabula. In the new reconstructions, the percentage of the maximum length posterior to this line is only 71.2% (NR1) and 73.1% (NR2). The subpubic angle in the new reconstructions (94° in NR1 and 98° and NR2) is more acute than in RA (110°).

DISCUSSION

Pelvic Morphology

The post-depositional damage to the Kebara 2 pelvis has been comprehensively described (Duday and Arensburg, 1991; Rak, 1991; Trinkaus, 2018). These prior assessments align with our own examinations through CT scans and the original fossils. In this study, we identified and corrected notable fractures of and distortions to the Kebara 2 right hipbone and sacrum by realigning dislocated fragments to more probable anatomical positions. Although the Kebara 2 pelvis is largely complete, like other fossils, the absence of certain fragments can contribute to increased interobserver error for any attempts at reconstructing it. To assess the magnitude and pattern of this error, we created two new reconstructions, by two different

researchers following roughly the same protocols (see Supplement S1.1). On the right hipbone, the virtual repositioning of bone fragments focused mainly around the ischiopubic region, which displayed the most extensive damage. The goal was to straighten out the ischiopubic ramus by rotating the pubic body anterolaterally. This primary step was followed by adjustments to the other fragments to align them with the revisions that had been made to ischiopubic ramus. For the sacrum, the unfused joints between the sacral vertebrae and the fragments making up the sacral alae were realigned. As expected, the two reconstructions have some differences between them, the major ones being the position of the pubis and the curvature of the ischiopubic ramus; NRhip1 has a more curved ischiopubic ramus and a more anterosuperiorly oriented pubis compared to NRhip2 (Fig. 1.3). Nevertheless, both new reconstructions have a more curved ischiopubic ramus and a more anterosuperiorly oriented pubis compared to the original fossil (Fig. 1.3).

Rak (1991) described the inferior margin of the ischiopubic ramus of the Kebara 2 pelvis to be pronouncedly concave in a manner that in recent humans is mostly found in females. Due to the anterosuperior rotation of the pubic body and the straightening of the ischiopubic ramus, the subpubic angle was reduced in the new reconstructions to the lower end of the range found in recent human females (Luo et al., 1993; Tague, 1994), although with angles of 94° (NR1) and 98° (NR2), respectively, these reconstructions have angles that also fall within the ranges of recent human males (Nwoha, 1995; Msamati et al., 2005; Karakas et al., 2013). The anterosuperior realignment of the pubic body also resulted in an increase in the anteroposterior length of the pelvic inlet and a smaller increase in the anteroposterior length of the outlet (see Table 1.4, NR2). These changes in anteroposterior length give the pelvic apertures of both new reconstructions a rounder (less oval) shape.

At the outlet, the maximum ML width represents one of the few dimensions where the two new reconstructions do not agree on the direction of change. While NR1 has a much narrower outlet than RA, NR2 has a slightly wider outlet than RA. The narrower width in NR1 creates a rounder (and smaller) outlet, while the outlet shape index for NR2 remains the same as in RA, even though the size of the outlet has increased. This discrepancy is the result of the different choices made in reconstructing the ischiopubic ramus (see Supplement S1.1 for more details). Nevertheless, although the outlet of NR1 is more circular than in RA and NR2, it is still mediolaterally wide in comparison to most recent humans (Tague, 1994).

The maximum AP length of the pelvic canal is also influenced by the more anteriorly repositioned S1 and sacral apex, which push the sacrum further into the pelvic canal space, indicating that Kebara 2 had a more android or heart-shaped pelvis than was apparent from the original. The position of the sacrum also impacts the position of the inlet within the pelvis and how much of the inlet is posterior to the anterior acetabular margins. According to Rak and Arensburg (1987), in recent human samples 89% of the inlet is posterior to the anterior acetabular margin, whereas the percentage for Kebara 2 is 75.2%. In both new reconstructions the percentage drops to even further away from the recent human average (71.2% in NR1 and 73.1% in NR2) due to the increase in superior pubic ramus length and the more sagittally-oriented pubic symphysis. Finally, the repositioning of the superior pubic ramus situates the anterior acetabular margins further away from the midline resulting in an even more laterally facing acetabula.

Uncertainty and Error

In accordance with our goal of acknowledging reconstruction uncertainty, potential sources of error must be addressed. One of these is the mirroring process,

particularly in the establishment of the sacral midline on which the left side was reflected. We endeavored to preserve the width of the body of S1 and the width of the most inferior part of the sacrum (apex). Nevertheless, NRsacrum2 presents a sacral width that is 2 mm narrower than in RA, and this reduction in sacral width could have affected other pelvic width measurements. In addition, by mirroring the right half to the left side, the resulting reconstructions are symmetric; however, because of the development anomalies discussed above, the reconstructed pelvises do not necessarily reflect the anatomy of Kebara 2 in life. Nonetheless, we believe that the new reconstructions are representative of Neandertal pelvic morphology in general.

The addition of modeling clay to represent the sacroiliac joint connective tissue would also have reduced the comparability of the new reconstructions to the original reconstruction, because it is not clear from the cast if Rak and Arensburg (1987) accounted for this tissue and, if so, at what magnitude. Rak (1991) did not provide measurements of the maximum AP length of the outlet so instead we used data from Tague (1992). Although there is no reason to believe that Rak (1991) and Tague (1992) would have measured maximum AP length of the outlet differently, it should be noted that the calculation for the outlet shape index for RA used data collected in two different studies. Finally, although mirroring allows us to estimate the dimensions of the Kebara 2 pelvis, and more generally, the male Neandertal pelvis, it results in reconstructions that are unrealistically symmetrical, which may be problematic for some analyses.

Implications of the New Reconstructions

Our new reconstructions of the Kebara 2 pelvis have implications for some of the conclusions previously drawn about its morphology and Neandertal morphology in general. According to Rak and Arensburg (1987), when compared to the mean of a

small sample (n = 18) of recent human males from the Hamann Todd collection, the size of the pelvic aperture of the original reconstruction did not differ from the size in recent human males. A subsequent, more extensive study by Tague (1992) showed that the Kebara 2 pelvis is at least 11% larger in both the AP and ML inlet diameters than the mean size for recent human males. According to our new reconstructions, the ML inlet width is slightly narrower, bringing Kebara 2 closer to the recent human male means from both studies. On the other hand, the AP inlet diameters of the new reconstructions suggest a difference between Kebara 2 and recent human males beyond that presented by Tague (1992), with NR1 being larger than both the original reconstruction, and the recent human male means.

The Kebara 2 pelvis has an elongated pubic ramus that is in some ways reminiscent of the morphology found in recent human females (Rak and Arensburg, 1987; Tague, 1992; Rosenberg et al., 1988; Trinkaus, 2006; Rosenberg, 2007; Weaver and Hublin, 2009). Rak and Arensburg (1987) argued that the length of the ramus could not be accounted for by the size of the pelvic inlet, suggesting that it was more likely to be functionally related to locomotion or posture than to obstetrics. However, other studies have pointed out that when Kebara 2 is compared to a more diverse sample, Kebara 2 falls well within the range of recent humans (Rosenberg et al., 1988; Tague, 1992). Our new reconstructions of Kebara 2 also fall within the ranges of recent human males. Additionally, substantial attention has been paid to the implications of Neandertal pelvic aperture morphology for childbirth (Rosenberg et al., 1988; Ponce de León et al., 2008; Weaver and Hublin, 2009; Rosenberg et al., 2010); however, given that the Kebara 2 pelvis is generally considered to come from a male, we are hesitant to reach conclusions about Neandertal birth mechanisms from the shape of its pelvic aperture without conducting analyses that are beyond the scope of this study.

The wide bi-iliac breadths found in Neandertals have been argued to be adaptations to the often-cold climates of Pleistocene Eurasia (Ruff, 1991; 1994; 2010; Holliday, 1997; Weaver and Hublin, 2009). Our new reconstructions of the Kebara 2 pelvis have comparable bi-iliac breadths to the original reconstruction, thereby retaining the configuration characteristic of Neandertals, and according to Tague (1992), the Kebara 2 pelvis has a bi-iliac breadth that is larger than in 99.5% of recent males.

CONCLUSIONS

We present two new reconstructions of the Kebara 2 pelvis, which provide us with the opportunity to reassess Neandertal pelvic morphology. Our study further illustrates the value of 3D imaging as a tool for fossil reconstruction because it allows researchers to develop multiple hypothetical reconstructions to better assess uncertainty (Gunz et al., 2009). For the majority of the measurements collected, the new reconstructions differ in similar ways from the original reconstruction by Rak and Arensburg (1987). Only for the maximum ML width of the outlet do the new reconstructions disagree on the direction of change from the original. Generally, the new reconstructions tend to accentuate features of the Kebara 2 pelvis—the long superior pubic ramus and anteriorly positioned pelvic inlet—that have already been discussed for Kebara 2 and other Neandertals.

CHAPTER 1 TABLES AND FIGURES

Table 1.1. Measurements of the disarticulated right innominate before and after new reconstruction (in mm).

Measurement	Original [a]	New reconstruction 1		New reconstruction 2	
			Difference (%)		Difference (%)
Maximum height	>217	>218	+0.46	>218	+0.46
Maximum width	158	156	-1.27	156	-1.27
Length of superior pubic ramus[b]	>87 (89)	(92)	+3.37	(91)	+2.25
Height of obturator foramen	59	59	0.00	58	-1.69
Length of obturator foramen	42	42	0.00	43	+2.38
Arcuate chord	128	130	+1.56	127	-0.78
Arcuate arc	149	151	+1.34	148	-0.67

[a] From Rak (1991).
[b] The length of the superior pubic ramus in the parenthesis reflects the estimated length after reconstructing the missing parts of the pubic body. The percent differences were calculated using the data in the parentheses.

Table 1.2. Measurements of the disarticulated sacrum before and after new reconstruction (in mm).

Measurement	Original [a]	New reconstruction 1		New reconstruction 2	
			Difference (%)		Difference (%)
Ventral height	115	109	-5.22	108	-6.09
Sacral width	122	119	-2.46	117	-4.10
Body length	33	32	-3.03	32	-3.03
Body width	55	55	0	53	-3.64

[a] From Rak (1991).

Table 1.3. Fiducial points used for virtually articulating the Kebara 2 pelvic bones.

Number	Fiducial points	Type
1	The most posterior point on the posterior-superior iliac spine	b
2	The most projecting point of the anterior-superior iliac spine	b
3	The most posterior point on the arcuate line where it meets the auricular surface	b
4	The most inferior point of the ischial tuberosity	b
5	The most anterior point on the portion of the pectineal line preserved on the fossil	b
6	The most superior point on the ala of the sacrum	b
7	The most superior point of the ventral margin of the second anterior sacral foramen	b
8	Midpoint of the sacral apex	m

Abbreviations: b = bilateral landmark; m = midsagittal landmark.

Table 1.4. Measurements and indices of the articulated pelvis before and after new reconstruction (in mm except otherwise indicated).

Measurement	Original [a]	New reconstruction 1		New reconstruction 2	
			Difference (%)		Difference (%)
Maximum width	313	311	-0.64	305	-2.56
Maximum AP inlet	117	125	+6.84	119	+1.71
Maximum ML inlet	141	139	-1.42	137	-2.84
Inlet index (AP/ML)	0.83	0.90	+8.43	0.87	+4.82
Distance between anterior-superior iliac spines	224	237	+5.80	231	+3.13
Maximum AP outlet	88[b]	87	-1.14	90	+2.27
Maximum ML outlet	104	96	-7.69	106	+1.92
Outlet index (AP/ML)	0.85	0.91	+7.06	0.85	0.00
Length of inlet portion in front of anterior acetabular margin	29	36	+24.14	32	+10.34
Length of inlet portion behind anterior acetabular margin	88	89	+1.14	87	-1.14
Percentage of inlet behind anterior acetabular margin	75.2	71.2	-5.32	73.1	-2.79
Distance between anterior-inferior iliac spines	204	208	+1.96	203	-0.49
Distance between anterior margins of acetabula	156	165	+5.77	168	+7.69
Distance between posterior margins of acetabula	196	197	+0.51	202	+3.06
Angle between plane of acetabular rim and sagittal plane	18°	20°	+11.11	24°	+33.33
Subpubic angle	110°	94°	-14.55	98°	-10.91

Abbreviations: AP = anteroposterior; ML = mediolateral.
[a] From Rak (1991) except where specified.
[b] From Tague (1992).

Figure 1.1. The Kebara 2 Neandertal right hipbone in lateral view. Note the postmortem damage, particularly along the ischiopubic ramus and the pubis. Scale bar = 1cm.
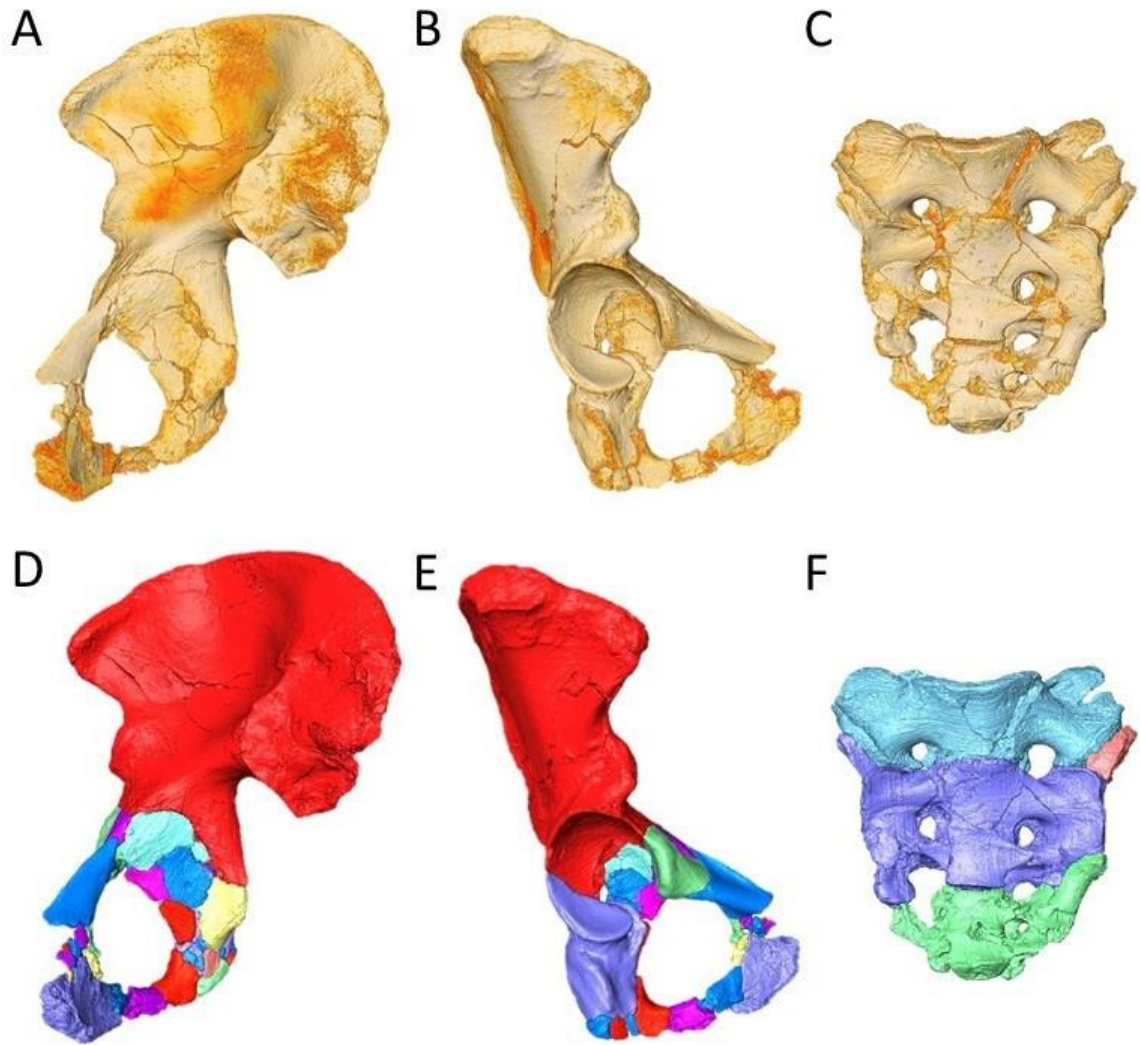
Figure 1.2. Segmentations of the fragments of the Kebara 2 right hipbone and sacrum. Volume renderings from CT scans of the hipbone in medial (A) and lateral (B) views, and the sacrum in anterior view (C). The color gradient in the volume renderings reflects higher (lighter) to lower (darker) bone density. Corresponding surface renderings of the hipbone are depicted in medial (D) and lateral (E) views, and the sacrum in anterior view (F). The different colors in the surface renderings indicate the 39 independently segmented fragments of the hipbone, and the 4 segmented fragments of the sacrum.
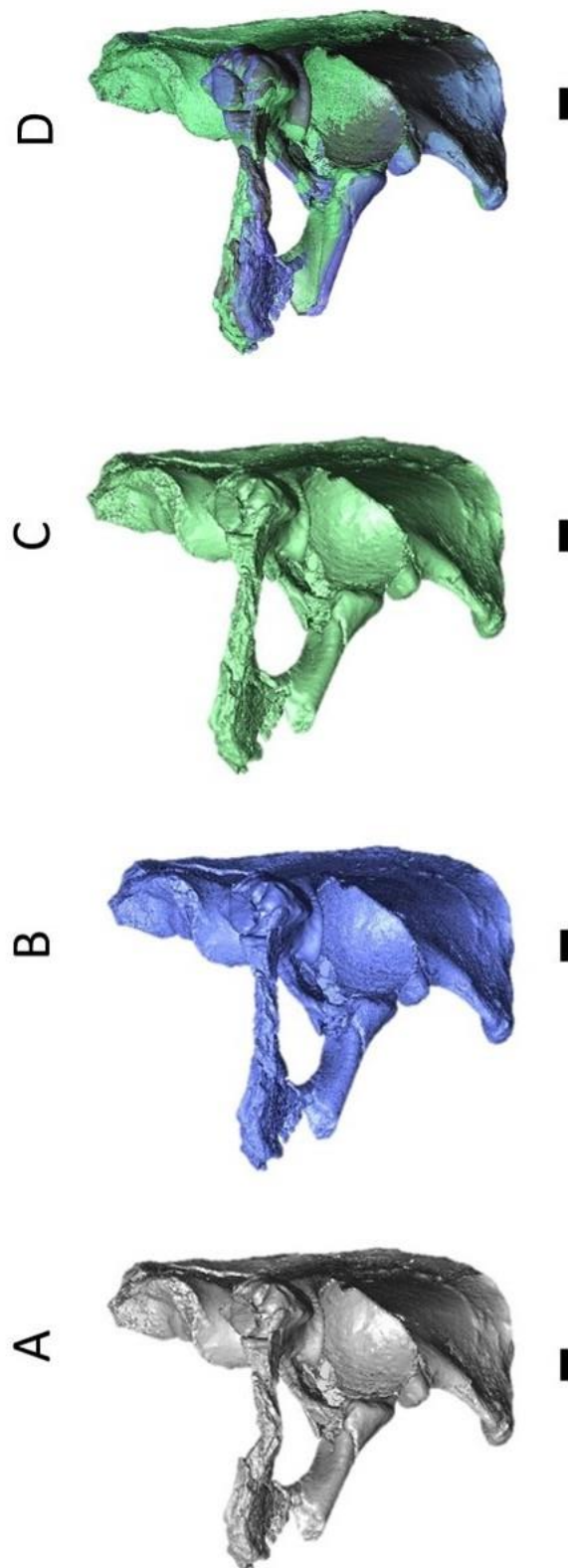
Figure 1.3. Realignment of the Kebara 2 ischiopubic ramus. A) the original hipbone; B) new reconstruction 1 (NRhip1); C) new reconstruction 2 (NRhip2); D) superimposition of A, B, and C in inferior view. Scale bars = 1cm.
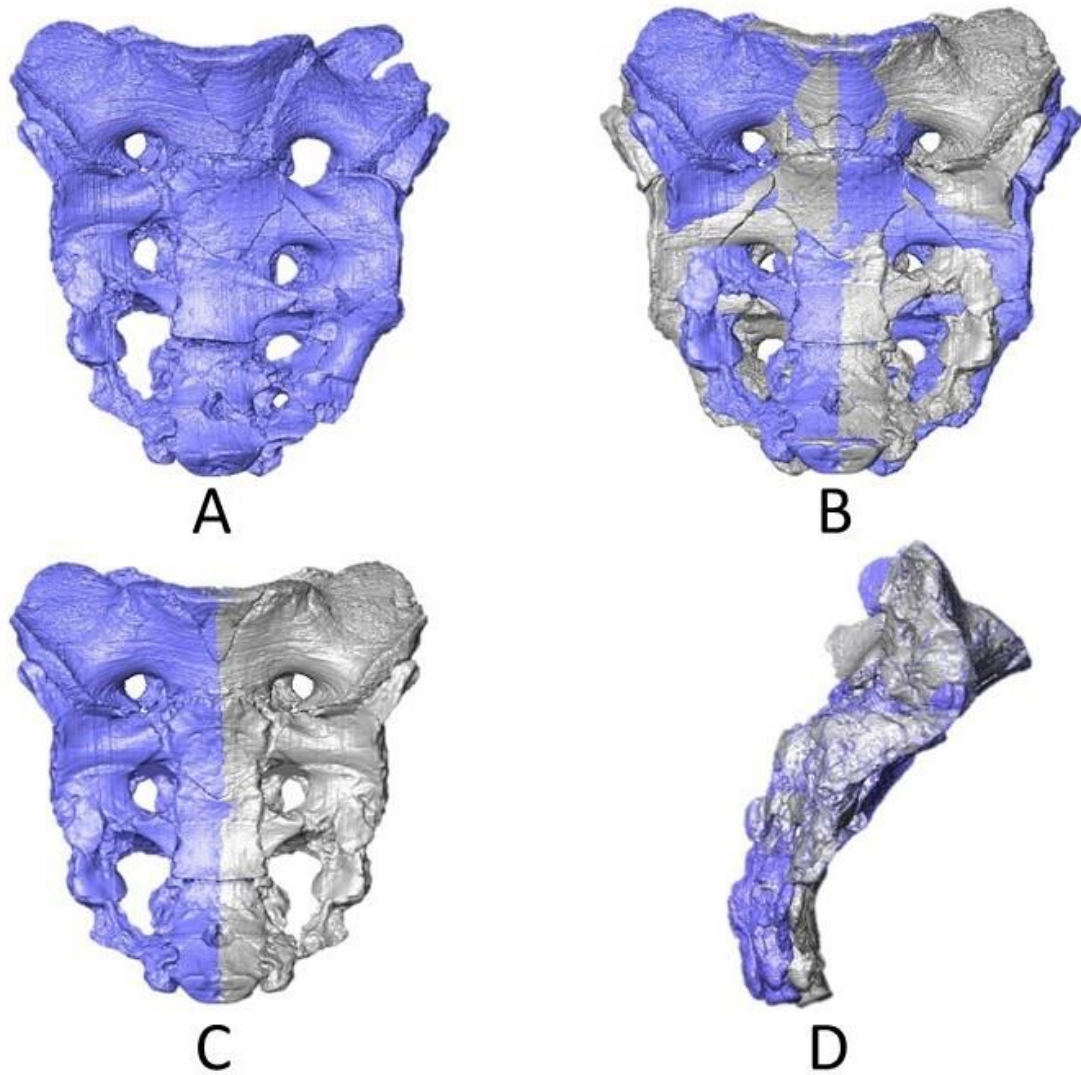
Figure 1.4. Reconstruction 1 of the Kebara 2 sacrum (NRsacrum1). A) the original sacrum; B) superimposition of reflected sacrum (gray) onto the original (blue) sacrum (the midline used in the superimposition was determined by the sagittal midline of the lumbosacral articular surface and the sacral apex); C) final result; D) overlap of the original sacrum (blue) with the reconstruction (gray) in sagittal view.
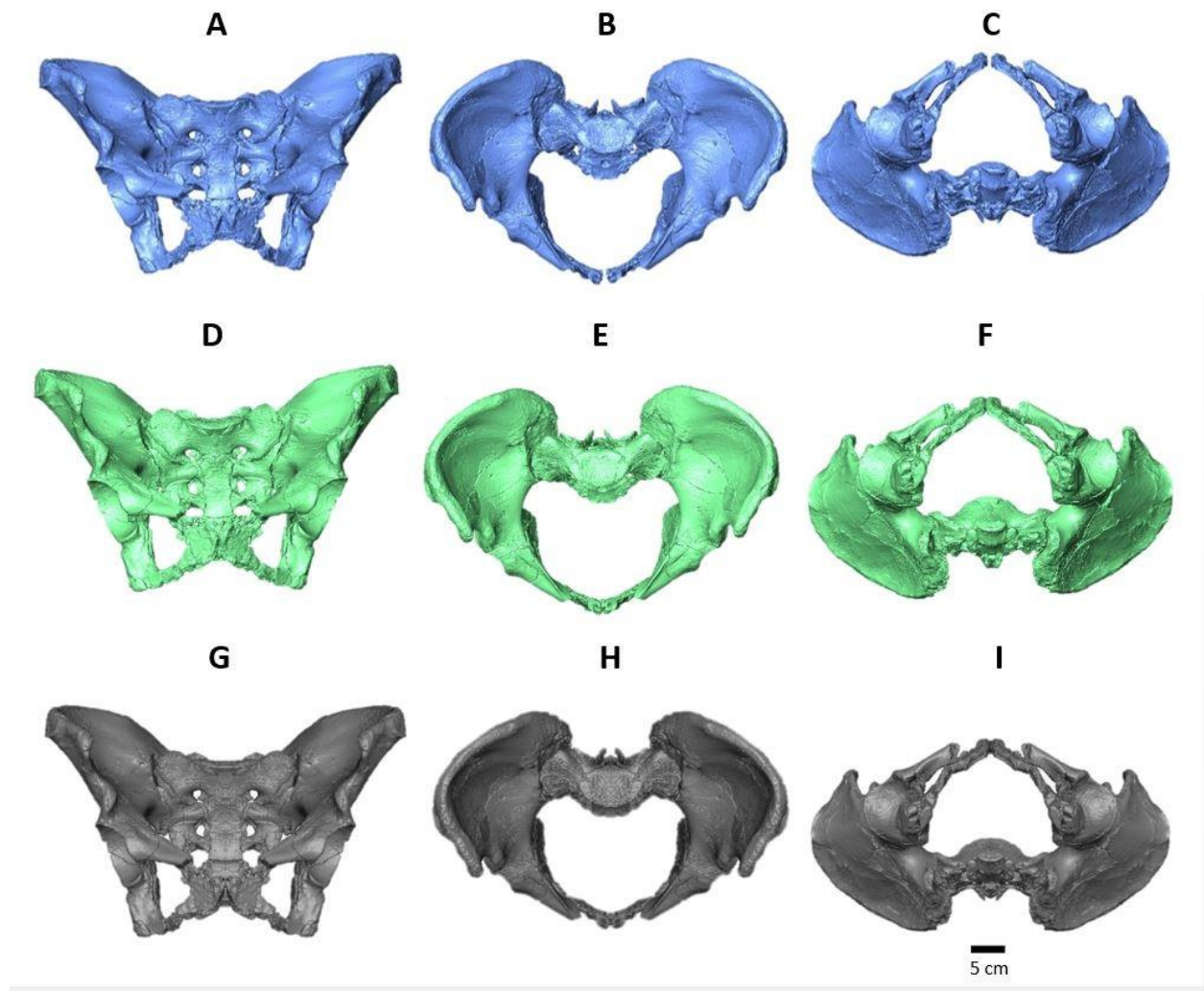
Figure 1.5. New reconstructions of the Kebara 2 pelvis. New reconstruction 1 (A–C; blue), New reconstruction 2 (D–F; green), and the original reconstruction by Rak and Arensburg (G–I; gray) in frontal (A, D, G), superior (B, E, H), and inferior (C, F, I) views. Scale bar = 5 cm.

CHAPTER 2: VARIATION IN THE SHAPE, SIZE, AND SPACING OF ADULT HUMAN PUBIC SYMPHYSES

Authors: Mayowa T. Adegboyega, Sara Jhanjar, Mark Grote, Timothy D. Weaver

ABSTRACT

Objectives

The pubic symphysis consists of anterior parts of the left and right hip bones but also soft tissue that affects the spacing of the bones. This study examines the shape, size, and spacing of adult human pubic symphyses (pubic symphysis morphology) using three-dimensional geometric morphometrics (3D-GM). The goals are to build a quantitative model to predict pubic symphysis morphology, and to assess the relationships between the anthropometric variables in the model and pubic symphysis morphology.

Materials and Methods

We collected 3D landmark and semilandmark data on the pubic symphysis and adjacent aspects of the pelvis from surface renderings generated from CT scans taken throughout the University of California Health system of 103 adults. We used geometric morphometrics to quantify pubic symphysis morphology and trained simple and 2-stage-least-squares linear regression models to predict pubic symphysis shape, and to assess the shape variation in the sample. We identified the best model and used principal components analysis to explore the effects of each variable on shape, and hypothetical shapes to illustrate these effects.

Results

The best model is a 2-stage least squares model that regresses pubic symphysis size against the additive effects of sex and age in the first stage, and then

interacts that predicted value with sex and age in the second stage. Other models that performed well included variables reflecting pelvic size and breadth.

Discussion

This study shows how linear regression modeling can be used to systematically estimate an individual's pubic symphysis morphology. This method could be used in addition to other reconstruction techniques to improve fossil pelvic reconstructions by more accurately estimating the morphology of this region of the pelvis.

INTRODUCTION

The pubic symphysis is a non-synovial joint that forms the anterior margin of the skeletal pelvis and connects the left and right pubic bones at the ventral midline (Becker et al., 2010; Gamble et al., 1986; Z. Li et al., 2007). The ends of both pubic bones are covered by a thin layer of hyaline cartilage (Sutro, 1936) and interposed by a fibrocartilaginous disc (Lei et al., 2015; Rosse et al., 1997), and the joint is reinforced by superior, inferior, anterior, and posterior pubic ligaments (Becker et al., 2010; Fick, 1904; Gamble et al., 1986; Standring, 2021). In humans, the pubic symphysis resists tension, shearing, and compression during weight bearing activities (Bar-Yosef et al., 1991; Becker et al., 2010; Benjamin & Evans, 1990; Gamble et al., 1986; Meissner et al., 1996; Walheim & Selvik, 1984), transfers the load from the upright trunk through the pelvic girdle to the lower limbs during bipedal locomotion (Lei et al. 2015; Neumann, 2016), and provides elasticity during pregnancy and childbirth to allow more room for the fetus to move through the birth canal (Becker, Woodley, and Stringer 2010; Wright, 1952; Bahlmann et al. 1993; Garagiola et al. 1989).

The pubic symphysis has undergone significant evolutionary changes within the hominin lineage (Gruss & Schmitt, 2015; Lewton, 2015; Rak & Arensburg, 1987). In comparison to most non-human primates, the pubic symphysis is shorter in superoinferior height, and it is interposed by a mediolaterally wider cartilaginous disc. Fusion between the pubic bones has been documented in some primate species (Tague, 1993), but symphyseal synostosis has not been documented in healthy humans. The increase in cartilage means the joint can experience some mobility in the maternal pelvis in response to pressure from the fetal head and shoulders (Gruss

& Schmitt, 2015), and as such, the human pubic symphysis has been described as a potential site of biomechanical weakness (Todd, 1920).

Human Pubic Symphysis Variation

The articular surfaces of the pubic bones are oval in shape and obliquely orientated in the sagittal plane (Fick, 1904; Knox, 1830; Luschka, 1862; Testus & Latarjet, 1928). Posteriorly, the surfaces run closely parallel to one another, but they usually diverge anteriorly, superiorly, and inferiorly (Aeby, 1858; Fick, 1904). The dimensions of the articular surfaces are reported to be between 30–35 mm long and 10–12 mm wide (Testus & Latarjet, 1928).

Several studies have attempted to quantify the morphological variation in human pubic symphysis joint width (Alicioglu et al., 2008; Bauman et al., 2011; Becker et al., 2014; Björklund et al., 1996; Gamble et al., 1986; Loeschcke, 1912; Testus & Latarjet, 1928); however, direct comparisons across studies are made difficult by poorly described data collection and analysis protocols in many of the earlier works (see: Becker et al., 2010, 2014). As a result, little can be inferred about the widely varying measurements of symphyseal width that have been presented. For example, Barnes (1934) estimated a mean male anterior symphyseal width of 4.2 mm while Alicioglu et al.,(2008) estimated it to be to 11.8 mm. In females, mean anterior symphyseal widths from 2.6 mm (Roberts, 1934) to 20 mm (Loeschcke, 1912) have been reported. It is important to also note that most studies of the pubic symphysis are conducted for clinical purposes with a focus on either pathological cases such as acute pubic symphysis inflammation and pubic symphysis dysfunction, or to assess the changes that occur during pregnancy (Aydın et al., 2016; Becker et al., 2010, see Table 2; Oligmüller, 2015), which means that they cannot be used as models of normative pubic symphysis form and functions. Very few of these studies investigate

the relationship between symphysis shape and other anthropometric data beyond the impact of sex on pubic symphysis width. Alicioglu et al., (2008) assessed the relationship between pubic symphysis width and age, sex, number of births, and body-mass index (BMI) and found that the anterior and posterior pubic symphysis narrows concurrently with ageing (though to a lesser degree with the latter) while the middle remained the same, and that number of births and body-mass index values did not affect symphyseal width though anterior and middle widths were significantly higher in women. Outside of clinical studies, much of the focus on the pubic symphysis has been to assess the developmental and degenerative changes that occur on the symphyseal surface for the purposes of bioarcheological and forensic age-at-death estimation (Brooks & Suchey, 1990; Chiba et al., 2014; Dudzik & Langley, 2015; Franklin, 2010; Gilbert & McKern, 1973; Lottering et al., 2014; Todd, 1920; White & Folkens, 2005), although a recent study demonstrated that below the age of 50, the outline of the symphyseal surface can also be used to estimate age-at-death (Bravo Morante et al. 2021).

Most of the aforementioned studies have been conducted postmortem, but quantitative in vivo analyses are limited to a few investigations (Alicioglu et al., 2008; Aydın et al., 2016; Bauman et al., 2011; Björklund et al., 1996; Schoellner et al., 2001; Weber et al., 1997; Wurdinger et al., 2002). These studies have also mostly focused on symphyseal width in the areas of obstetrics (which limited analyses of male morphology), and on age-at-death estimation from the symphyseal faces. There have not been comprehensive analyses of the size, shape, and spacing of this joint that could be useful for in comparative analysis with fossil hominins or for inferring missing pelvic dimensions.

Geometric Morphometrics and Regression-Based Predictive Analysis

Three-dimensional (3-D) geometric morphometrics (GM) has become an established analytical toolbox for the statistical analysis of biological shape variation and improving fossil reconstructions (Benazzi et al., 2009; Brassey et al., 2018; García-Martínez et al., 2014; Gunz et al., 2009; Gunz & Mitteroecker, 2013; Mitteroecker & Gunz, 2009; O'Higgins et al., 2011; Schlager et al., 2018; Slice, 2005; Slice, 2007; Torres-Tamayo et al., 2020; Weaver & Hublin, 2009). The advantages of 3D-GM include the ability to analyze shape separately from the effects of size and to visualize the results of multivariate statistical analyses.

Amongst the many 3D-GM methods available, a statistical approach applying multiple multivariate linear regressions to a reference sample has proven to be an accurate way to predict missing shape data (Bookstein et al., 2003; Gunz et al., 2004; 2009; Stelzer et al., 2018; Weber & Bookstein, 2011). This technique involves regressing shape variables (e.g., 3-D superimposed landmarks on an anatomical structure) with the missing values on other variables in a reference sample of complete specimens to predict the missing 3-D landmark coordinates.

In this study, we trained simple and 2-stage-least-squares linear regression models to predict pubic symphysis shape using several anthropometric variables such as sex, age, height, weight, centroid sizes of the pubic symphysis and the pelvis, and pelvic breadth. We began by training different regression models on our sample to identify a model that best predicted shape. Then, we followed this by investigating the variation in the sample by exploring the relationships between pubic symphysis morphology the variables used in the model . This study could help us better understand pubic symphysis shape variation, and it could help us develop new

models for estimating missing pubic symphysis morphological data to complement methods for reconstructing hominin pelvic specimens.

MATERIALS AND METHODS

Samples and Data

The sample consisted of 103 adult humans (n = 52, males; n = 51, females) ranging between the ages of 20 to 96 years old who had undergone abdominal and pelvis computed tomography (CT) imaging between May 2019 and November 2020 through the University of California Health system in California, USA. We obtained approval from the University of California, Davis Institutional Review Board to use these patient's data in this study. The scans were taken using one of the following medical CT scanners at slice thicknesses of 1 – 1.5 mm: Siemens Somatom Definition DS 64, Siemens Somatom Definition AS 128, Siemens Somatom Sensation PCH 64, and the GE Light Speed VCT 64. Individuals who presented with injuries including but not limited to pelvic fractures, neuromuscular disorders, and pubic symphysis diastasis, or were identified as having undergone treatments in the past for pelvic injuries were not included in the study as these conditions might influence pubic symphysis morphology.

The CT scans were imported as DICOM (.dcm) files into Avizo Lite 9 (FEI Visualization Sciences Group, 2015) for segmentation and data collection. The skeletons were first segmented from soft tissue using automated density thresholding tools, then the pelvic bones (the left and right hipbones and the sacrum) were manually segmented from the rest of the skeleton, and finally 3-D surface renderings to be used for data collection were generated for each segmented pelvis.

Along with the CT scans, a series of biometric and morphometric data were collected for each individual from their electronic medical records. The CT scan data

were anonymized before being imported, so searching for corresponding medical records was done using medical record numbers (MRN). The information collected from the medical records included sex (male or female), age in years, weight in kilograms, and height in meters at the time of the scan. The other predictors variables that were used in the regression models were generated from the landmark data collected on the pelvic surface renderings. These variables were maximum pelvic breadth and centroid size of the pelvis and of the pubic symphysis face.

Landmarks and Semilandmarks

The set of 3D landmarks and semilandmarks were designed to define two overlapping shapes. The first set of points defines the shape of the pubic symphysis in a living human whose pelvis is still fully articulated, and the second set of points defines the shape of the entire pelvis for the purposes of calculating pelvic centroid size, which is the measure of size used almost universally in geometric morphometrics i.e., the square root of the sum of squared distances of all the landmarks of an object from their centroid (Dryden & Mardia, 1998; Goodall, 1991; Rohlf & Slice, 1990).

Landmarks and semilandmarks were collected along the visible symphyseal margins because the cartilage in the joint obstructs the bony symphysis faces, preventing us from collecting accurate surface semilandmarks on the symphyseal faces. Three anatomical landmarks (Dryden & Mardia, 1998) were collected on each side (totaling 6 landmarks per symphysis), on the most superior and most inferior points of each side, and on the most anterior points on each pubic tubercle. Semilandmarks were manually placed along the margins of each left and right pubic symphyses. Afterwards, the semilandmarks were then resampled so each individual had the same number of equidistant semilandmarks and then slid along curves to

minimize bending energy (Gunz et al., 2005). The total count was 14 semilandmarks on each side in R (R CoreTeam, 2019) making a total of 28 semilandmarks per symphysis. A landmark set of 54 pelvic landmarks were collected to define the shape of the whole pelvis. The 6 pubic symphysis landmarks are included in these landmarks (Fig. 2.1; Table 2.1).

Geometric Morphometric Analyses

All landmarks and semilandmarks of were imported into R and were registered using Generalized Procrustes Analysis (GPA) which translates all the shapes to the origin, scales them to the unit centroid size to remove size as a confounding variable, and rotates them around the origin to minimize the sum of squared distances between them (Gower, 1975; Zelditch et al., 2012). GPA was carried out first using only the pubic symphysis landmark because we surmised that this would generate the most appropriate registration for our region of focus. The second GPA, using all of the pelvic landmarks and semilandmarks, was carried out to extract information about pelvic centroid sizes within the sample and to generate a measure of maximum pelvic breadths for every pelvis. Pelvic breadth was calculated as the Euclidean distance – the square root of the sum of squared difference – between the left and right pubic tubercle landmark coordinates. The values generated therefore represent a within-sample Procrustes registered scale of pelvic breadth.

As part of the GPAs, the semilandmarks were slid to minimize the bending energy between each specimen and the Procrustes mean shape (Gunz et al., 2005; Schlager et al., 2021). The centroid sizes of the pubic symphyses as defined by the landmarks and semilandmarks were also generated in the Procrustes registration process.

<u>Predicting shape</u>

We trained several multivariate linear regression models on different combinations sex, age, pubic symphysis centroid size, pelvis centroid size, height, weight, and pelvic breadth with the goal of identifying the model that will most accurately predict pubic symphysis shape. First, we calculated the natural log of each variable except for sex, so from this point on, any mention of these variables will be referring to its log transformed value. Then, we established several guiding principles to constrain our model space which are as follows:

1. **Sex is a constant predictor**. The sexual dimorphism of the pubic symphysis in particular has been well established (Becker et al., 2010; Lottering et al., 2014), so to acknowledge this effect, we included sex as a variable in every model except for the null model.

2. **All body size variables are endogenous variables**. We hypothesize that the body size variables namely height, weight, pelvic breadth, and pubis symphysis and pelvis centroid sizes are not independent of sex and age and so we used two-stage least squares regression (2SLS) models to more robustly capture their total effects on pubic symphysis shape. In 2SLS models the endogenous variables (i.e., variables that are influenced by the independent or exogenous variables), become the dependent variable in the first stage regression equation, and the predicted values from these regressions replace the original values of those variables in the second stage regression model. In our models, sex and age are the only truly exogenous variables, while all body size variables are treated as endogenous.

3. **Height and weight always appear together**. Our previous investigation revealed strong collinearity between height and weight, but instead of

applying our first principle, we created a log transformed matrix of height and weight data which results in a logged index of height and weight, i.e., a log of body mass index (BMI).

Leave one out cross validation (LOOCV) was used to calculate the prediction errors – mean squared errors of the Procrustes distance between each original specimen and its prediction – for each model. We interpreted LOOCV as a measure of model performance. LOOCV is a type of cross-validation where just a single observation is held out for validation. The 2SLS analysis was carried out for each prediction excluding the individual whose shape was being predicted. Thus, a prediction for that individual was calculated while excluding the individual from the predictive model to avoid self-inference, and the same was done for every other individual in the sample. This ensures that individuals did not unduly influence the training sample used to develop the models to predict their shape (Torres-Tamayo et al., 2020). The prediction error is then calculated by taking the mean of every individual's squared error evaluation for each model. The model with the lowest means squared error was identified as the best model and was further investigated in the next steps.

<u>Assessing shape variation</u>

Following the predictive modelling, we used two approaches to understand the biological implications of the predictor variables on shape focusing on our best model. First, we employed principal components analysis (PCA) to investigate general patterns of variation (Cox, 2021) in the dataset. A plot of principal component 1 (PC1) and principal component 2 (PC2) which account for 42.43% of the sample variation is reported here. We also generated plots of PC1 and PC2 against the variables in the best model to further elucidate the relationships between

those variables and pubic symphysis shape. Second, we created wireframe models of hypothetical symphyseal shapes to elucidate the effects of each of those variables holding the other variables constant. All geometric morphometric analyses were performed in R (R CoreTeam, 2019) using the following packages: Morpho v. 2.9 (Schlager et al., 2021), geomorph v. 4.0 (Adams et al. 2021; Baken et al 2021), boot v. 1.3 (Canty & Ripley, 2016; Davison & Hinkley 1997), and plyr v. 1.8.6 (Wickham et al., 2019) packages.

RESULTS

Model Predictions

To constrain the model space, we excluded models that did not fit our guiding principles from consideration (see Section 3.3.1). The full list of models that were fit, along with the prediction errors, is presented in the Supplementary Tables and Figures (Supplement S2.1); however, the best 5 models are described here in the main text (Table 2.2). The best model, (M4 in Table 2.2; M7 in Supplement S2.1) was a 2SLS regression model that first regressed sex and age on centroid size in the first stage, and then interacted the result with both sex and age in the second stage. The next best model, M5 (Table 2.2 ;M13 in Supplement S2.1), is very similar, except it includes pelvis centroid size in the place of pubic symphysis centroid size thereby revealing a strong correlation between pubic symphysis size and pelvis size. The next three models, M1 -M3, share the same prediction errors. M2 and M3 (Table 2.2; M11 and M23 in Supplement S2.1 respectively) interact sex with pelvis centroid size and pelvic breadth respectively and do not include age, indicating that model performance falls when age is excluded. M3 also additionally indicates the correlation between pelvic breadth and shape. M1 (Table 2.2 ; Supplement S2.1) is a

simple regression of just sex, which underscores how sex is the best single predictor of pubic symphysis shape. Though the differences between the prediction errors are very small, M4 stands out with an error that is more different from the best model, M5, than the differences between the following 3 best models combined. To visually assess how well the best model performed, we superimposed a generated prediction onto its corresponding observed shape (Fig. 2.2).

Principal Components Analysis

To investigate patterns of shape variation, we analyzed the first 2 principal components, which account for a total of 42.43% of the shape variation in our sample. To further investigate the patterns of variation, we plotted PC1 and PC2 against the entire set of model variables, and we include all of these plots in the supplementary tables and figures (Supplement S2.2-2.8). Here in the main text, we only present the analyses of PC1 and PC2 in relation to the variables present in the best model in the main text.

Effect of sex

When we plotted PC1 against PC2 (Fig. 2.3A), we observed significant levels of sexual dimorphism in pubic symphysis shape although there is significant overlap between males and females suggesting that the certain shapes exist in both sexes. Both PC1 and PC2 capture some aspect of pubic symphysis sexual dimorphism though most of the sexual dimorphism is captured by PC1. The minimum PC1 value represents a shape most commonly seen in females and the maximum PC1 value represents a shape most commonly seen in males. This symphysis has articular surfaces that are dorsoventrally narrow and the symphyseal width is relatively large when compared to the maximum PC1 value. Additionally, the pubic tubercles are more posterolaterally positioned than the maximum PC1 value, which has more

dorsoventrally wide symphyseal surfaces and a narrower symphyseal width. At first glance, PC2 seems to capture some contrasting patterns of shape variation as PC1. The minimum PC2 value represents dorsoventrally narrow symphyseal surfaces with a narrow symphyseal width, and the maximum PC2 value represents wide symphyseal surfaces with a wide symphyseal width. However, when data were sorted by sex, PC2 seems to also be reflecting shape variation relating to age which we analyze more specifically in other analyses.

Effect of age

The shape variation represented by PC1 does not reveal any discernable relationship with age for the entire sample; however, when the data were sorted by sex, males and females exist into moderately distinct regions of shape spaces across all ages, and there seems to be a stronger relationship between age and shape in males compared to females (Fig 3b). PC2 also does not seem to have any relationship to age for the whole sample, but once the data were sorted by sex, the sample can be seen to extend into more distinct regions of shape space as age increases. Additionally, PC2 appears to be positively correlated with age in males and negatively correlated with age in females (Fig 3c). This means that females that are nearer to the lower values of PC2 tend to be older whereas the males tend to be younger and vice versa.

Effect of size

PC1 and pubic symphysis centroid size are positively associated for the whole sample; however, a sex sorted plot suggests that PC1 and centroid size covary far more strongly for males than females, suggesting that there are stronger signatures of allometry in males compared to females (Fig. 2.3D). PC2, however, does not seem

to be associated with pubic symphysis centroid size in either the entire sample or after sorting by sex (Fig. 2.3E).

Hypothetical Models

We generated wireframe models of hypothetical pubic symphyses to highlight the effects of the variables in the best predictive model. For example, we generated wireframes for hypothetical 25-year-old females, one with a small, and the other with a large centroid size to isolate the effects of size on the shape. Figure 4 illustrates some shape comparisons for the variables in our best model and we describe those patterns of variation here.

Effect of sex

Figure 4a-d depict female shapes, and Figure 4e-h depict male shapes for hypothetical adults who are young and small, young and large, old and small, and old and large, in this order. The main differences between males and females are that the symphyseal surfaces are dorsoventrally wider and rounder in males compared to females, and the symphyseal width is wider in females in general. Additionally, the pubic tubercles are positioned more posterolaterally in the females while the males have more anteriorly positioned tubercles that are closer to the midline.

Effect of age

The main effect of age on our predictions can be seen in the symphyseal widths. In the younger predictions (Fig. 2.4A, B, E, F), the symphysis is wider compared to the older predictions (Fig. 2.4C, D, G, H). The inferior borders of the symphyseal surfaces were also less round, i.e., more pointed in the older individuals.

Effect of size

The symphyseal widths also reflect the main shape difference between the smaller and larger predictions. The smaller predictions (Fig. 2.3A, C, E, G) had wider symphyses than the larger predictions (Fig. 2.4 B, D, F, H) when comparisons were made within the sexes and within the younger and older predictions. In both smaller and larger males, the pubic tubercles are more superiorly positioned in relation to the superior margins of the pubic tubercles.

DISCUSSION

Our analysis shows that the pubic symphysis shape can be predicted using geometric morphometric tools including quantitative predictive modeling. In this section, we discuss the limitations of the study, the results of the regression models, the impact of each predictor variable from our best models on shape, and a potential application of this approach to fossil pelvis reconstructions.

Limitations of the Study

It is worth mentioning that due to the small number of individuals sampled in this study, we can expect the presence of some "noise" in the analyses, giving individuals who are outliers an oversized effect on the results. For example, the PCAs suggests that there is a stronger covariance between shape and size in males compared to females, but further investigation is needed to confirm if this is broadly true across all humans, or if this due to peculiarities within our sample. Notwithstanding, we have been able to capture major morphological characteristics of the pubic symphysis and in the following sections we will discuss what it means for the biology of the joint.

Model Predictions

We have shown that predictive modelling is a viable means of estimating pubic symphysis morphology in adult humans. The clear difference in the performance of the best model compared to the null model highlights the need to consider sex especially but also age, and size when predicting pubic symphysis morphology. If we consider the results of the second-best model, the need to consider pelvic size also becomes apparent.

Shape Variation

Our analyses confirms that the human pubic symphysis is sexually dimorphic much like other regions of the pelvis (Arsuaga & Carretero, 1994; Bookstein et al., 2003; Fischer & Mitteroecker, 2015; Kurki, 2011; Tague, 1992; Walrath & Glantz, 1996). The average female has a dorsoventrally narrower symphyseal surface shape compared to males across age and size. This corresponds to females having more gracile pubic bones which allows them to maximize the space of the birth canal (Standring, 2021; White & Folkens, 2005). The symphyseal widths which correspond to the shape of the cartilaginous symphysis are wider in females and the pubic tubercles are positioned farther from the midline in females because females have elongated pubic bones that in addition to the wider cartilage, contribute to the increases the width of the birth canal (Bruzek, 2002).

Most anthropological and forensic studies of the pubic symphysis have focused on the developmental and degenerative changes to the surface texture for the purposes of conducting adult age estimation (Brooks & Suchey, 1990; Chiba et al., 2014; Dudzik & Langley, 2015; Franklin, 2010; Gilbert & McKern, 1973; Lottering et al., 2014; Todd, 1920; White & Folkens, 2005). These past studies have all made a distinction between male and female changes on the symphyseal surface in relation

to age. Our results show that the sexual dimorphism attributed to the surface morphology also extend to the symphyseal outline. We can also see from the hypothetical shape models that the shape of the pubic symphysis varies with age with older individuals having narrow symphyseal widths and more pointed inferior borders across males and females which we propose is likely related to degenerative processes such as the ossification of the cartilaginous soft tissue. These observations support further geometric morphometric exploration of the pubic symphysis towards the goal of developing additional tools means of conducting both adult sex and age estimation.

Our best model indicates that changes to size have different impacts on older and younger adults. This could suggest that the continued growth of the pelvis into young adulthood continues to cause changes to pelvic shape, however as individuals enter their later years, there might be a slowdown on the change in size. The model also indicates that changes to size have different impacts on male and female symphyses, which is in step with the different developmental trajectories that male and female pelvises continue after puberty into young adulthood (Huseynov et al., 2016) . These include the changes we previously described that increase the width of the of the birth canal in female adults.

Predicting Fossil Shapes

The absence of soft tissue in the hominin fossil record coupled with the consistent poor preservation of pubic bones limits the ability of researchers to ascertain the true articulation of this anterior joint in many extinct hominins (Adegboyega et al., 2021; Karasik et al., 1998; Todd, 1920). In previous reconstructions, researchers have relied heavily on the sacroiliac articulation of the sacrum and the hipbones when orienting the pelvic bones. Most reconstructions have

left very little space for the pubic symphysis or have simply joined both pubic bones together (Adegboyega et al., 2021; Berge & Goularas, 2010; Bonmatí et al., 2010; Claxton et al., 2016; Häusler & Schmid, 1995; Schmid, 1983; Tague & Lovejoy, 1986). However missing information about sacroiliac joint cartilage thickness reduced the accuracy of hipbone placement thereby compounding pubic symphysis estimation error (Claxton et al., 2016; Li, 2002). Furthermore, damage to the auricular surfaces of the hip bones and the sacrum, introduces even more uncertainty to the orientation of the bones leading to potentially different reconstructions depending on the reconstructor's choices as was the case with the different reconstructions of the AL 288-1 pelvis (Häusler & Schmid, 1995; Lovejoy, 1979; Schmid, 1983). These issues have been more recently highlighted in Chapter 1 (Adegboyega et al., 2021) where pubic symphysis uncertainty contributed to different reconstructions and morphological interpretations of the same fossil pelvis. Our predictive model-based approach provides a more systematic means of inferring the shape of the pubic symphysis and we have shown that it can be done to different levels of accuracy depending on the data that is available to go into the model. We have shown that if we are able to estimate the sex and age of the individual, we can make decent predictions about their shape, additional information about their age and pubic symphysis or pelvic size, can be used to make even more accurate predictions when other means of inferring pubic symphysis shape are not viable. Applying this modeling approach to fossil hominins with well-preserved sacroiliac joints will help us assess the efficacy of this method on extinct species.

CONCLUSION

This study demonstrates the applicability of regression modelling, in predicting pubic symphysis morphology, and in elucidating patterns of pubic symphysis shape variation across various shape predictors. The results also support more geometric morphometric studies of this region, for the purposes of constructing robust quantitative models for age and sex estimation. Additionally, though researcher anatomical expertise is still required in fossil reconstruction, we have shown that a statistically driven approach could help to systematically predict the shape of missing soft tissue thereby reducing the subjectively involved in pubic symphysis articulation during pelvic reconstruction.

CHAPTER 2 TABLES AND FIGURES

Table 2.1. Landmarks and semilandmarks

Landmark	Definition	Type
1, 29	Apex of the anterior superior iliac spine*	b
2, 30	Most superior point on the iliac crest	b
3, 31	Apex of the posterior superior iliac spine*	b
4, 32	Apex of the posterior inferior iliac spine*	b
5, 33	Most inferior point of the arcuate line of the ilium	b
6, 34	Midpoint of the superolateral edge of the iliac tubercle	b
7, 35	Deepest point of the greater sciatic notch	b
8, 36	Point where the iliopubic ramus meets the arcuate line	b
9, 37	Apex of the ischial spine	b
10, 38	Most superior point of the ischial tuberosity	b
11, 39	Most inferior point of the ischial tuberosity	b
12, 40	Most superior point of the medial aspect of the pubic symphysis	b
13, 41	Most inferior point of the medial aspect of the pubic symphysis	b
14, 42	Most anterior point of the pubic tubercle	b
15, 43	Most anterior point of the obdurator foramen[†]	b
16, 44	Most superior point of the obturator foramen[†]	b
17, 45	Most posterior point of the obturator foramen[†]	b
18, 46	Point on the acetabulum margin corresponding to where ilium and superior pubic ramus meet[†]	b
19, 47	Point on the acetabulum margin furthest away from landmark 18	b
20, 48	Most inferior point on the anterior lunate surface of the acetabulum margin	b
21, 49	Point on the acetabulum margin furthest away from landmark 20	b
22, 50	Deepest point of the acetabular fossa	b

23	Most ventral point on the midline of the sacral promontory	m
24, 51	Most lateral point on the sacral body	b
25, 52	Apex of the sacral wing	b
26	Most dorsal point on the midline of the sacral body	m
27, 53	Most lateral point on the right sacral wing that falls on the Linea terminalis	b
28	Most caudal point on the midline of the sacral apex	m
54	Point on the midline of the sacrum between sacral vertebrae 3 and 4	m
55 – 82	Curve semilandmarks along the pubic symphysis	b

Abbreviations: b = bilateral landmark; m = midsagittal landmark.
* Weaver (2002) landmark definitions have been used.
† Betti et al. (2013) landmark definitions have been used.

Table 2.2. Best prediction models

| Model	First stage model formula	Second stage model formula	MSE
null	Shape ~ 1	NA	0.02696
M1	Shape ~ Sex	NA	0.02510
M2	Log pelvis centroid size ~ Sex	Shape ~ Sex * Log pelvis centroid size	0.02510
M3	Log pelvic breadth ~ Sex	Shape ~ Sex * Log pelvic breadth	0.02510
M4	Log pubic symphysis centroid size ~ Sex + Log age	Shape ~ (Sex + Log age) * Log pubic symphysis centroid size	0.02505
M5	Log pelvis centroid size ~ Sex + Log age	Shape ~ (Sex + Log age) * Log pelvis centroid size	0.02508
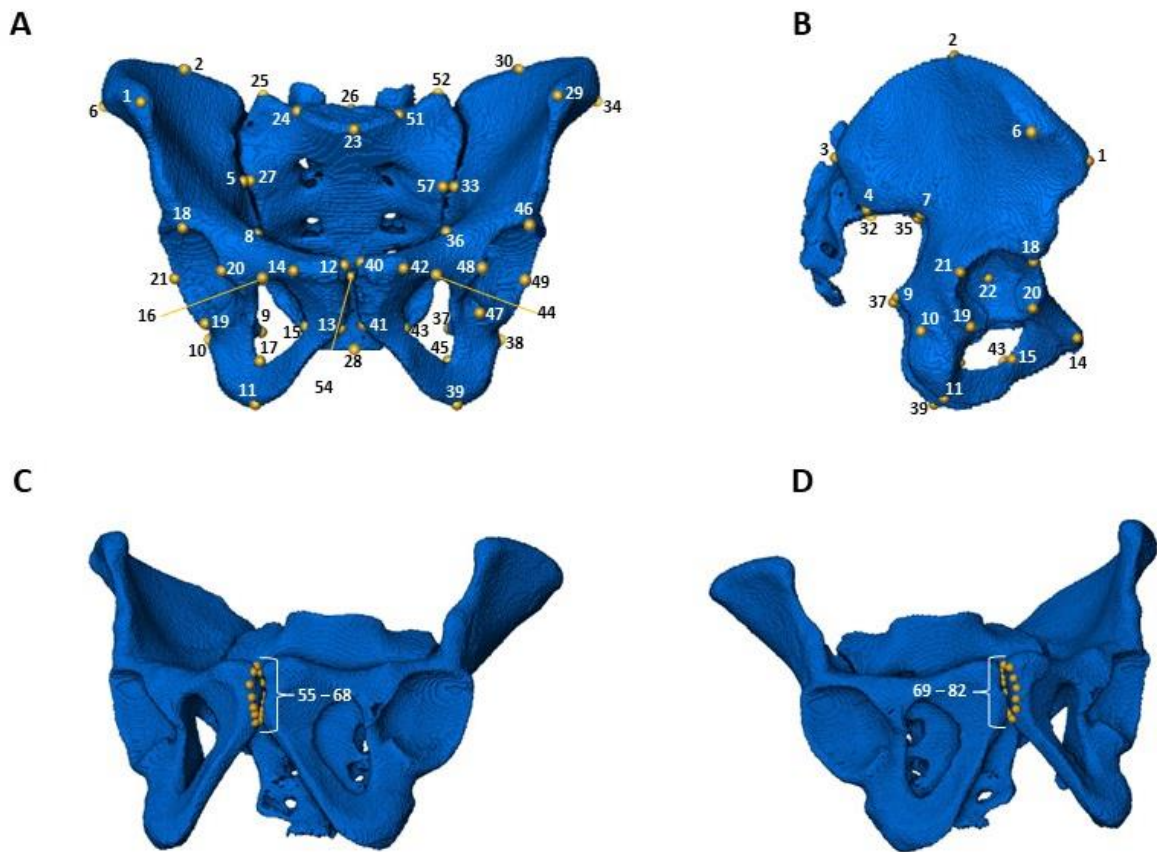
Figure 2.1. Landmarks and semilandmarks. Landmarks used in this study are show on a pelvis from the (A) anterior view, and (B) lateral view. The semilandmarks are show on the (C) right and (D) left pubic symphysis.
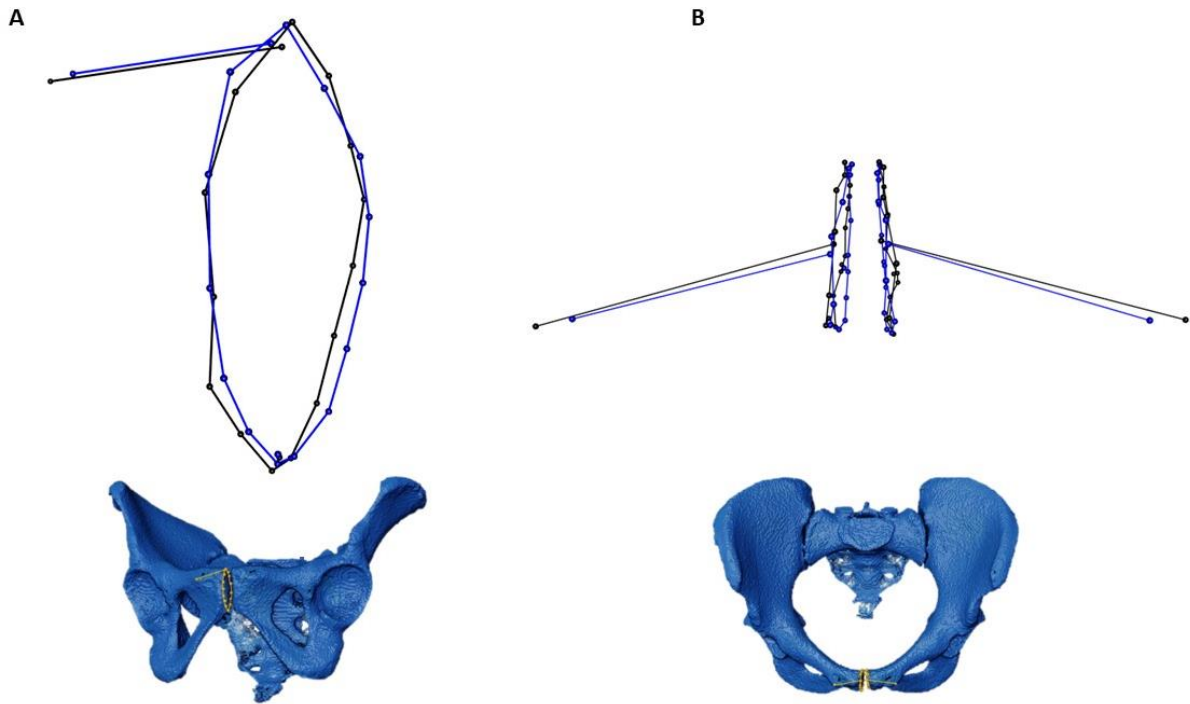
Figure 2.2. Observed vs predicted pubic symphysis shape contrast. (A) Contrast of an observed (black) and predicted (blue) right pubic symphysis face and pubic tubercle. (B) Contrast of the pubic symphysis in the superior view.
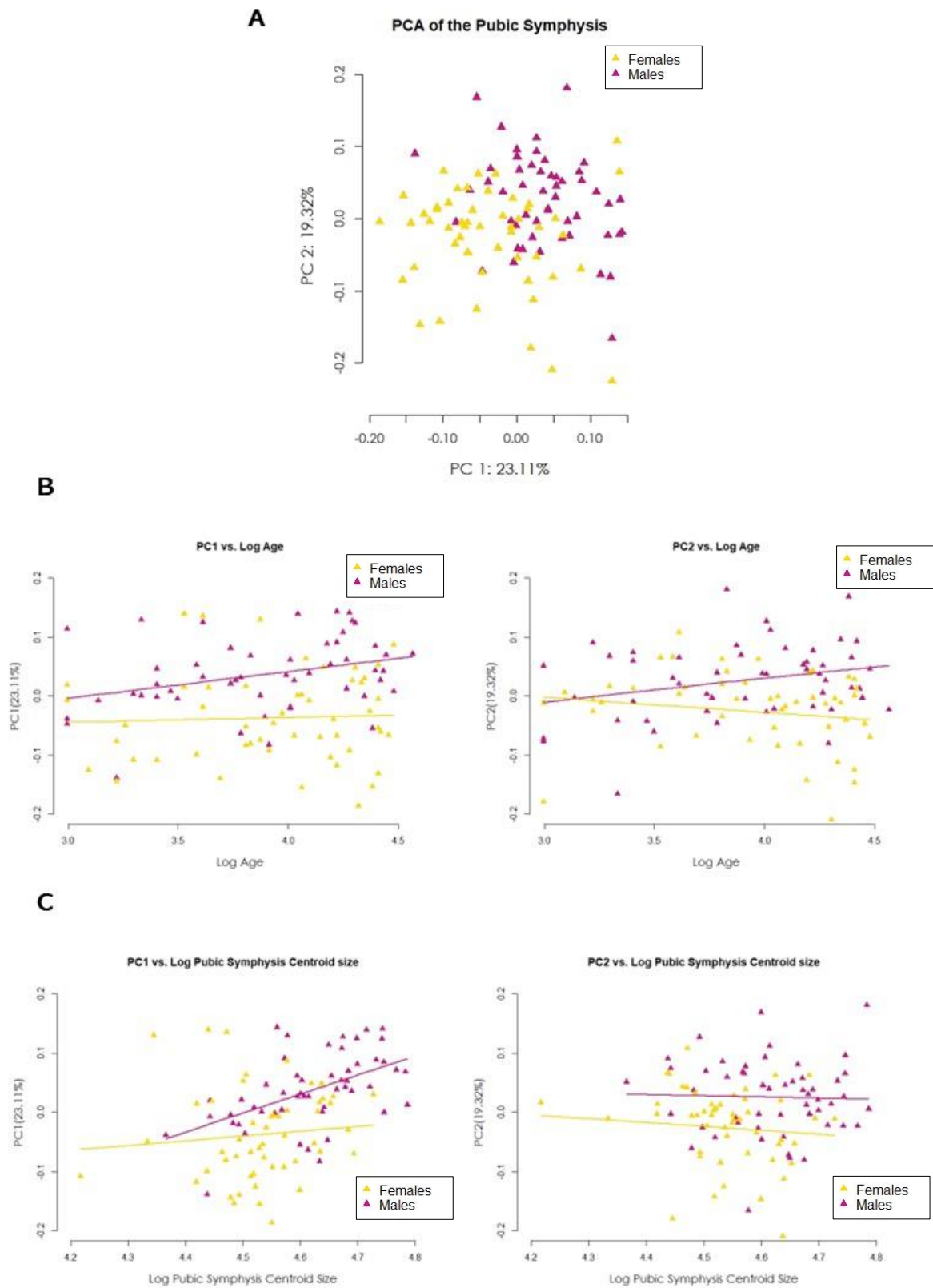
Figure 2.3. Principal components analysis of pubic symphysis shape. (A) PC1 and PC2, (B) PC1 and PC2 against age, and (C)PC1 and PC2 against log pubic symphysis centroid size.

Figure 2.4. Hypothetical predictions of pubic symphysis shape. The two rows depicts hypothetical predictions of pubic symphysis shape for adult females (top row) and adult males (bottom row) who are (A)&(E) young and small, (B)&(F) young and big, (C)&(G) old and small (D)&(H) old and big.

CHAPTER 3: PREDICTING THE POSITION OF HIP BONES WITHIN THE PELVIC GIRDLE: A CASE STUDY OF THE KEBARA 2 NEANDERTHAL
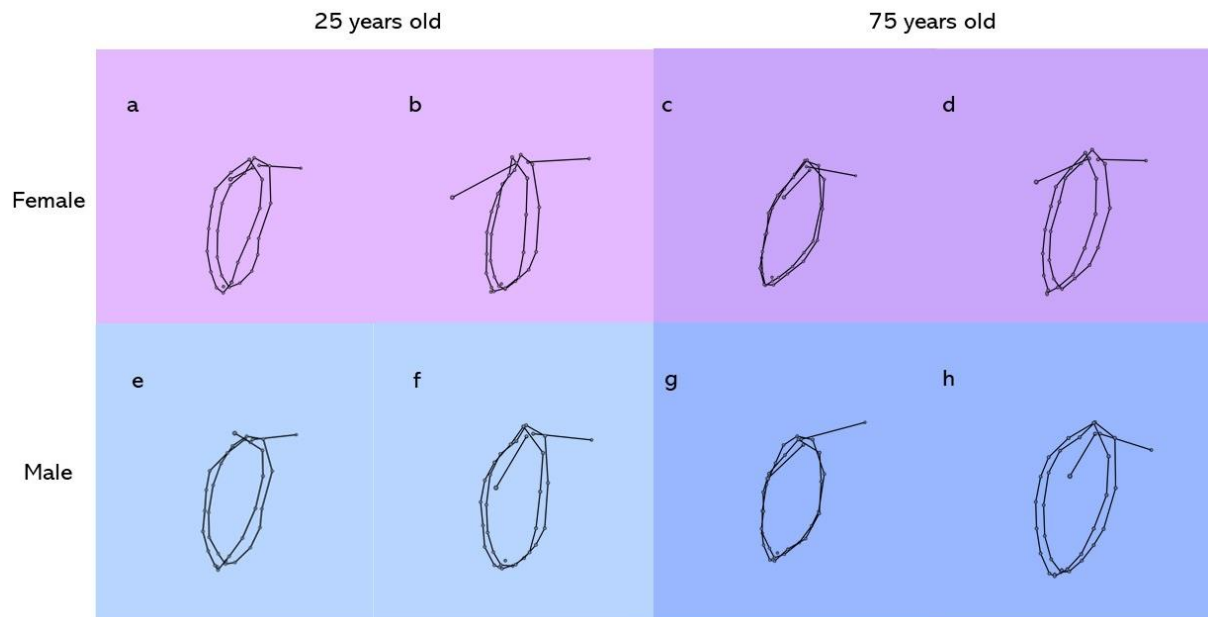
Authors: Mayowa T. Adegboyega, Mark Grote, Timothy D. Weaver

ABSTRACT

Hominin pelvises are particularly vulnerable to fragmentation and distortion during the fossilization process, which even in better preserved fossils, often leads to only one adequately preserved side and a sacrum that is missing or too fragmentary to help with positioning. Reconstructing a full pelvis, which is crucial for many functional or evolutionary interpretations, requires researchers to rely on their anatomical expertise therefore adding subjectivity to the process. The bilateral symmetry of the pelvis offers an opportunity to use one side to reconstruct missing data on the other side by predicting only a few quantities: the translations and rotations needed to transform a hip bone onto the location of its pair. In this study, we trained a statistical model to predict the location of the missing hip bone from the preserved hip bone of the other side without using the sacrum. To build this model, 44 landmarks and 72 curve semilandmarks were collected on a training sample of medical CT scans of 103 adults from throughout the University of California Health system. We trained a reduced rank regression (RRR) model to predict the translation and rotation values that would position each right hip bone on its left pair. Then, we applied the model to two reconstructions of the Kebara 2 Neanderthal pelvis and assessed how well the model predictions corresponded with the reconstructions. Our results showed that regression modelling based on a human training sample can be used to accurately predict 'missing' human hip bones and Kebara 2's left hip bone. We believe that this method can be employed in conjunction with a researcher's anatomical expertise and other reconstruction techniques to reduce subjectivity in fossil pelvis reconstruction.

INTRODUCTION

The bony pelvis is a basin shaped complex that consists of a pair of hip bones, a sacrum, and a coccyx. The hip bones articulate anteriorly at the pubic symphysis and posteriorly with the sacrum, which also articulates inferiorly with the coccyx (Standring, 2021). In the human body, the cavity formed by these bones protects and supports abdominal organs and functions as the birth canal in females. The shape of the cavity has undergone many changes through the evolution of the human lineage and these changes have impacted childbirth (Arsuaga et al., 1999; Gruss & Schmitt, 2015; Huseynov et al., 2016; Kappelman, 1996; Rosenberg, 1992; Rosenberg & DeSilva, 2017; Rosenberg & Trevathan, 2002; Ruff, 1995, 2010; Simpson et al., 2008; Stansfield et al., 2021; Tague & Lovejoy, 1986; Trinkaus, 1984; Walrath, 2003; Weaver & Hublin, 2009). Additionally, research has shown that the form and orientation of the pelvis has implications for thermoregulation (Holliday, 1997; Ruff, 1991, 1994, 1995, 2010; Weaver & Hublin, 2009; but see Simpson et al., 2008), posture, and locomotion (Bailey et al., 2019; Been et al., 2013, 2017; Lovejoy et al., 2009; Middleton et al., 2017; Lovejoy, 2005; Stern et al., 1983). In order to properly investigate the impact of the aforementioned pressures on pelvic shape, we need reliable fossils to include in future studies.

Existing pelvic reconstruction techniques

In the fossil record, the poor preservation of bones of the pelvis coupled with the absence of soft tissue limits researcher's abilities to ascertain the geometry of the pelvis in extinct hominins, limiting our understanding of evolutionary trajectories and processes. Researchers have often relied on the presence of a well-preserved sacrum that can confidently be articulated with what remains of the hip bones. Even with a sacrum, many reconstructions have had to utilize the bilateral symmetry of the

pelvis to mirror a reconstructed hemipelvis along the midsagittal line to form a full pelvic inlet (Adegboyega et al., 2021; Berge & Goularas, 2010; Claxton et al., 2016; Rak and Arensburg 1987). In the absence of a sacrum, Weaver & Hublin (2009) fit together the right and mirrored left-sided fragments by matching overlapping anatomy to create a more complete right hip bone and then estimated sacral and other missing anatomical landmarks before also mirroring the hemipelvis to create the left side. In these cases, either a sacrum or estimated sacrum was used to position the hip bones.

When the pubic symphysis is not preserved, a great amount of care must be taken to orient the reconstruction at the sacroiliac joint, as there is no other way to independently confirm that the hip bones have been angled correctly without the anterior constraints provided by the pubic symphysis (Claxton et al., 2016; Li, 2002). These issues are well highlighted in Adegboyega et al., (2021) where even in the face of a relatively well-preserved sacroiliac joint, the pubic symphysis uncertainty contributed to differences in the reconstructions and morphological interpretations of the Kebara 2 Neanderthal pelvis. In many cases however, the sacroiliac joint cannot be relied upon at all, either due to the poor preservation of the bones or to the complete absence of the sacrum. Under these conditions, the placement of the hip bones falls entirely on the estimated shape and size of the pubic symphysis which researchers use to complete the inlet anteriorly. In sum, previous pelvic reconstruction approaches rely on having or estimating a sacrum (see Weaver and Hublin, 2009) or on assumptions made about the pubic symphysis joint.

Existing approaches to missing data estimation

Both physical and virtual techniques have been employed in previous pelvis reconstructions however, virtual reconstruction methods are becoming more popular

due to their ability to minimize the risk of damage to already fragile fossil elements and allow for multiple reconstructions (Gunz et al., 2009; Weber & Bookstein, 2011; Zollikofer et al., 2005). One of the virtual techniques that have been growing in popularity is 3D geometric morphometrics (3DGM) largely due to its ability to be employed towards missing data estimation (Benazzi et al., 2009; Brassey et al., 2018; Gunz et al., 2009; Gunz & Mitteroecker, 2013; Mitteroecker & Gunz, 2009a; Schlager et al., 2018; Slice, 2005; Slice, 2007).

There are two main 3D GM methods for missing data estimation, which in principle we could use to estimate the form and orientation of the other hip bone. The first is thin-plate spline to predict the coordinates of the missing landmarks by deforming a reference sample to the target specimen with missing landmarks, but this method does not work well across joints because it relies on an assumption of a smoothly curving surface (Bookstein, 1989, 1992; Gunz et al., 2005; Mitteroecker & Gunz, 2009). The second is regression; this method does not have the problem of over smoothing, but it does not make use of the bilateral symmetry of the pelvis so every missing coordinate has to be individually predicted (Bookstein et al., 2003; Gunz et al., 2009).

The Kebara 2 Neanderthal pelvis

The Kebara 2 Neanderthal is a Levantine Neanderthal partial skeleton dated to ~60ka (Valladas & Valladas, 1991). The skeleton, which is presumed to have belonged to an adult male, has been crucial to our understanding of Neanderthal postcranial anatomy. For example, it has been used to represent Neanderthal body breadth and pelvic canal shape, which in turn have been used to understand Neanderthal climactic adaptation, birth mechanisms, infant head size, and other functions (Adegboyega et al., 2021; Been et al., 2010, 2017; Chapman et al., 2017;

García-Martínez et al., 2014; Gómez-Olivencia et al., 2009, 2013, 2017, 2018; Rak & Arensburg, 1987; Torres-Tamayo et al., 2020; Vandermeersch, 1991). The pelvis consists of a left hip bone, which is missing the pubis as far back as the root of the superior pubic ramus and the entire ischiopubic ramus, a right hip bone, which is fragmentary but ultimately relatively well preserved, and a sacrum, which is essentially complete although exhibiting some developmental anomalies and postmortem damage (Adegboyega et al., 2021; Duday & Arensburg, 1991; Rak & Arensburg, 1987; Trinkaus, 2018).

This pelvis has undergone several reconstructions using both physical and virtual methods. The first reconstruction by Rak and Arensburg (1987; see also Rak, 1991) was achieved by articulating a cast of the right half of the sacrum with a cast of the right hip bone to form a hemipelvis. The missing region of the pubis was reconstructed following the curvature of the Linea terminalis (i.e., the inlet rim) so the full pelvis was only visible when physically mirror imaged. Sawyer and Maley (2005) used the sacrum, right ilium, and ischium of Kebara 2 in conjunction with the left ilium and ischium from Feldhofer 1, and the pubis, from La Ferrassie 1 to build a complete pelvis but the composite nature of the reconstruction and the artistic license employed "in order to maintain symmetric continuity" make it difficult to assess (Torres-Tamayo et al., 2020). Adegboyega et al., (2021) applied virtual and physical reconstruction techniques to produce two reconstructions of the Kebara 2 pelvis. Virtual techniques were applied independently by two researchers to surface renderings generated from CT scans to realign misaligned fragments of the hip bones and sacrum based on the same general reconstruction protocol and each researcher's assumptions about how the fragments should be aligned. These techniques also allowed the researchers to create mirror images of the right hip bone and the right

half of the sacrum to create a new left side to replace the poorly preserved left side. Physical techniques were then used to articulate 3D printouts of the reconstructed elements, which in turn were used to articulate the virtual elements using landmarks data and image warping techniques to create two articulated virtual pelvic girdles that matched the physical replicas. Presenting more than one reconstruction allowed for the assessment of the assumptions and choices made by different researchers and how they impact the reconstructions the present. This process yielded two reconstructions with the most noticeable differences in the shape and size of the pelvic outlet. Some of these differences can be attributed to independent choices made by each researcher when aligning the bone fragments; however, some of them are also the result of different choices that were made when orienting the hip bones at the sacroiliac joint. This problem raises the need for more systematic methods that could be used to support researchers' anatomical expertise and reduce uncertainty in fossil pelvis reconstructions.

Study aims

We investigate whether the bilateral symmetry of the pelvis can be used to accurately predict the form and position of a hip bone from the hip bone of the other side. Specifically, we use reduced rank regression (RRR) to predict the translations and rotations needed to transform a hip bone onto the location of its pair. The novelty of this method is that unlike existing missing data estimation methods used in hominin fossil reconstructions, where the set of 3D coordinates of the missing elements are predicted, we only predicted the translation and rotational matrices that could transform one hip bone to the location of its pair on the other side. After evaluating the approach in living humans, we applied it to the two reconstructions of the Kebara 2 Neanderthal pelvis presented in (Adegboyega et al., 2021).

MATERIALS AND METHODS

Samples, data, and software

Data were collected from 103 adult humans ($n = 52$, males; $n = 51$, females) ranging between the ages of 20 to 96 years old who had undergone abdominal and pelvis computed tomography (CT) imaging between May 2019 and November 2020 through the University of California health system in California, USA. We obtained approval from the University of California, Davis Institutional Review Board to use these patient's data in this study. The scans were taken using one of the following medical CT scanners at slice thicknesses of $1 - 1.5$ mm: Siemens Somatom Definition DS 64, Siemens Somatom Definition AS 128, Siemens Somatom Sensation PCH 64 and the GE Light Speed VCT 64. Individuals who presented with injuries including but not limited to pelvic fractures, neuromuscular disorders, and pubic symphysis diastasis, or were identified as having undergone treatments in the past for pelvic injuries were not included in the study as these conditions might influence their pelvic shape.

The CT scans were imported as DICOM (.dcm) files into Avizo Lite 9 (FEI Visualization Sciences Group, 2015) where the skeletons were first segmented from soft tissue using automated density thresholding tools, and then the pelvic bones (the left and right hip bones and the sacrum) were manually segmented from the skeletons. 3D surface renderings for each segmented pelvis were generated in Avizo for use in the analyses. To test the predictive model on a pelvis outside of the *Homo sapiens* shape range, we used the surface renderings of the two Kebara 2 Neanderthal pelvis reconstructions (NR1 and NR2) reported in Chapter 1 (Adegboyega et al., 2021). The analyses were carried out in R using the following

packages: Morpho v 2.9 (Schlager et al., 2021), geomorph v 4.0 (Adams et al. 2021; Baken et al 2021), Directional v 5.3 (Tsagris et al., 2022), rrpack v 0.1-11 (Chen et al., 2019), and shapes v 1.2.6 (Dryden, 2021).

Landmarks and semilandmarks

Three-dimensional landmark and semilandmarks were collected on each pelvis in Avizo. A set of anatomical landmarks (Dryden & Mardia, 1998) were manually collected on the left and right hip bones to represent their forms and positions within the pelvic girdle; curve semilandmarks points were collected along the pubic crest, pectineal line, and the arcuate line of the inlet rim of both hip bones; and curve semilandmarks were collected along the margins of the articular surfaces of the bony pubic symphyses. Afterwards, the semilandmark sets were resampled in R (R CoreTeam, 2019) to ensure roughly equidistant homologous points for each individual (Gunz et al., 2005). The final count of semilandmarks was 72 semilandmarks; 22 semilandmarks along the inlet rim of each hip bone, making a total of 44 inlet semilandmarks per pelvis; and 14 semilandmarks along each pubic symphysis making a total of 28 symphysis semilandmarks per pelvis (Fig. 1; Table 1).

Superimposition

To begin our analysis, we designated the right hip bone as the predictor and the left hip bone as the target, i.e., the object whose position was to be predicted. We conducted our analysis in two stages, first training and testing the model on the human sample, and then testing the model on the NR1 and NR2. In both stages, we superimposed the hip bones in the sample with a Generalized Procrustes Analysis (GPA) of only the coordinates on the right hip bone to ensure that the shape data from the left side did not influence the features from the right side used for prediction, and to model a scenario whereby only the one hip bone is available. GPA

translates all the shapes to the origin, scales them to unit centroid size to remove size, and rotates them around the origin to minimize the sum of squared distances between them (Gower, 1975; Zelditch et al., 2012). During the GPA, the semilandmarks were slid to minimize the bending energy between each specimen and the Procrustes mean shape (Philipp Gunz et al., 2005; Schlager et al., 2021). Additionally, the centroid sizes for each right hip bone were retrieved after the scaling step. Centroid size is the measure of size used almost universally in geometric morphometrics and is calculated as the square root of the sum of squared distances of all the landmarks of an object from their centroid (Dryden & Mardia, 1998; Goodall, 1991; Klingenberg, 2016; Rohlf & Slice, 1990).

Preparing the predictors and targets

To prepare our predictor coordinates, we began by scaling up the Procrustes registered coordinates of our human right hip bones, by multiplying each coordinate by the centroid size of the hip bone. Then, we determined the transformation necessary to convert the right hip bone into the left side within each pelvic girdle. The transformation consists of 1) reflection: creating a mirror image of the right hip bone; 2) translation: moving the mirrored hip bone to the position of the observed left hip bone; and 3) rotation: turning the reflected hip bone to fit the orientation of the left hip bone (Fig. 2).

We relied on the bilateral symmetry of the pelvis to recreate the left hip bone from the right side. The first step of the transformation was to reflect the right hip bone in place to create a mirror image, i.e., a left hip bone. This was done by multiplying each hip bone's landmarks by a 3D reflection matrix through the y-z plane.

$$\mathrm{Ref}_x = \begin{pmatrix} -1 & 0 & 0 \\ 0 & 1 & 0 \\ 0 & 0 & 1 \end{pmatrix}.$$

Afterwards for each reflected right hip bone, we obtained the 3x1 translation and 3x3 rotation matrices that were needed to transform the reflected right hip bone to the location and orientation of the left hip bone. Because the reflected right and left hip bones do not have exactly the same form (i.e., the pelvis is not perfectly bilaterally symmetric), the location and orientation were defined as those that minimized the Procrustes distance between the reflected right hip bone and the left hip bone. The translation matrix contains the values that need to be added to the x, y, and z coordinates of reference (reflected right hip bone) to move it to the location of the target (left hip bone). The rotation matrix reflects the angles needed to position the target as the reference. We reduced the rotation matrix into three Euler angles which when combined with the translation matrix resulted in a single 6x1 transformation matrix for each individual. The six actions encoded in each individual's 6x1 transformation matrix are those needed to create a bilaterally symmetric left hip bone from a reflected right hip bone.

Predicting human left hip bones

Our goal was to build a model to predict the six actions from the landmark coordinates of a reflected right hip bone. There are p = 58 x 3 = 192 such coordinates, three (x, y, z) for each of the 58 landmarks and semilandmarks of a right hip bone. The sample matrix of predictors then has n = 103 rows, one for each individual, and 192 columns, therefore it is less than full rank. Standard least squares methods fail when n < p and we seek a numerically stable lower dimensional solution. Reduced Rank Regression (RRR; Izenman, 1975) is a standard tool for model fitting in such situations, conveniently implemented in the R library rrpack (Chen et al., 2019).

We began by centering and scaling the reflected right hip bone coordinates and six variables encoding the actions, so that all the variables had a mean of zero and a standard deviation of one. This prevents variables of a larger order of magnitude from having oversized influence on the reduced-rank solution. We chose a six-dimensional RRR model to reflect the fact that six distinct actions are being predicted.

Following model fitting, the predicted actions were returned to their original scales and then applied to the reflected right hip bones to predict the left side. Because RRR is computationally efficient, and the sample is relatively small, we were able to assess prediction error by explicit ("brute force") leave-one-out methods. In leave-one-out, each case is removed from the sample in turn, and a model fitted to the remaining cases is used to predict the held-out case. The six actions and subsequently the left hip bone are predicted for each individual in this way. This process produces unbiased out-of-sample prediction errors and faithfully mirrors the procedure for predicting a fossil specimen from a modern training sample.

Predicting the reconstructed left hip bones of Kebara 2

The next step was to test the fitted RRR model on NR1 and NR2. Because Kebara 2 is missing some of the pubic bone, we used the thin plate spline interpolation (Bookstein, 1989, 1992) to impute the missing landmarks and semilandmarks using the human training sample as a reference. We then slid the semilandmarks of the training dataset including a Kebara reconstruction and the newly constituted coordinates were Procrustes registered onto the human sample using only the right hip bone landmarks (as was done with the human training sample). The same process was carried out as before whereby all the hip bones were scaled back up to their original size after registration, the right hip bone was

reflected, the translation and rotation matrices needed to convert the reflected right hip bone were obtained, the predictors and responses were scaled, and the model was fit using RRR. As with the human training sample, the predicted transformations were returned to their original scales and then applied to the reflected right hip bones. Finally, leave-one-out was used to assess the model prediction errors.

Assessing model performance

To visually assess how well the model performed, we generated wireframe contrasts depicting predicted left hip bones and the observed left hip bones from the human training sample and for NR1 and NR2. We report a selection of the human predictions and both Kebara predictions here. We also used kernel density plots to compare the Euclidean prediction errors to those from a mean form model, and to the pairwise Euclidean distances between the human individuals in the sample. The first comparison assesses how much the prediction improves when information about the form of each individual's hip bone is included in the model. The second comparison assess how similar the predicted and observed forms are relative to the differences in pelvic form between the individuals in the sample. The error density for the mean form model was generated from the squared errors between each individual's prediction and the mean form of all the predictions, and the pairwise error density was generated from the Euclidean distances between all pairs of left hip bones. The Kebara 2 errors, which were the pairwise Euclidean distances between the model predictions and the observed forms for each reconstruction were marked on the density plots.

RESULTS

Comparison of predicted with observed hip bones

Wireframe contrasts of the observed and predicted left hip bones of two individuals in the human training sample are reported here. Overall, based on visual assessment, the prediction errors are low (Fig. 3.3); cases with the average prediction error are very close to their observed coordinates (Fig. 3.3A), and even the in the cases with higher prediction errors (Fig. 3.3B), the positioning is still quite similar. The Kebara 2 prediction errors are also low. NR1's prediction in particular is very close to its observed coordinates (Fig. 3.4) and NR2 which upon observation has a higher prediction error, is still very similar to its observed coordinates (Fig. 3.5).

Comparison of prediction errors

Kernel densities were plotted to further assess model performance. The plots (Fig. 3.6) depict Euclidean distances between the predictions and the observed forms. Fig 3.6A compares prediction errors between the RRR model, a mean shape model, and pairwise Euclidean distances among left hip bones of all the individuals in the sample.

The plot shows that the RRR model performs favorably (mean value = 102.52) in comparison to the mean shape model (mean value = 183.71) and the pairwise distances(mean value = 257.79). The prediction errors for the two Kebara reconstructions (NR1 =87.74; NR2 = 121.27; Fig 3.6B) are well within the error distribution of the training sample.

DISCUSSION

Novelty of the method

The two main 3D GM method for missing data estimation––thin-plate split and multivariate regression––both aim to predict the coordinates of each of the landmarks characterizing the missing part (Gunz et al., 2004; Gunz et al., 2009; Stelzer et al., 2018; Torres-Tamayo et al., 2020). Here, instead of predicting numerous landmark coordinates, we predict only six values that describe the actions needed to create a bilaterally symmetric left hip bone from a reflected right hip bone. By making use of the bilateral symmetry of the pelvis, our approach substantially reduces how many quantities need to be predicted and uses the relative positions of the landmarks on the preserved side to constrain the relative positions of the landmarks on the predicted side. This is similar conceptually to reflecting a partial cranium and fitting the reflection to the original (Gunz et al., 2009), except that our approach does not rely on having overlapping anatomy in the original and reflection.

Validity of the predictors

The human training sample used in this study was randomly selected from patient CT scans that were acquired from UC Davis health system medical records. We did not explicitly select a diverse set of individuals; however, according to the United States Census Bureau (2021) in the 2020 United States Census, the self-reported racial and ethnic makeup of California was very diverse. When Californians were asked to select all the racial groups they identified with, the reported racial makeup of the state was as follows: White 54.6%; Black 7.1%; Hispanic or Latino 39.4%; Asian 17.8%; American Indian and Alaska Native 3.6%; Native Hawaiian and Other Pacific Islander alone 0.9%; Some Other Race alone 31.6%; Two or More Other Races 14.6%. Because the data derive from health centers in California, we are

confident that the that the individuals in our sample reflect a broad range of population histories and thus our sample reflects a significant portion of global pelvic form variation.

Nonetheless, this study is based on predictive models that were trained exclusively on present-day humans, therefore an implicit assumption of our approach when it is applied to a Neandertal hip bone is that Neanderthals had similar relationships between hip bone form and positioning as in humans which may not be the case. While Neanderthal and human pelvises share many traits, the Neanderthal pelvis retains more ancestral traits like having more flared iliac blades, a mediolaterally wider inlet, and longer pubic bones (Adegboyega et al., 2021; Arsuaga et al., 1999; Ponce de León et al., 2008; Rak & Arensburg, 1987; Rosenberg, 2007; Weaver & Hublin, 2009). These morphological differences could be associated with different relationships between hip bone form and positioning. Nevertheless, our model predictions for Kebara 2 were largely consistent with the reconstructions presented by Adegboyega et al., (2021) who used the sacrum to position the hip bones, suggesting if there were different relationships in human and Neandertals, the difference were not great enough to bias predictions based on Neandertal hip bones. To expand our approach to making predictions for a wider range of hominin taxa, for example, Pliocene hominins such as *Ardipithecus* or *Australopithecus*, the inclusions of a variety of extant hominoids might be necessary as a human training sample alone might not be sufficient for characterizing the relationships between hip bone form and positioning (Lovejoy et al., 2009; White et al., 2015).

We selected the Kebara 2 pelvis for this study because unlike other Neandertal pelvic remains that require extensive reconstruction, e.g., Tabun C1 (Ponce de León et al., 2008; Weaver and Hublin, 2009), the well preserved Kebara 2 pelvis retains a

substantial portion of the anatomy. This means that the uncertainty that is commonly associated with pelvis reconstruction is reduced with Kebara 2, making it a suitable fossil specimen with which to test this predictive method.

Assessing model performance

The results of our study show that within humans and Neandertals, it is possible to accurately predict hip bones within a pelvic girdle by using a transformed 'present' side as a replacement for the 'missing' side. When we compared the Euclidean errors from our model to errors from a mean form model, the errors from the RRR model were substantially lower. The errors were also small relative to between individual variation in pelvic form. We were able to observe this visually with the wireframe contrasts which showed that in both the human sample and Kebara 2, the model positioned and oriented the predictions with very little error. Because the pelvis is not perfectly bilaterally symmetrical some of the prediction error being captured is differences between the sizes and shapes of the left and right sides. We considered symmetrizing the pelvises in the training sample, which would have reduced the prediction errors; however, we thought it was important to report the more realistic expectation of this method to highlight the natural asymmetry that is lost in the mirroring process of most pelvic reconstructions and thus capture the total error expect when this method is applied to a real fossil context.

We also noticed that the pairwise comparison between the predicted and observed for Kebara 2 yielded a lower prediction error for NR1 (87.74) than for NR2 (121.27). Furthermore, when compared to the human mean prediction error (102.52), NR1's prediction error was closer to the mean than NR2. This disparity might be the result of the different anatomical assumptions that were used to complete each reconstruction. It is possible that the lower prediction error for NR1

means that NR1 should be preferred, but because we do not have the true Kebara pelvis to compare to, we hesitate to draw this conclusion. Because the model performed better when predicting NR1 over R2, it is tempting to suggest that the first reconstruction is more valid however, because there is no true Kebara pelvis to compare our results to and the Neanderthal pelvic fossil space is sparse we cannot reliably make this assessment, however this does suggest that statistical shape analysis could be employed to assess and validate reconstructions of a specimen, if enough representations from that species become available to make confident assertions about patterns of shape variation.

As was mentioned above, this method has the potential to be applied more broadly to other hominin pelvises and to other bilaterally symmetric anatomical structures given that good reference samples are selected and the associations and covariations between those structures is well understood (Gunz et al., 2009; Stelzer et al., 2018; Torres-Tamayo et al., 2018). If applied appropriately, predictive method such as the one described here can provide statistical support to more manual or subjective reconstruction processes thereby reducing interobserver error in fossil pelvis reconstructions.

CONCLUSION

In this study, we used reduced rank regression analysis to predict the translation and rotation values need to transform a human right hip bone to the left side. By also testing the method on the Kebara 2 pelvis, we showed that this method could be used to reconstruct the pelvises of Neanderthals, and potentially other members of the genus *Homo*. This work contributes to the growing application of 3D GM to predicting missing aspects of fossil morphology. In this study, we were able to

uses regression analysis to recreate 'missing' hip bones within our human sample, but even more encouragingly, the model was also able to predict make an accurate prediction in a Neanderthal. The method we have proposed here aims to reduce subjectivity in hominin pelvis reconstructions through the application of statistical predictions to systematically constrain the placement of hip bones even without the presence of a sacrum or other anatomical references and reduce the reliance of researcher's individual anatomic presumptions. We would like to emphasize that this method does not replace physical or other virtual reconstruction techniques, but rather, it can help to support these other methods by constraining areas of uncertainty.

CHAPTER 3 TABLES AND FIGURES

Table 3.1. Landmarks and semilandmarks

Landmark	Definition
1, 23	Apex of the anterior superior iliac spine*
2, 24	Most superior point on the iliac crest
3, 25	Apex of the posterior superior iliac spine*
4, 26	Apex of the posterior inferior iliac spine*
5, 27	Most inferior point of the arcuate line of the ilium
6, 28	Midpoint of the superolateral edge of the iliac tubercle
7, 29	Deepest point of the greater sciatic notch
8, 30	Point where the iliopubic eminence meets the arcuate line
9, 31	Apex of the ischial spine
10, 32	Most superior point of the ischial tuberosity
11, 33	Most inferior point of the ischial tuberosity
12, 34	Most superior point of the medial aspect of the pubic symphysis
13, 35	Most inferior point of the medial aspect of the pubic symphysis
14, 36	Most anterior point of the pubic tubercle
15, 37	Most anterior point of the obdurator foramen[†]
16, 38	Most superior point of the obturator foramen[†]
17, 39	Most posterior point of the obturator foramen[†]
18, 40	Point on the acetabulum margin corresponding to where ilium and iliopubic ramus meet[†]
19, 41	Point on the acetabulum margin furthest away from landmark 18
20, 42	Most inferior point on the anterior lunate surface of the acetabulum margin
21, 43	Point on the acetabulum margin furthest away from landmark 20
22, 44	Deepest point of the acetabular fossa
45 – 72	Curve semilandmarks along the pubic symphysis
73 – 116	Curve semilandmarks along the Linea terminalis of the hip bone

All landmarks are bilateral.
* Weaver (2002) landmark definitions have been used.
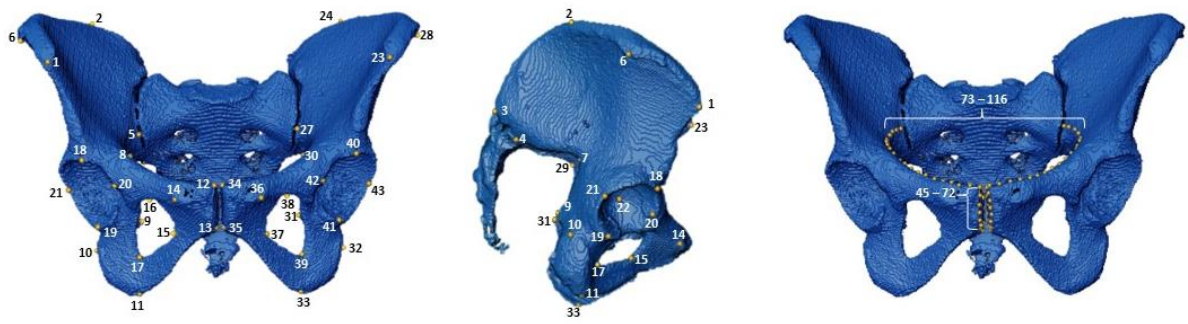† Betti et al. (2013) landmark definitions have been used.

Figure 3.1. Landmarks and semilandmarks. Landmarks and semilandmarks used in the study are shown is the anterior view (A), lateral view of the left side (B), inferior view (C).
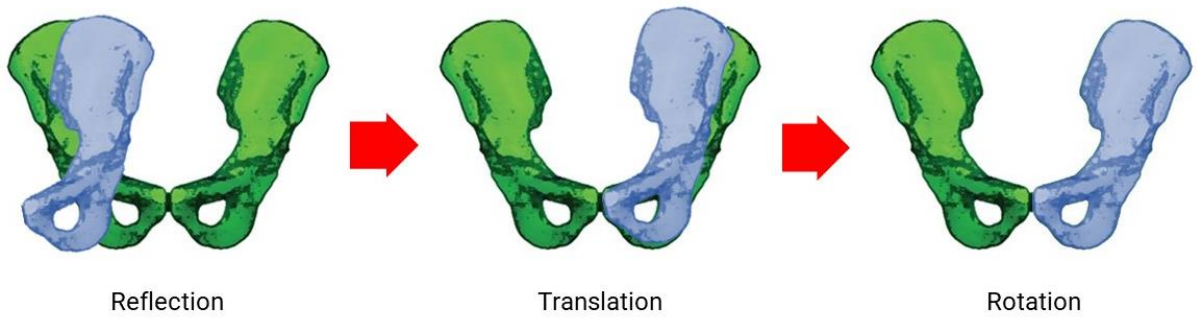

Figure 3.2. Transformations. A graphical representation of the reflection (left), translation (middle), and rotation (right) need to transform the right hip bone to the left hip bone.
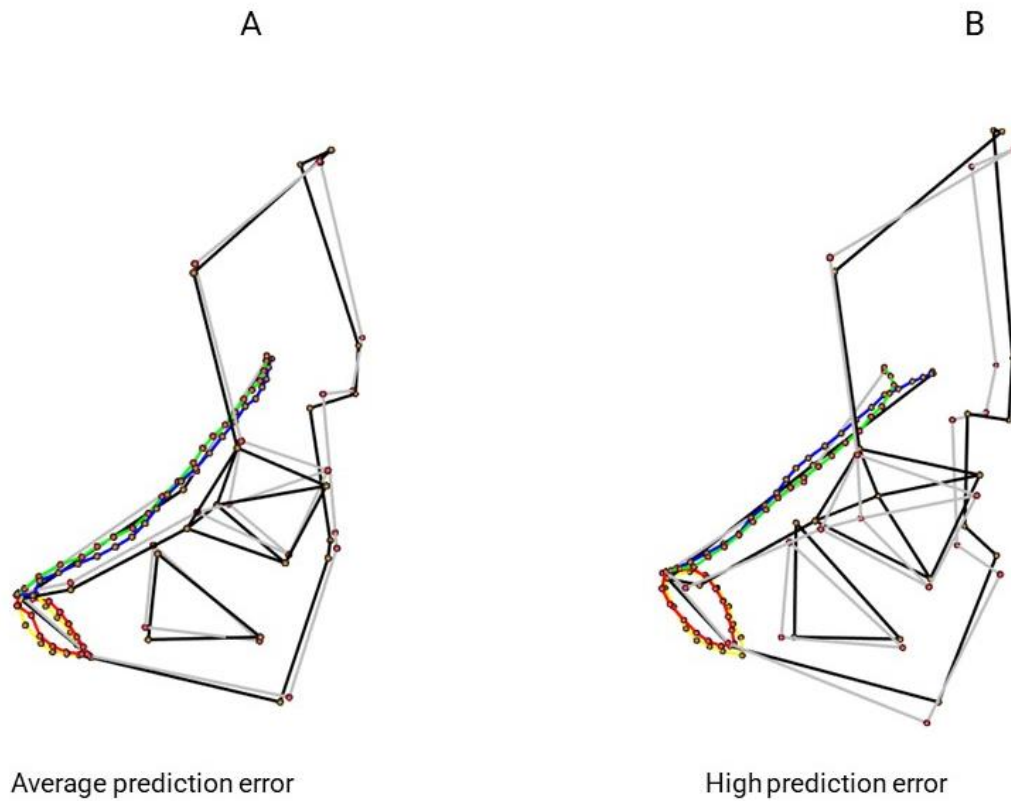
Figure 3.3. Human prediction contrasts. Contrasts of predicted vs. observed left hip bones from the human training set of an individual with a prediction error close to the mean (A), and an individual with a high prediction error (B). The hip bone is black (observed) and grey (predicted); the Linea terminalis is in blue (observed) and grey (predicted); and the pubic symphysis is yellow (observed) and red (predicted). Both predictions are very close to their observed coordinates however, (A) is slightly more medially positioned and (B) is more anterolaterally positioned.
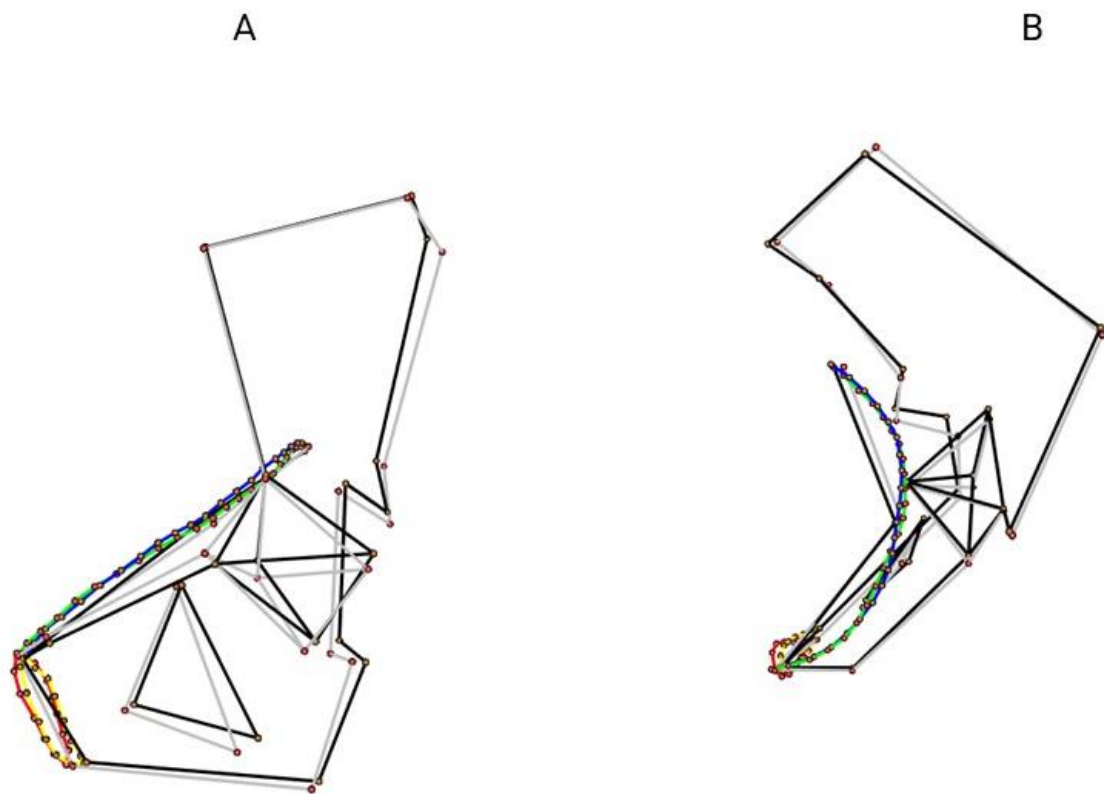
Figure 3.4. Kebara new reconstruction 1 prediction contrasts. Contrasts of the predicted vs. observed left hip bones of the Kebara pelvis reconstruction 1 made by Adegboyega et al. (2021). The hip bone is black (observed) and grey (predicted); the inlet rim is in blue (observed) and grey (predicted); and the pubic symphysis is yellow (observed) and red (predicted). The predictions is very close to their observed coordinates however, it is slightly tilted upwards in the sagittal plane from the center so that the posterior ends of the obdurator foramen and the acetabulum are more anteriorly positioned.
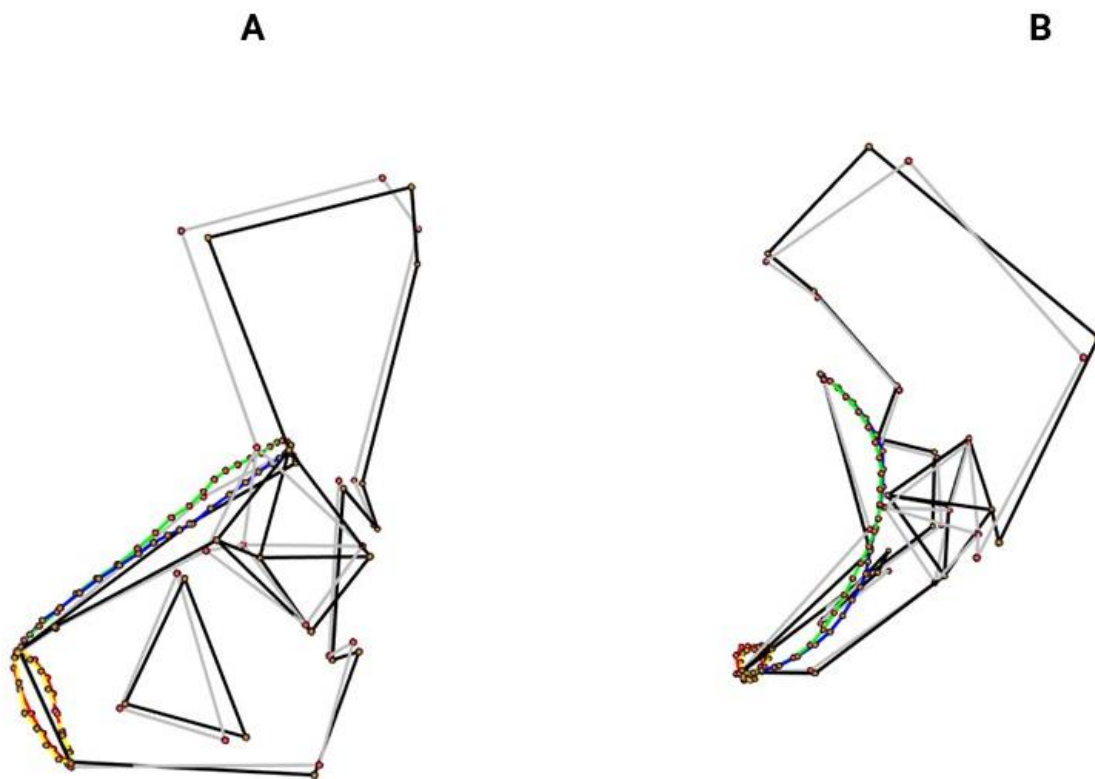
Figure 3.5. Kebara new reconstruction 2 prediction contrasts. Contrasts of the predicted vs. observed left hip bones of the Kebara pelvis reconstruction 2 made by Adegboyega et al. (2021). The hip bone is black (observed) and grey (predicted); the inlet rim is in blue (observed) and grey (predicted); and the pubic symphysis is yellow (observed) and red (predicted). Though the prediction is not as close to the observed coordinate as with NR1 (more anterosuperiorly positioned and more medially rotated than the observed), it is still very close.
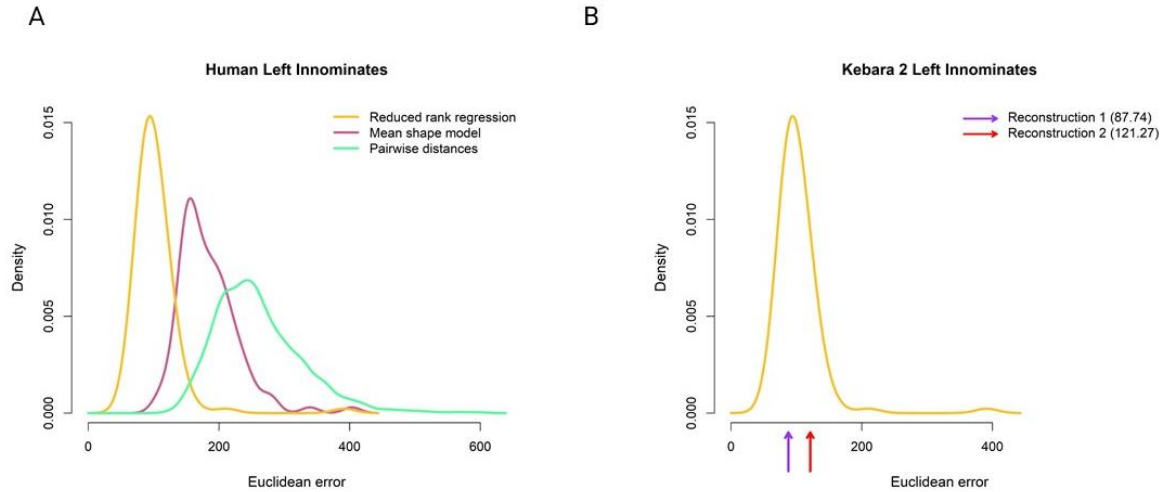
Figure 3.6. Left hip bone prediction error density plots. (A) A density plot showing the distribution of Euclidean leave-one-out prediction errors from the Reduced Rank Regression model (in gold) compared to a distribution of Euclidean distances between each individual and the mean shape (in pink), and finally, the distribution of Euclidean distances between each pair of individuals in the training sample (in green). (B) The model prediction errors for the Kebara 2 reconstructions compared to the leave-one-out prediction errors.

CONCLUSION

The overarching goal of this project was to develop solutions to some the challenges to anthropological study that arise from of an incomplete human fossil record. Fragmentation, complete disintegration, and the loss of soft tissue have long restricted our understanding of the human past and because there is no way to prevent these processes, or to predict the location of every fossil in the fossil record, the next best option is to be able to extract more information about human evolution from the current array of fossil specimens. Hominin pelvises are notoriously scarce but immensely important to our understanding of the evolution of human anatomy and behavior. With the help of virtual anthropological techniques including 3D imaging and 3D geometric morphometrics, we were able to learn more about this critical bony complex.

The two new reconstructions of the Kebara 2 pelvis (Chapter 1) allow us to visualize more accurate representations of Kebara's pelvis specifically, and Neanderthal morphology in general. As a result, future studies will be better equipped to clarify the evolutionary processes that shaped their body plans and how they compare to the processes that led to *Homo sapiens* morphology. The differences between these reconstructions raises the issue of reconstructor bias and they highlight how much individual choices can impact the final fossil morphology. In the subsequent studies, human samples and Kebara 2 were analyzed to clarifying how pelvic bones are oriented in relation to one another. The analysis of the pubic symphysis joint (Chapter 2) showed that symphyseal shape can be predicted with regression modelling and revealed systematic patterns of variation along age, sex and size. One obvious application of this method is to use it to estimate the spacing of this joint not just in Kebara, but in other fossil reconstructions; an aspect that has been

largely ignored in previous attempts at reconstituting hominin pelvises. The following study (Chapter 3) in which we predicted the position of hip bones within the pelvis further emphasizes the utility of regression modelling for inferring the association of pelvic bones. We exploited the pelvis' bilateral symmetry to develop a novel method whereby we only predicted the actions needed to transform one side into the other thereby reducing the number of variables to be predicted. This model presents a new opportunity to create a missing side of the pelvis from a single and even fragmentary fossil hip bones even when the sacrum is unavailable to properly orient disarticulated hip bones in relation to one another. It can also be used in cases where both hip bones are present to properly orient them to visualize the pelvic inlet.

There is room to develop upon the analyses we have conducted herein to create even better hominin pelvis reconstructions. For example, we hope that by creating more than one Kebara 2 pelvis, we help to promote the practice of testing out different configurations and assessing reconstruction accuracy to arrive at the best version or versions of any individual specimen. Using the different statistical models discussed in this work alongside other data estimation techniques and the findings of other shape variation studies, also has the potential to help us create even more accurate and complete hominin pelvis reconstructions. The models we present here can also be improved upon. By assessing other factors that could potentially be influencing the shape of the pubic symphysis such as childbirth and population history, we could uncover even better models for predicting symphyseal shape. Also, by expanding our training sets to include earlier hominins and extant hominoids, we could likewise expand the range of hominins for whom we can make accurate morphological predictions about.

We have been able to demonstrate that virtual anthropology is an effective suite of tools to help improve fossil reconstructions. More studies and innovation in this area could revolutionize our ability to look into the past to understand the evolution, patterns or variation, and lifeways of our ancestors and this in turn will help us to better understand who we are today, and where we might be headed in the future.

SUPPLEMENTARY TABLES AND FIGURES

CHAPTER 1: VIRTUAL RECONSTRUCTION OF THE KEBARA 2 NEANDERTAL PELVIS

Supplement S1.1. Reconstructions

<u>New Reconstruction 1</u>

    This reconstruction was done by the first author (M.T.A.). CT scans of the right hipbone and the sacrum were generated with a Bio Imaging Research (BIR) ACTIS 225/300 industrial CT scanner from the Max Planck Institute for Evolutionary Anthropology (Leipzig, Germany) and imported as tagged image files (TIFF) into Avizo Lite 9 (Thermo Fisher Scientific, Waltham). The CT data have a resolution of 0.09 mm and 0.08 mm for all dimensions for the hipbone and sacrum respectively. Each fragment that comprised the right hipbone and the sacrum was identified and segmented into individual surface renderings and labeled Surface 1–39 for the hip bone and Surface 1S–4S for the sacrum (Supplement 3). The segmentation process involved visually inspecting each slice of the virtual volume rendering in the X, Y, and Z planes in the segmentation editor in Avizo. We used the tools of the segmentation editor to manually separate bone fragments into individual surface renderings based on visual identification of the borders of each piece. We separated bone from sediment in a similar manner, relying on visual observations of the difference in densities between the bones and the sedimentary matrix. The initial goal was to correct the misalignment at the ischiopubic ramus, which was identified by Ruff (1995) and discussed by Weaver and Hublin (2009); however, other areas where fragments were misaligned were identified on the pubis, and at the internal wall of the acetabulum. The steps of the reconstruction were as follows. Surface 4, which makes up part of the pubic ramus, was rotated and translated so that its inferodorsal margin was flush with that of Surface 2. These two surfaces were merged and renamed Surface Pubis, so that subsequent translations would apply to

them as a unit (Supplement s4). Surface Pubis was then translated anteriorly and rotated superiorly so that its inferodorsal margin was flush with Surface 1, so that the inferior border of the obturator foramen was also straightened, revealing the gentle curve of the interior margin of the hip bone (Fig. 1.3B). The rest of the surfaces making up the pubic region (Surfaces 6, 10, 23, 24, 25, 26, 27, 28, and 39) were adjusted to be flush with Surface Pubis on the internal wall. The steps taken thus far disconnected the superior pubic ramus such that it now hung posteriorly to the pubic region, so fragments comprising the superior pubic ramus (Surfaces 5, 8, 9, 14, 15, 34, 36, 37) were each rotated superiorly and translated anteriorly to align them. The fragments that made up the ischium (Surfaces 3, 7, 11, 12, 13, 16, 17, 18, 19, 20, 21, 29, 30, 31, 32, 33) were determined to not have undergone any significant displacement so they remained in their original positions. Surfaces 22 and 35 of the acetabulum were adjusted slightly to align with the other surfaces of the ischium and the superior pubic ramus. Further adjustments were made to Surfaces 15 and 37 of the superior pubic ramus to ensure that all margins continued seamlessly. The ilium (Surface 38) was fit to the rest of the pelvis, and for the final step, all the surfaces of the right hip bone were merged into a single surface.

Surface 3S of the sacrum was rotated anterosuperiorly to close the gap created by the unfused sacral bodies (Surfaces 2S and 3S). Surface 4S was then translated anteriorly with the goal of improving the alignment of the ventral body and both sacral alae. Because of the sacrum's asymmetry, we could not make precise alignments between the surfaces; instead, we selected for the best compromise between the three. Finally, Surface 1S was aligned to fit on the rest of the sacrum, and all of the sacral surfaces were merged into a single surface.

The ventral margins of the right hip bone and sacral auricular surfaces (on Surface 2S) were well preserved, so we used them to guide the articulation of the sacrum and

hip bone. Once we achieved satisfactory alignment, the two surfaces were merged

and then mirrored along the sagittal midline of the sacrum. We determined the

position of this line by finding the center of the apex (half of the sacral base width)

and the base (half of the sacral base width) of the sacrum and drawing a line that

connected them. The true left sides of the sacra were removed, and the final complete

pelvis was merged.

New Reconstruction 2

Instructions provided to P.A.S.:

      The segmented surfaces created by the first author (M.A.) for NR1 were

provided to another author (P.A.S.) for use in creating NR2. Groups of fragments

that would need to be translated together such as Surface Pubis, Surface Ischium,

and Surface superior pubic ramus (Supplement S2) were premerged, but P.S. was

provided with instructions on how to separate them into individual fragments if

needed. Because P.S. had no previous interaction with the specimen, some

instructions were provided to guide him during the reconstruction process. These

instructions identified the problem areas and general information on the directions

to move the fragment in, but P.S. was also instructed to deviate from these

suggestions whenever he felt it was necessary. No numerical translation data were

provided. Assembling the full pelvis was performed as in NR1.

Differences between New Reconstruction 1 and New Reconstruction 2:

      Most of the steps taken for NR2 followed the steps taken for NR1; however,

there was a significant difference between the reconstruction of ischiopubic ramus in

NR1 and NR2. While in NR1 the pubis was rotated anteriorly to align with Surface 1

(at the center of the ischiopubic ramus) and Surface Ischium; in NR2 the ischiopubic

ramus was adjusted to be a straight line between Surface 2 (the most anterior fragment of the pubis) and Surface Ischium. This resulted in the observed difference between the maximum anteroposterior length of the pelvic canal where NR1, whose pubic bone was moved more anteriorly, has a longer maximum anteroposterior length than NR2, whose pubic symphysis remained largely in the same position. In the sacrum of NR2, Surface 3S is rotated so that a slight gap is still visible between the S2 and S3 sacral vertebrae. This decision was made to account for the intervertebral cartilage that would have present between unfused vertebrae. No such gap was left in NR1. The result is a more ventrally curved sacrum and thus a more anteriorly positioned outlet in NR1 than in NR2.

Supplement S1.2. Surface Groups List Used for the NR2 Reconstruction

Surface groups	Surface numbers
Surface 1	1
Surface 4	4
Surface 22	22
Surface 35	35
Surface 38	38
Surface Ischium	3, 7, 11, 12, 13, 16, 17, 18, 19, 20, 21, 29, 30, 31, 32, 33
Surface Pubis	2, 6, 10, 23, 24, 25, 26, 27, 28, 39
Surface Superior pubic ramus	5, 8, 9, 14, 15, 34, 36, 37
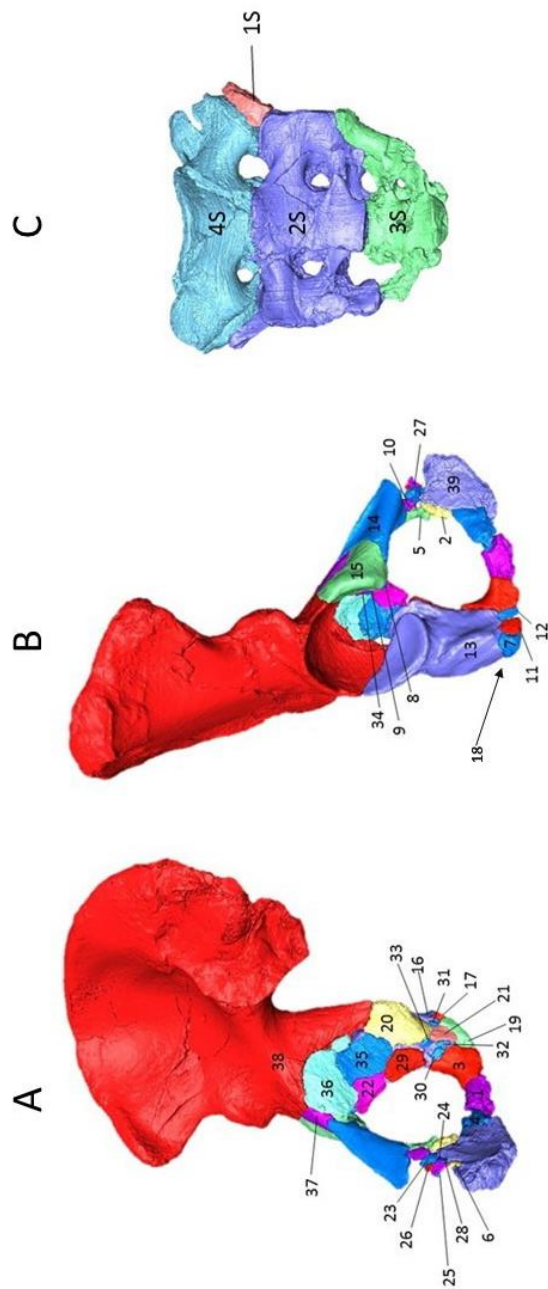
Supplement S1.3. Numbered Surface Renderings of the Right Hip Bone and Sacrum. The hip bone is shown in medial (A) and lateral (B) views. The sacrum is shown in anterior view (C). The different colors of the surface renderings indicate independently segmented fragments. One of the fragments (fragment 18) is not visible. Fragment 18 is wedged between fragments 13, 17, and 19, and its approximate position is indicated by the arrow.
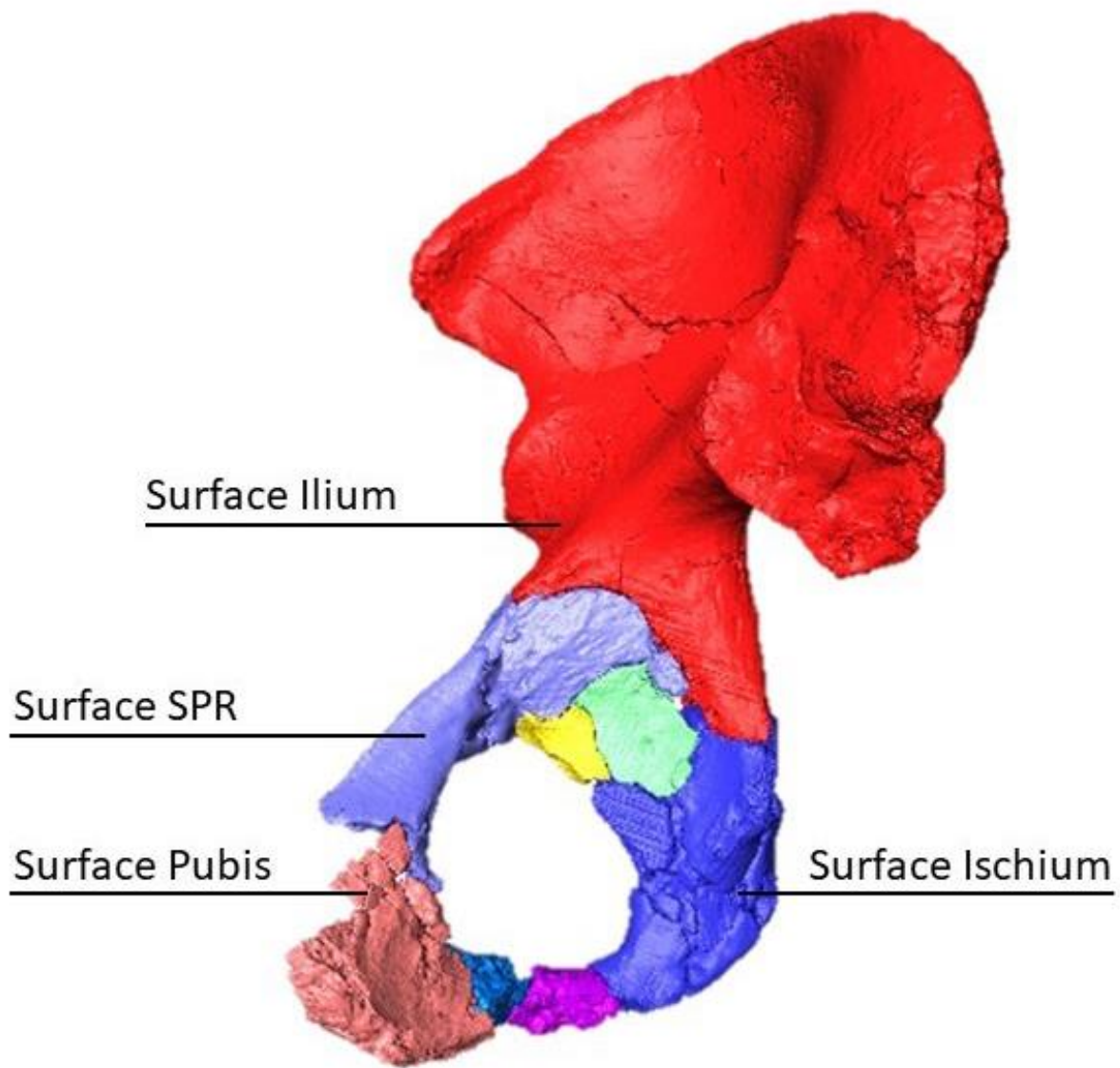
Supplement S1.4. Surface Groups on the Right Hip Bone. The different colors represent groups of surface renderings used in the New Reconstruction 2. These groups correspond to the list in Supplement S2.

CHAPTER 2: VARIATION IN THE SHAPE, SIZE, AND SPACING OF ADULT HUMAN PUBIC SYMPHYSES

Supplement S2.1. Full List of Regression Models

| Model	First Stage Model Formula	Second Stage Model Formula	MSE
null	Shape ~ 1	NA	0.02696
M1	Shape ~ Sex	NA	0.02510
M2	Shape ~ Sex + Log age	NA	0.02516
M3	Shape ~ Sex * Log age	NA	0.02524
M4	Log pubic symphysis centroid size ~ Sex	Shape ~ Sex + Log pubic symphysis centroid size	0.02510
M5	Log pubic symphysis centroid size ~ Sex	Shape ~ Sex * Log pubic symphysis centroid size	0.02510
M6	Log pubic symphysis centroid size ~ Sex + Log age	Shape ~ Sex + Log age + Log pubic symphysis centroid size	0.02516
M7	Log pubic symphysis centroid size ~ Sex + Log age	Shape ~ (Sex + Log age) * Log pubic symphysis centroid size	0.02505
M8	Log pubic symphysis centroid size ~ Sex * Log age	Shape ~ Sex * Log age + Log pubic symphysis centroid size	0.02524
M9	Log pubic symphysis centroid size ~ Sex * Log age	Shape ~ Sex * Log age * Log pubic symphysis centroid size	0.02518
M10	Log pelvis centroid size ~ Sex	Shape ~ Sex + Log pelvis centroid size	0.02510
M11	Log pelvis centroid size ~ Sex	Shape ~ Sex * Log pelvis centroid size	0.02510
M12	Log pelvis centroid size ~ Sex + Log age	Shape ~ Sex + Log age + Log pelvis centroid size	0.02516
M13	Log pelvis centroid size ~ Sex + Log age	Shape ~ (Sex + Log age) * Log pelvis centroid size	0.02508

M14	Log pelvis centroid size ~ Sex * Log age	Shape ~ Sex * Log age + Log pelvis centroid size	0.02524
M15	Log pelvis centroid size ~ Sex * Log age	Shape ~ Sex * Log age * Log pelvis centroid size	0.02513
M16	Log height + Weight ~ Sex	Shape ~ Sex + Log height+ Log weight	0.02554
M17	Log height + Weight ~ Sex	Shape ~ Sex * (Log height+ Log weight)	0.02615
M18	Log height + Weight ~ Sex + Log age	Shape ~ Sex + Log age + Log height+ Log weight	0.02558
M19	Log height + Weight ~ Sex + Log age	Shape ~ (Sex + Log age) * (Log height+ Log weight)	0.02688
M20	Log height + Weight ~ Sex * Log age	Shape ~ Sex * Log age + Log height+ Log weight	0.02565
M21	Log height + Weight ~ Sex * Log age	Shape ~ Sex * Log age * (Log height+ Log weight)	0.02765
M22	Log pelvic breadth ~ Sex	Shape ~ Sex + Log pelvic breadth	0.02510
M23	Log pelvic breadth ~ Sex	Shape ~ Sex * Log pelvic breadth	0.02510
M24	Log pelvic breadth ~ Sex + Log age	Shape ~ Sex + Log age + Log pelvic breadth	0.02516
M25	Log pelvic breadth ~ Sex + Log age	Shape ~ (Sex + Log age) * Log pelvic breadth	0.02514
M26	Log pelvic breadth ~ Sex * Log age	Shape ~ Sex * Log age + Log pelvic breadth	0.02524
M27	Log pelvic breadth ~ Sex * Log age	Shape ~ Sex * Log age * Log pelvic breadth	0.02523

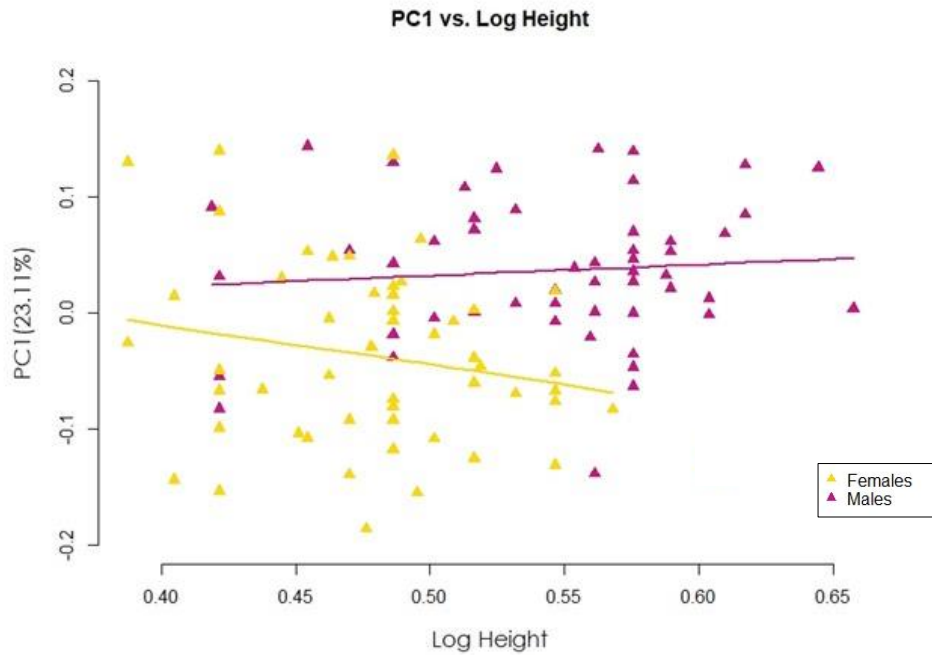**Supplement S2.2. PC1 and PC2 vs. Log pelvis centroid size.** (A) PC1, and (B) PC2 against log pelvis centroid size.
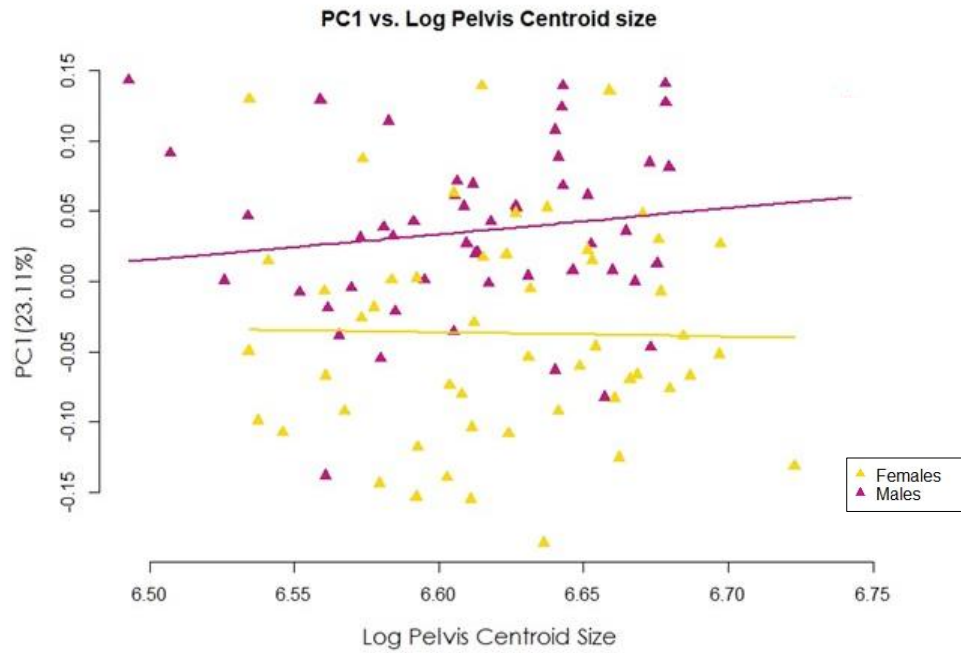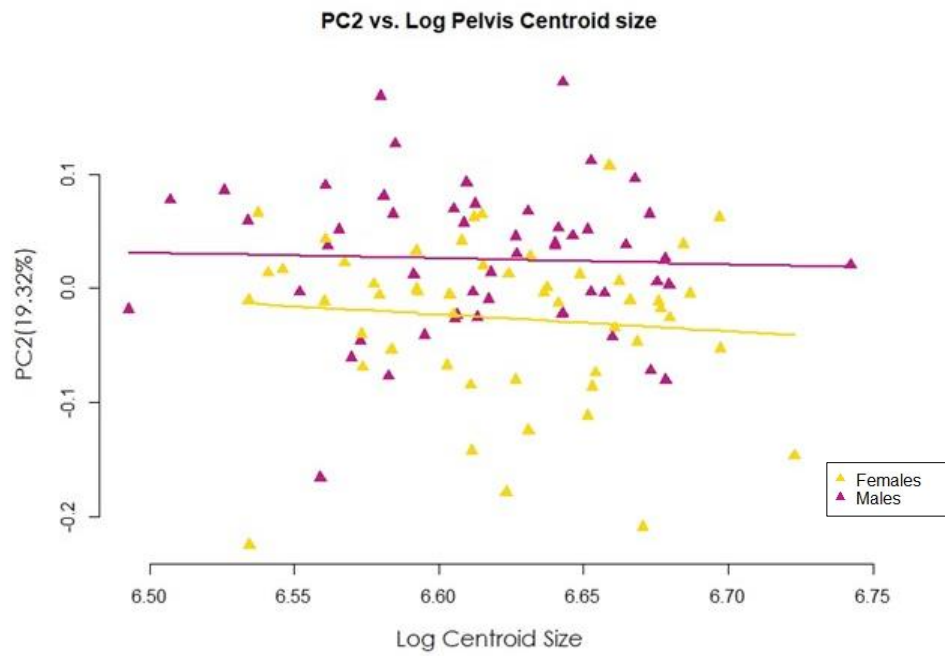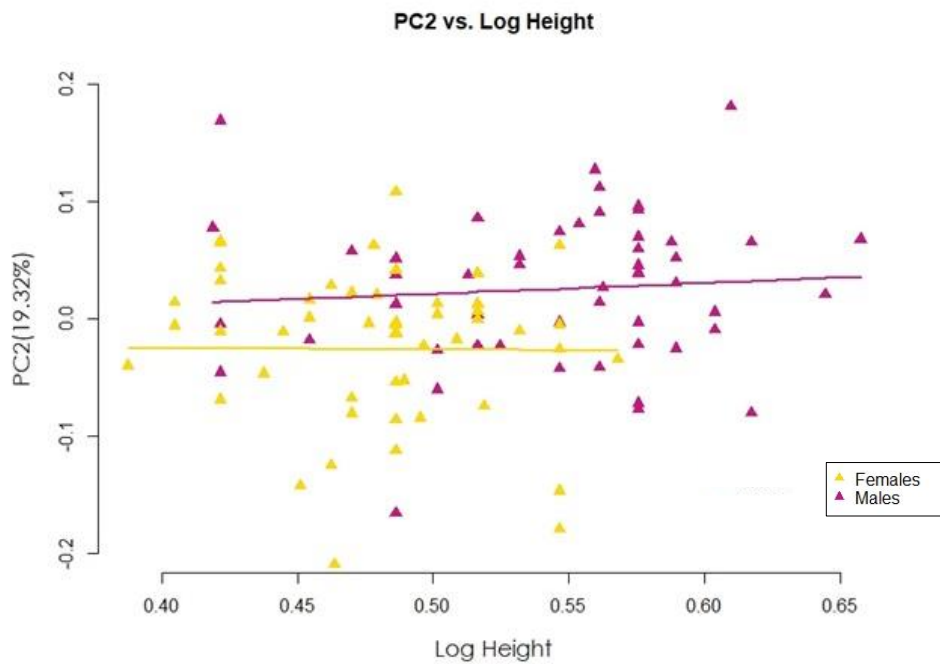
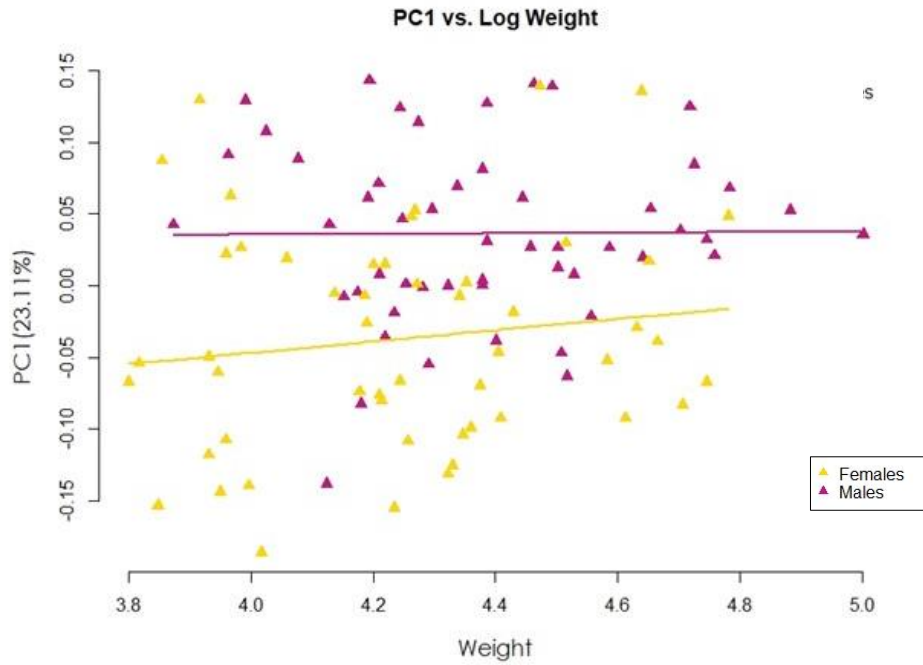**Supplement S2.3. PC1 and PC2 vs. Log height.** (A) PC1, and (B) PC2 against log height.
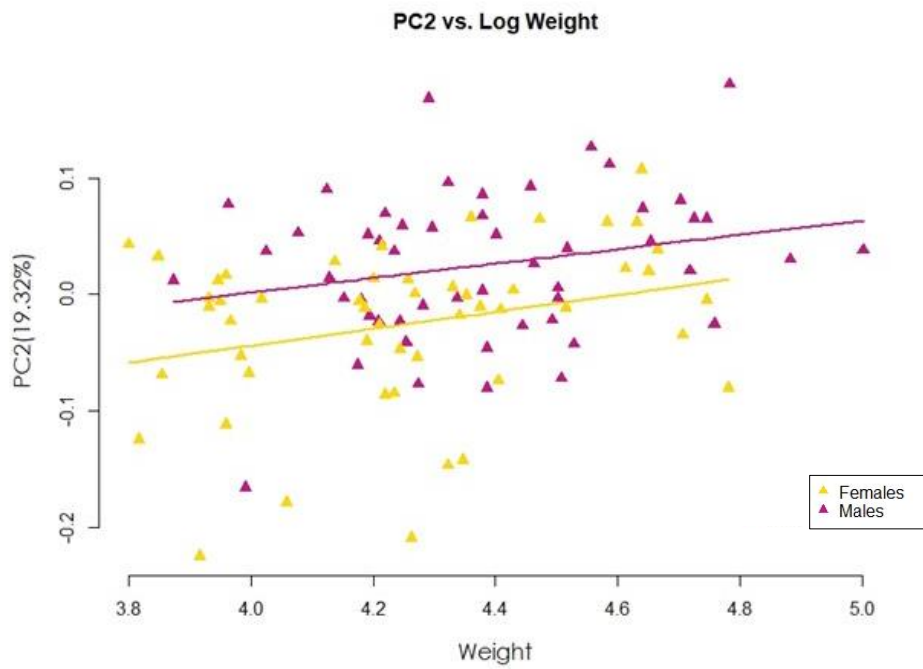
A

B

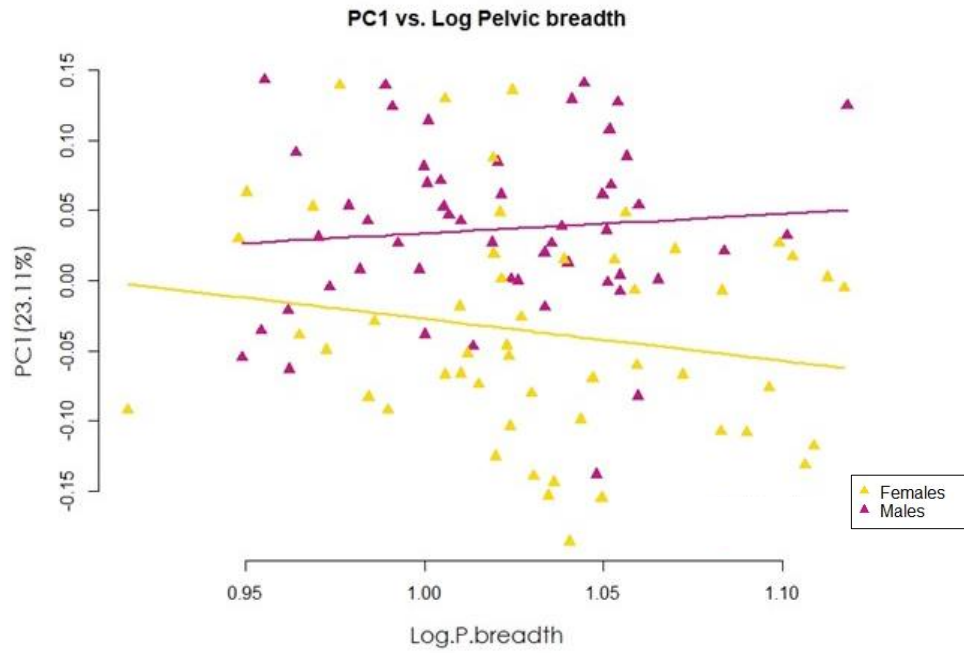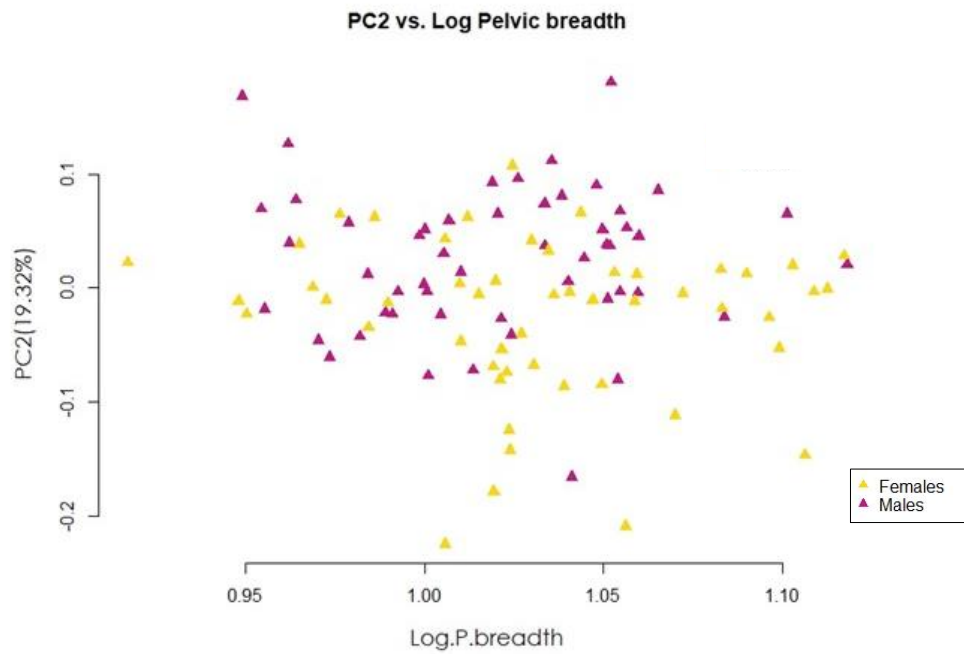**Supplement S2.7. PC1 and PC2 vs. Log weight.** (A) PC1 and (B) PC2 against log weight.

Supplement S2.8. PC1 and PC2 vs. Log pelvic breadth. (A) PC1 and (B) PC2 against log pelvic breadth.

REFERENCES

Abitbol, M. M. (1987). Obstetrics and posture in pelvic anatomy. *Journal of Human Evolution*, 16(3), 243–255. https://doi.org/10.1016/0047-2484(87)90001-7

Adams D., Collyer, M., Kaliontzopoulou, A., Baken, E. (2021). Geomorph: Software for geometric morphometric analyses. R package version 4.0.2. Retrieved from https://cran.r-project.org/package/geomorph

Adegboyega, M. T., Stamos, P. A., Hublin, J.-J., & Weaver, T. D. (2021). Virtual reconstruction of the Kebara 2 Neanderthal pelvis. *Journal of Human Evolution*, *151*, 102922. https://doi.org/10.1016/j.jhevol.2020.102922

Aeby, C. (1858). Über die Symphyse Ossium Pubis des Menschen nebst Beitragen zur Lehre vom hyalinen Knorpel und seiner Verknöcherung. *Z. Rationelle Med. Serie*, *4*(3), 1–25.

Alicioglu, B., Kartal, O., Gurbuz, H., & Sut, N. (2008). Symphysis pubis distance in adults: a retrospective computed tomography study. *Surgical and Radiologic Anatomy*, *30*(2), 153–157. https://doi.org/10.1007/s00276-007-0295-0

Antón, S. C., Taboada, H. G., Middleton, E. R., Rainwater, C. W., Taylor, A. B., Turner, T. R., Turnquist, J. E., Weinstein, K. J., & Williams, S. A. (2016). Morphological variation in homo erectus and the origins of developmental plasticity. *Philosophical Transactions of the Royal Society B: Biological Sciences*, *371*(1698). https://doi.org/10.1098/rstb.2015.0236

Arsuaga, J. L., & Carretero, J. M. (1994). Multivariate analysis of the sexual dimorphism of the hip bone in a modern human population and in early hominids. *American Journal of Physical Anthropology*, *93*(2), 241–257. https://doi.org/10.1002/ajpa.1330930208

Arsuaga, J. L., Lorenzo, C., Carretero, J.-M., Gracia, A., Martínez, I., García, N., Castro, J.-M. B. de, & Carbonell, E. (1999). A complete human pelvis from the Middle Pleistocene of Spain. *Nature*, *399*(6733), 255–258. https://doi.org/10.1038/20430

Aydın, S., Bakar, R. Z., Aydın, Ç. A., & Özcan, P. (2016). Assessment of postpartum symphysis pubis distention with 3D ultrasonography: a novel method. *Clinical Imaging*, *40*(2), 185–190. https://doi.org/10.1016/j.clinimag.2015.10.015

Bahlmann, F., Merz, E., Macchiella, D., & Weber, G. (1993). Sonographische darstellung des symphysenspaltes zur beurteilung eines symphysenschadens in der schwangerschaft und post partum. *Zeitschrift Fur Geburtshilfe Und Perinatologie*, *197*(1), 27–30. https://scholar.google.com/scholar_lookup?hl=en&volume=197&publication_year=1993&pages=27-30&journal=Z+Geburtsh+u+Perinat&author=F+Bahlmann&author=E+Merz&author=D+Macchiella&title=Sonographische+Darstellung+des+Symphysenspaltes+zur

+Beurteilung+eines+Symph

Bailey, J. F., Shefi, S., Soudack, M., Kramer, P. A., & Been, E. (2019). Development of Pelvic Incidence and Lumbar Lordosis in Children and Adolescents. *The Anatomical Record*, *302*(12), 2132–2139. https://doi.org/10.1002/AR.24209

Bar-Yosef, O., Arensburg, B., Laville, H., Meignen, L., Tillier, A.-M., Valladas, G., Valladas, H., & Vandermeersch, B. (1991). *Le squelette Mousterien de Kebara 2*. Centre National de la Recherche Scientifique.

Bar-Yosef, O., Vandermeersch, B., Arensburg, B., Goldberg, P., Laville, H., Meignen, L., Rak, Y., Tchernov, E., & Tillier, A. M. (1986). New data on the origin of modern man in the Levant. *Current Anthropology*, *27*(1), 63–64.

Barnes, M. J. (1934). The symphysis pubis in the female. *American Journal of Rentogen*, *32*, 333–352. https://ci.nii.ac.jp/naid/10014839687/

Bauman, M., Marinaro, J., Tawil, I., Crandall, C., Rosenbaum, L., & Paul, I. (2011). Ultrasonographic Determination of Pubic Symphyseal Widening in Trauma: The FAST-PS Study. *The Journal of Emergency Medicine*, *40*(5), 528–533. https://doi.org/10.1016/j.jemermed.2009.08.041

Becker, I., Stringer, M. D., Jeffery, R., & Woodley, S. J. (2014). Sonographic anatomy of the pubic symphysis in healthy nulliparous women. *Clinical Anatomy*, *27*(7), 1058–1067. https://doi.org/10.1002/ca.22423

Becker, I., Woodley, S. J., & Stringer, M. D. (2010). The adult human pubic symphysis: a systematic review. *Journal of Anatomy*, *217*(5), 475–487. https://doi.org/10.1111/j.1469-7580.2010.01300.x

Been, E., Gómez-Olivencia, A., Kramer, P. A., & Barash, A. (2017). 3D Reconstruction of Spinal Posture of the Kebara 2 Neanderthal. In A. Marom & E. Hovers (Eds.), *Vertebrate Paleobiology and Paleoanthropology* (pp. 239–251). Springer. https://doi.org/10.1007/978-3-319-46646-0_18

Been, E., Peleg, S., Marom, A., & Barash, A. (2010). Morphology and function of the lumbar spine of the Kebara 2 Neandertal. *American Journal of Physical Anthropology*, *142*(4), 549–557. https://doi.org/10.1002/ajpa.21256

Been, E., Pessah, H., Peleg, S., & Kramer, P. A. (2013). Sacral Orientation in Hominin Evolution. *Advances in Anthropology*, *03*(03), 133–141. https://doi.org/10.4236/aa.2013.33018

Benazzi, S., Stansfield, E., Milani, C., & Gruppioni, G. (2009). Geometric morphometric methods for three-dimensional virtual reconstruction of a fragmented cranium: The case of Angelo Poliziano. *International Journal of Legal Medicine*, *123*(4), 333–344. https://doi.org/10.1007/s00414-009-0339-6

Benjamin, M., & Evans, E. J. (1990). Fibrocartilage. *Ncbi.Nlm.Nih.Gov*, *171*, 1–15. https://www.ncbi.nlm.nih.gov/pmc/articles/pmc1257123/

Berge, C. (1991). Size- and locomotion-related aspects of hominid and anthropoid pelves: An osteometrical multivariate analysis. *Human Evolution*, *6*(5–6), 365–376. https://doi.org/10.1007/BF02435530

Berge, C., & Goularas, D. (2010). A new reconstruction of Sts 14 pelvis (Australopithecus africanus) from computed tomography and three-dimensional modeling techniques. *Journal of Human Evolution*, *58*(3), 262–272. https://doi.org/10.1016/j.jhevol.2009.11.006

Betti, L., von Cramon-Taubadel, N., Manica, A., & Lycett, S. J. (2013). Global Geometric Morphometric Analyses of the Human Pelvis Reveal Substantial Neutral Population History Effects, Even across Sexes. *PloS One*, *8*(2), e55909. https://doi.org/10.1371/journal.pone.0055909

Betti, L., von Cramon-Taubadel, N., Manica, A., & Lycett, S. J. (2014). The interaction of neutral evolutionary processes with climatically-driven adaptive changes in the 3D shape of the human os coxae. *Journal of Human Evolution*, *73*, 64–74. https://doi.org/10.1016/j.jhevol.2014.02.021

Björklund, K., Bergström, S., Lindgren, P. G., & Ulmsten, U. (1996). Ultrasonographic measurement of the symphysis pubis: A potential method of studying symphyseolysis in pregnancy. *Gynecologic and Obstetric Investigation*, *42*(3), 151–153.

Bonmatí, A., Gómez-Olivencia, A., Arsuaga, J. L., Carretero, J. M., Gracia, A., Martínez, I., Lorenzo, C., Bérmudez de Castro, J. M., & Carbonell, E. (2010). Middle Pleistocene lower back and pelvis from an aged human individual from the Sima de los Huesos site, Spain. *Proceedings of the National Academy of Sciences*, *107*(43), 18386–18391. https://doi.org/10.1073/pnas.1012131107

Bookstein, F. L. (1989). Principal warps: Thin-plate splines and the decomposition of deformations. *IEEE Transactions on Pattern Analysis and Machine Intelligence*, *11*(6), 567–585. https://doi.org/10.1109/34.24792

Bookstein, F. L. (1992). Morphometric Tools for Landmark Data. In *Morphometric Tools for Landmark Data: Geometry and Biology*. Cambridge University Press. https://doi.org/10.1017/CBO9780511573064

Bookstein, F. L., Gunz, P., Mitteroecker, P., Prossinger, H., Schæfer, K., & Seidler, H. (2003). Cranial integration in *Homo*: singular warps analysis of the midsagittal plane in ontogeny and evolution. *Journal of Human Evolution*, *44*(2), 167–187. https://doi.org/10.1016/S0047-2484(02)00201-4

Bramble, D. M., & Lieberman, D. E. (2004). Endurance running and the evolution of *Homo*. In *Nature* (Vol. 432, Issue 7015, pp. 345–352).

https://doi.org/10.1038/nature03052

Brassey, C. A., O'Mahoney, T. G., Chamberlain, A. T., & Sellers, W. I. (2018). A volumetric technique for fossil body mass estimation applied to *Australopithecus afarensis*. *Journal of Human Evolution*, *115*, 47–64. https://doi.org/10.1016/j.jhevol.2017.07.014

Brooks, S., & Suchey, J. M. (1990). Skeletal age determination based on the os pubis: a comparison of the Acsadi-Nemeskeri and Suchey-Brooks methods. *Human Evolution*, *5*(3), 227–238.

Bruzek, J. (2002). A method for visual determination of sex, using the human hip bone. *American Journal of Physical Anthropology*, *117*(2), 157–168. https://doi.org/10.1002/ajpa.10012

Cartmill, M., & Schmitt, D. (1996). Pelvic rotation in human walking and running: Implications for early hominid bipedalism. *American Journal of Physical Anthropology*, *48*, 25–44.

Chapman, T., Beyer, B., Sholukha, V., Semal, P., Feipel, V., Louryan, S., & Van Sint Jan, S. (2017). How different are the Kebara 2 ribs to modern humans? *Journal of Anthropological Sciences*, *95*, 183–201. https://doi.org/10.4436/jass.95004

Chiba, F., Makino, Y., Motomura, A., Inokuchi, G., Torimitsu, S., Ishii, N., Kubo, Y., Abe, H., Sakuma, A., Nagasawa, S., Saitoh, H., Yajima, D., Hayakawa, M., Miura, M., & Iwase, H. (2014). Age estimation by quantitative features of pubic symphysis using multidetector computed tomography. *International Journal of Legal Medicine*, *128*(4), 667–673. https://doi.org/10.1007/s00414-014-1010-4

Claxton, A. G., Hammond, A. S., Romano, J., Oleinik, E., & DeSilva, J. M. (2016). Virtual reconstruction of the *Australopithecus africanus* pelvis Sts 65 with implications for obstetrics and locomotion. *Journal of Human Evolution*, *99*, 10–24.

Collard, M., & Cross, A. (2017). Thermoregulation in Homo erectus and the Neanderthals: A reassessment using a segmented model. *Vertebrate Paleobiology and Paleoanthropology*, *9783319466446*, 161–174. https://doi.org/10.1007/978-3-319-46646-0_12

Cox, S. L. (2021). A geometric morphometric assessment of shape variation in adult pelvic morphology. *American Journal of Physical Anthropology*, *176*(4), 652–671. https://doi.org/10.1002/ajpa.24399

Dryden, I. L., & Mardia, K. (1998). Statistical shape analysis: Wiley series in probability and statistics. *New York, NY: John Wiley & Sons, Ltd.*

Duday, H., & Arensburg, B. (1991). La pathologie. In O. Bar-Yosef & B. Vandermeersch (Eds.), *Le squelette moustérien de Kebara* (pp. 179 - 193). Centre National de la Recherche Scientifique.

Dudzik, B., & Langley, N. R. (2015). Estimating age from the pubic symphysis: A new component-based system. *Forensic Science International*, *257*, 98–105. https://doi.org/10.1016/j.forsciint.2015.07.047

Fick, R. (1904). Handbuch der anatomie und mechanik der gelenke unter berücksichtigung der bewegenden muskeln. *Erster Teil: Anatomie der Gelenke* (Vol. 2). Jena: Verlag von Gustav Fischer.

Fischer, B., & Mitteroecker, P. (2015). Covariation between human pelvis shape, stature, and head size alleviates the obstetric dilemma. *Proceedings of the National Academy of Sciences*, *112*(18), 5655–5660. ttps://doi.org/10.1073/pnas.1420325112

Fischer, B., & Mitteroecker, P. (2017). Allometry and Sexual Dimorphism in the Human Pelvis. *The Anatomical Record*, *300*(4), 698–705. https://doi.org/10.1002/AR.23549

Franklin, D. (2010). Forensic age estimation in human skeletal remains: Current concepts and future directions. *Legal Medicine*, *12*(1), 1–7. https://doi.org/10.1016/j.legalmed.2009.09.001

Gamble, J. G., Simmons, S. C., & Freedman, M. (1986). The symphysis pubis. Anatomic and pathologic considerations. *Clinical Orthopaedics and Related Research*, *203*(NA;), 261–272. https://doi.org/10.1097/00003086-198602000-00033

Garagiola, D., Tarver, R., Gibson, L., Rogers, R., & Wass, J. (1989). Anatomic changes in the pelvis after uncomplicated vaginal delivery: a CT study on 14 women. *American Journal of Roentgenology*, *153*(6), 1239–1241. https://doi.org/10.2214/ajr.153.6.1239

García-Martínez, D., Barash, A., Recheis, W., Utrilla, C., Torres-Sánchez, I., García Río, F., & Bastir, M. (2014). On the chest size of Kebara 2. *Journal of Human Evolution*, *70*(1), 69–72. https://doi.org/10.1016/j.jhevol.2014.02.003

Gilbert, B. M., & McKern, T. W. (1973). A method for aging the femaleOs pubis. *American Journal of Physical Anthropology*, *38*(1), 31–38. https://doi.org/10.1002/ajpa.1330380109

Gómez-Olivencia, A., Arlegi, M., Barash, A., Stock, J. T., & Been, E. (2017). The Neandertal vertebral column 2: The lumbar spine. *Journal of Human Evolution*, *106*, 84–101. https://doi.org/10.1016/j.jhevol.2017.01.006

Gómez-Olivencia, A., Barash, A., García-Martínez, D., Arlegi, M., Kramer, P., Bastir, M., & Been, E. (2018). 3D virtual reconstruction of the Kebara 2 Neandertal thorax. *Nature Communications 2018 9:1*, *9*(1), 1–8. https://doi.org/10.1038/s41467-018-06803-z

Gómez-Olivencia, A., Been, E., Arsuaga, J. L., & Stock, J. T. (2013). The Neandertal

vertebral column 1: The cervical spine. *Journal of Human Evolution*, *64*(6), 608–630. https://doi.org/10.1016/j.jhevol.2013.02.008

Gómez-Olivencia, A., Eaves-Johnson, K. L., Franciscus, R. G., Carretero, J. M., & Arsuaga, J. L. (2009). Kebara 2: new insights regarding the most complete Neandertal thorax. *Journal of Human Evolution*, *57*(1), 75–90. https://doi.org/10.1016/j.jhevol.2009.02.009

Goodall, C. (1991). Procrustes Methods in the Statistical Analysis of Shape. *Journal of the Royal Statistical Society: Series B (Methodological)*, *53*(2), 285–321. https://doi.org/10.1111/j.2517-6161.1991.tb01825.x

Gower, J. C. (1975). Generalized procrustes analysis. *Psychometrika*, *40*(1), 33–51. https://doi.org/10.1007/BF02291478

Gruss, L. T., & Schmitt, D. (2015). The evolution of the human pelvis: changing adaptations to bipedalism, obstetrics and thermoregulation. *Philosophical Transactions of the Royal Society B: Biological Sciences*, *370*(1663), 20140063. https://doi.org/10.1098/rstb.2014.0063

Gunz, P., Mitteroecker, P., Bookstein, F. L., & Weber, G. (2004). Computer aided reconstruction of incomplete human crania. In S. Campana, R. Scopigno, G. Carpentiero, & M. Cirillo (Eds.), *Enter the Past: Computer Applications and Quantitative Methods in Archaeology* (pp. 96–98). Archaeopress, Oxford.

Gunz, P., & Mitteroecker, P. (2013). Semilandmarks: a method for quantifying curves and surfaces. *Hystrix, the Italian Journal of Mammalogy*, *24*(1), 103–109. https://doi.org/https://doi.org/10.4404/hystrix-24.1-6292

Gunz, P., Mitteroecker, P., & Bookstein, F. L. (2005). Semilandmarks in three dimensions. *Modern Morphometrics in Physical Anthropology*, 73–98. https://doi.org/10.1007/0-387-27614-9_3

Gunz, P., Mitteroecker, P., Neubauer, S., Weber, G. W., & Bookstein, F. L. (2009). Principles for the virtual reconstruction of hominin crania. *Journal of Human Evolution*, *57*(1), 48–62. https://doi.org/10.1016/j.jhevol.2009.04.004

Häusler, M., & Schmid, P. (1995). Comparison of the pelves of Sts 14 and AL288-1: implications for birth and sexual dimorphism in Australopithecines. *Journal of Human Evolution*, *29*(4), 363–383. https://doi.org/10.1006/JHEV.1995.1063

Herries, A. I. R., Martin, J. M., Leece, A. B., Adams, J. W., Boschian, G., Joannes-Boyau, R., Edwards, T. R., Mallett, T., Massey, J., Murszewski, A., Neubauer, S., Pickering, R., Strait, D. S., Armstrong, B. J., Baker, S., Caruana, M. V., Denham, T., Hellstrom, J., Moggi-Cecchi, J., Mokobane, S., Penzo-Kajewski, P., Rovinsky, D. S., Schwartz G. T., Stammers, R. C., Wilson, C., Woodhead, J., Menter, C. (2020). Contemporaneity of *Australopithecus*, *Paranthropus*, and early *Homo erectus* in South Africa. *Science, 368*(6486). https://doi.org/10.1126/science.aaw7293

Hill, W. C. O., & Heinemann, W. (1954). Man's ancestry. *American Journal of Physical Anthropology*, *12*(4), 627–628. https://doi.org/10.1002/ajpa.1330120415

Holliday, T. W. (1997). Body proportions in Late Pleistocene Europe and modern human origins. *Journal of Human Evolution*, *32*(5), 423–448. https://doi.org/10.1006/jhev.1996.0111

Horan, F. (2009). Gray's Anatomy: the anatomical basis of clinical practice. *The Journal of Bone and Joint Surgery. British Volume*, *91-B*(7), 983–983. https://doi.org/10.1302/0301-620x.91b7.22719

Huseynov, A., Zollikofer, C. P. E., Coudyzer, W., Gascho, D., Kellenberger, C., Hinzpeter, R., & Ponce de León, M. S. (2016). Developmental evidence for obstetric adaptation of the human female pelvis. *Proceedings of the National Academy of Sciences*, *113*(19), 5227–5232. https://doi.org/10.1073/pnas.1517085113

Izenman, J. A. (1975). Reduced-Rank Regression for the Multivariate Linear Model. *Journal Of Multivariate Analysis*, *5*, 248–264.

Kappelman, J. (1996). The evolution of body mass and relative brain size in fossil hominids. *Journal of Human Evolution*, *30*(3), 243–276. https://doi.org/10.1006/jhev.1996.0021

Karasik, D., Arensburg, B., Tillier, A.-M., & Pavlovsky, O. M. (1998). Skeletal Age Assessment of Fossil Hominids. *Journal of Archaeological Science*, *25*(7), 689–696. https://doi.org/10.1006/jasc.1997.0264

Kibii, J. M., Churchill, S. E., Schmid, P., Carlson, K. J., Reed, N. D., De Ruiter, D. J., & Berger, L. R. (2011). A partial pelvis of *Australopithecus sediba*. *Science*, *333*(6048), 1407–1411. https://doi.org/10.1126/science.1202521

Klingenberg, C. P. (2016). Size, shape, and form: concepts of allometry in geometric morphometrics. *Development Genes and Evolution*, *226*(3), 113–137. https://doi.org/10.1007/s00427-016-0539-2

Knox, R. (1830). A system of human anatomy translated from the fourth edition of the french "traite d'anatomie descriptive" of M. H. Cloquet (2nd Edition, pp. 196–198). Wells and Lilly, Court Street.

Kurki, H. K. (2011). Pelvic dimorphism in relation to body size and body size dimorphism in humans. *Journal of Human Evolution*, *61*(6), 631–643. https://doi.org/10.1016/j.jhevol.2011.07.006

Lei, J., Zhang, Y., Wu, G., Wang, Z., & Cai, X. (2015). The Influence of pelvic ramus fracture on the stability of fixed pelvic complex fracture. *Computational and Mathematical Methods in Medicine*, *2015*, 1–11. https://doi.org/10.1155/2015/790575

Lewton, K. L. (2015). Allometric scaling and locomotor function in the primate pelvis. *American Journal of Physical Anthropology*, *156*(4), 511–530. https://doi.org/10.1002/ajpa.22696

Li, Y. (2002). Postnatal development of pelvic sexual dimorphism in four anthropoid primates. In *ProQuest Dissertations and Theses* (Issue 3046493).

Li, Z., Kim, J.-E., Davidson, J. S., Etheridge, B. S., Alonso, J. E., & Eberhardt, A. W. (2007). Biomechanical response of the pubic symphysis in lateral pelvic impacts: A finite element study. *Journal of Biomechanics*, *40*(12), 2758–2766. https://doi.org/10.1016/j.jbiomech.2007.01.023

Loeschcke, H. (1912). Untersuchungen über entstehung und bedeutung der spaltbildungen in der symphyse, sowie über physiologische erweiterungsvorgänge am becken schwangerer und gebärender. *Archives of Gynecology and Obstetrics*, *96*(3), 525–560. https://doi.org/10.1007/BF02100216

Lottering, N., Reynolds, M. S., MacGregor, D. M., Meredith, M., & Gregory, L. S. (2014). Morphometric modelling of ageing in the human pubic symphysis: Sexual dimorphism in an Australian population. *Forensic Science International*, *236*, 195.e1-195.e11. https://doi.org/10.1016/j.forsciint.2013.12.041

Lovejoy, C. O. (1988). Evolution of human walking. *Scientific American*, *259*(5), 118–125. https://doi.org/10.1038/scientificamerican1188-118

Lovejoy, C. O. (2005). The natural history of human gait and posture. *Gait & Posture*, *21*(1), 113–124. https://doi.org/10.1016/j.gaitpost.2004.06.010

Lovejoy, C. O. (1979). Reconstruction of the pelvis of AL-288 (Hadar Formation, Ethiopia). *American Journal of Physical Anthropology*, *50*(3), 460.

Lovejoy, C. O., Heiple, K. G., & Burstein, A. H. (1973). The gait of Australopithecus. *American Journal of Physical Anthropology*, *38*(3), 757–779. https://doi.org/10.1002/ajpa.1330380315

Lovejoy, C. O., & McCollum, M. A. (2010). Spinopelvic pathways to bipedality: why no hominids ever relied on a bent-hip–bent-knee gait. *Philosophical Transactions of the Royal Society B: Biological Sciences*, *365*(1556), 3289–3299. https://doi.org/10.1098/RSTB.2010.0112

Lovejoy, C. O., Suwa, G., Spurlock, L., Asfaw, B., & White, T. D. (2009). The Pelvis and Femur of Ardipithecus ramidus : The Emergence of Upright Walking. *Science*, *326*(5949), 71. https://doi.org/10.1126/science.1175831

Luders, E., Narr, K. L., Thompson, P. M., & Toga, A. W. (2009). Neuroanatomical correlates of intelligence. *Intelligence*, *37*(2), 156–163. https://doi.org/10.1016/j.intell.2008.07.002

Luschka, H. von. (1862). *Die Anatomie des Menschen in Rücksicht auf die Bedürfnisse der praktischen Heilkund* (Vol. 1). Verlag der H. Laupp'schen Buchhandlung Laupp & Siebeck.

Meissner, A., Fell, M., Wilk, R., Boenick, U., & Rahmanzadeh, R. (1996). [Biomechanics of the pubic symphysis. Which forces lead to mobility of the symphysis in physiological conditions?]. *Der Unfallchirurg*, *99*(6), 415–421.

Middleton, E. R., Winkler, Z. J., Hammond, A. S., Plavcan, J. M., & Ward, C. V. (2017). Determinants of Iliac Blade Orientation in Anthropoid Primates. *Anatomical Record*, *300*(5), 810–827. https://doi.org/10.1002/ar.23557

Mitteroecker, P., & Gunz, P. (2009). Advances in Geometric morphometrics. *Evolutionary Biology*, *36*(2), 235–247. https://doi.org/10.1007/S11692-009-9055-X

Morante, G. B., Fischer, B., López, M. C. B., & Bastir, M. (2021). The outline of the pubic symphyseal surface is sexually dimorphic and changes with age in humans. *Journal of Anthropological Sciences*, *99*, 83–95. https://doi.org/10.4436/jass.99003

Müller-Vahl, K. R., Berding, G., Brücke, T., Kolbe, H., Meyer, G. J., Hundeshagen, H., Dengler, R., Knapp, W. H., & Emrich, H. M. (2000). Dopamine transporter binding in Gilles de la Tourette syndrome. *Journal of Neurology*, *247*(7), 514–520. https://doi.org/10.1007/PL00007806

Nejad, A. H., Jamali, A., Wootton-Gorges, S. L., Boakes, J. L., & Ferguson, T. A. (2012). Symphysis pubis width in the pediatric population. *Journal of Trauma and Acute Care Surgery*, *73*(4), 923–927. https://doi.org/10.1097/TA.0b013e31825159b5

Neumann, D. A. (2016). Kinesiology of the Musculoskeletal System: Foundations for Rehabilitation. *Pagina 595* (3rd Edition).

O'Higgins, P., Cobb, S. N., Fitton, L. C., Gröning, F., Phillips, R., Liu, J., & Fagan, M. J. (2011). Combining geometric morphometrics and functional simulation: an emerging toolkit for virtual functional analyses. *Journal of Anatomy*, *218*(1), 3–15. https://doi.org/10.1111/j.1469-7580.2010.01301.x

Oligmüller, A.-K. (2015). Sonographic measurement of the width of the pubic symphysis during pregnancy and analysis of the influencing factors. (Doctoral dissertation, Freie Universität Berlin).

Ponce de León, M. S., Golovanova, L., Doronichev, V., Romanova, G., Akazawa, T., Kondo, O., Ishida, H., & Zollikofer, C. P. E. (2008). Neanderthal brain size at birth provides insights into the evolution of human life history. *Proceedings of the National Academy of Sciences*, *105*(37), 13764–13768. https://doi.org/10.1073/pnas.0803917105

Rak, Y., & Arensburg, B. (1987). Kebara 2 Neanderthal pelvis: First look at a complete

inlet. *American Journal of Physical Anthropology*, *73*(2), 227–231. https://doi.org/10.1002/ajpa.1330730209

Rak, Yoel. (1991). The pelvis. In O. Bar-Yosef & B. Vandermeersch (Eds.), *Le squelette moustérien de Kébara* (Vol. 2, pp. 147–156). Centre National de la Recherche Scientifique.

Roberts, R. E. (1934). Discussion on the physiology and pathology of the pelvic joints in relation to child-bearing. *Proc R Soc Med*, *17*, 1211–1217.

Rohlf, F. J., & Slice, D. (1990). Extensions of the procrustes method for the optimal superimposition of landmarks. *Systematic Zoology*, *39*(1), 40–59. https://doi.org/10.2307/2992207

Rosenberg, K. R. (1992). The evolution of modern human childbirth. *American Journal of Physical Anthropology*, *35*(S15), 89–124.

Rosenberg, K. R. (1998). Morphological variation in west Asian postcrania: implications for obstetric and locomotor behavior. In T. Akazawa, K. Aoki., & O. Bar-Yosef (Eds.), *Neandertals and modern humans in Western Asia* (pp. 367–379). NY: Plenum Press.

Rosenberg, K. R. (2007). Neandertal pelvic remains from Krapina: peculiar or primitive? *Periodicum Biologorum*, *109*(4), 387–392.

Rosenberg, K. R., & DeSilva, J. M. (2017). Evolution of the Human Pelvis. *The Anatomical Record*, *300*(5), 789–797. https://doi.org/10.1002/ar.23580

Rosenberg, K. R., & Trevathan, W. (2002). Birth, obstetrics and human evolution. *BJOG: An International Journal of Obstetrics and Gynaecology*, *109*(11), 1199–1206. https://doi.org/10.1046/j.1471-0528.2002.00010.x

Rosenberg, K. R., & Trevathan, W. R. (2001). The evolution of human birth. *Scientific American*, *285*(5), 72–77.

Rosenberg, K. R., & Trevathan, W. R. (2005). Bipedalism and human birth: The obstetrical dilemma revisited. *Evolutionary Anthropology: Issues, News, and Reviews*, *4*(5), 161–168. https://doi.org/10.1002/evan.1360040506

Rosse, C., Gaddum-Rosse, P., & Hollinshead, W. H. (1997). *Hollinshead's textbook of anatomy* (5th editio, Vol. 741). New York: Lippincott Williams & Wilkins.

Ruff, C. B. (1991). Climate and body shape in hominid evolution. *Journal of Human Evolution*, *21*(2), 81–105. https://doi.org/10.1016/0047-2484(91)90001-C

Ruff, C. B. (1994). Morphological adaptation to climate in modern and fossil hominids. *American Journal of Physical Anthropology*, *37*(S19), 65–107.

Ruff, C. B. (1995). Biomechanics of the hip and birth in earlyHomo. *American Journal*

of Physical Anthropology, *98*(4), 527–574.
https://doi.org/10.1002/ajpa.1330980412

Ruff, C. B. (1998). Evolution of the Hominid Hip. In E. Strasser, J. G. Fleagle, A. L. Rosenberger, & H. M. McHenry (Eds.), *Primate Locomotion* (pp. 449–469). Springer US. https://doi.org/10.1007/978-1-4899-0092-0_23

Ruff, C. B. (2010). Body size and body shape in early hominins–implications of the Gona pelvis. *Journal of Human Evolution*, *58*(2), 166–178.

Saunders, J. B., Inman, V. T., & Eberhart, T. (1953). The major determinants in normal and pathological gait. *J Bone Joint Surg*, *35*, 543–558.

Sawyer, G. J., & Maley, B. (2005). *Neanderthal Reconstructed*. https://doi.org/10.1002/ar.b.20057

Sawyer, G. J., & Maley, B. (2005). Neanderthal reconstructed. *The Anatomical Record Part B: The New Anatomis*t, 283B(1), 23–31. https://doi.org/10.1002/ar.b.20057

Schlager, S., Jefferis, G., & Dryden, I. L. (2021). Calculations and Visualisation Related to Geometric Morphometrics. In *CRAN Repository: Package "Morpho": Vol. 2.8* (pp. 1–164).

Schlager, S., Profico, A., Vincenzo, F. Di, & Manzi, G. (2018). Retrodeformation of fossil specimens based on 3D bilateral semi-landmarks: Implementation in the R package "Morpho." *PLOS ONE*, *13*(3), e0194073. https://doi.org/10.1371/journal.pone.0194073

Schmid, P. (1983). [A reconstruction of the skeleton of A.L. 288-1 (Hadar) and its consequences]. *Folia primatologica; international journal of primatology*, *40*(4), 283–306. https://doi.org/10.1159/000156111

Schmitt, D., Lemelin, P., & Trueblood, A. C. (1999). Shock wave transmission through the human body during normal and compliant walking. *American Journal of Physical Anthropology*, 28,243–244.

Schoellner, C., Szöke, N., & Siegburg, K. (2001). Der schwangerschaftsassoziierte symphysenschaden aus orthopädischer sicht - untersuchungen zu veränderungen an der symphysis pubica in der schwangerschaft, unter der geburt und post partum. *Zeitschrift Für Orthopädie Und Ihre Grenzgebiete*, *139*(05), 458–462. https://doi.org/10.1055/s-2001-17991

Schwarcz, H. P., Buhay, W. M., Grün, R., Valladas, H., Tchernov, E., Bar-Yosef, O., & Vandermeersch, B. (1989). ESR dating of the Neanderthal site, Kebara Cave, Israel. *Journal of Archaeological Science*, *16*(6), 653–659. https://doi.org/10.1016/0305-4403(89)90029-0

Shapiro, H. L. (1956). Man, culture, and society. *Oxford University Press, NY*.

Simpson, S. W., Quade, J., Levin, N. E., Butler, R., Dupont-Nivet, G., Everett, M., & Semaw, S. (2008). A female *Homo erectus* pelvis from Gona, Ethiopia. *Science*, *322*(5904), 1089–1092. https://doi.org/10.1126/science.1163592

Slice, D. (2005). Modern Morphometrics in Physical Anthropology. In D. E. Slice (Ed.), *Modern Morphometrics in Physical Anthropology*. Springer, US. https://doi.org/10.1007/0-387-27614-9

Slice, D. E. (2007). Geometric Morphometrics. *Annual Review of Anthropology*, *36*(1), 261–281. https://doi.org/10.1146/annurev.anthro.34.081804.120613

Stansfield, E., Fischer, B., Grunstra, N. D. S., Pouca, M. V., & Mitteroecker, P. (2021). The evolution of pelvic canal shape and rotational birth in humans. *BMC Biology*, *19*(1). https://doi.org/10.1186/s12915-021-01150-w

Stelzer, S., Gunz, P., Neubauer, S., & Spoor, F. (2018). Using the covariation of extant hominoid upper and lower jaws to predict dental arcades of extinct hominins. *Journal of Human Evolution*, *114*, 154–175. https://doi.org/10.1016/j.jhevol.2017.10.012

Stern, J. T., & Susman, R. L. (1983). The locomotor anatomy of *Australopithecus afarensis*. In *American Journal Of Physical Anthropology,* 60(3), 279-317.

Susman, R. L., Stern, J. T., & Jungers, W. L. (1984). Arboreality and bipedality in the Hadar hominids. *Folia Primatologica; International Journal of Primatology*, *43*(2–3), 113–156. https://doi.org/10.1159/000156176

Sutro, C. J. (1936). The pubic bones and their symphysis. *Archives of Surgery*, *32*(5), 823. https://doi.org/10.1001/archsurg.1936.01180230078006

Tague, R. G. (1992). Sexual dimorphism in the human bony pelvis, with a consideration of the Neandertal pelvis from Kebara cave, Israel. *American Journal of Physical Anthropology*, *88*(1), 1–21. https://doi.org/10.1002/ajpa.1330880102

Tague, R. G. (1993). Pubic symphyseal synostosis and sexual dimorphism of the pelvis inPresbytis cristata andPresbytis rubicunda. *International Journal of Primatology*, *14*(4), 637–654. https://doi.org/10.1007/BF02215452

Tague, R. G., & Lovejoy, C. O. (1986). The obstetric pelvis of AL 288-1 (Lucy). *Journal of Human Evolution*, *15*(4), 237–255.

Testus, J., & Latarjet, A. (1948). Traité d'anatomie humaine (8th edn). Doin, Paris

Todd, T. W. (1920). Age changes in the pubic bone I. The male white pubis. *American Journal of Physical Anthropology*, 3(3), 285-344.

Torres-Tamayo, N., García-Martínez, D., Lois Zlolniski, S., Torres-Sánchez, I., García-Río, F., & Bastir, M. (2018). 3D analysis of sexual dimorphism in size, shape and breathing kinematics of human lungs. *Journal of Anatomy*, *232*(2), 227–237.

https://doi.org/10.1111/joa.12743

Torres-Tamayo, N., Schlager, S., García-Martínez, D., Sanchis-Gimeno, J. A., Nalla, S., Ogihara, N., Oishi, M., Martelli, S., & Bastir, M. (2020). Three-dimensional geometric morphometrics of thorax-pelvis covariation and its potential for predicting the thorax morphology: A case study on Kebara 2 Neandertal. *Journal of Human Evolution*, *147*, 102854. https://doi.org/10.1016/j.jhevol.2020.102854

Trevathan, W. R. (2015). Primate pelvic anatomy and implications for birth. *Philosophical Transactions of the Royal Society B: Biological Sciences*, *370*(1663), 20140065. https://doi.org/10.1098/rstb.2014.0065

Trevathan, W. R. (2017). Human birth: An evolutionary perspective. *Human Birth: An Evolutionary Perspective*, 1–268. https://doi.org/10.4324/9780203789599/human-birth-wenda-trevathan

Trinkaus, E. (1984). Neandertal Pubic Morphology and Gestation Length. *Current Anthropology*, *25*(4), 509–514. https://doi.org/10.1086/203173

Trinkaus, E. (2011). The postcranial dimensions of the La Chapelle-aux-saints 1 Neandertal. *American Journal of Physical Anthropology*, *145*(3), 461–468.

Trinkaus, E. (2018). The labyrinth of human variation. *Proceedings of the National Academy of Sciences of the United States of America*, *115*(16), 3992–3994. https://doi.org/10.1073/pnas.1804794115

Valladas, Helene, Joron, J. L., Valladas, G., Arensburg, B., Bar-Yosef, O., Belfer-Cohen, A., Goldberg, P., Laville, H., Meignen, L., Rak, Y., Tchernov, E., Tillier, A. M., & Vandermeersch, B. (1987). Thermoluminescence dates for the Neanderthal burial site at Kebara in Israel. *Nature*, *330*(6144), 159–160. https://doi.org/10.1038/330159a0

Valladas, Hélène, & Valladas, G. (1991). Datation par la thermoluminescence de silex chauffés des grottes de Kébara et de Qafzeh. In O. Bar-Yosef & B. Vandermeersch (Eds.), *Le Squelette Moustérien de Kébara 2.* (Vol. 2, pp. 43–48), Centre National de la Recherche Scientifique.

Vandermeersch, B. (1991). La ceinture scapulaire et les membres supérieurs. In O. Bar-Yosef & B. Vandermeersch (Eds.), *Le squelette Moustérien de Kébara 2* (Vol. 2, pp. 157–178),Centre National de la Recherche Scientifique.

Vansickle, C. (2017). Measuring Lateral Iliac Flare by Different Methods Risks Obscuring Evolutionary Changes in the Pelvis. *The Anatomical Record*, *300*(5), 956–963. https://doi.org/10.1002/AR.23581

Vix, V. A., & Ryu, C. Y. (1971). The adult symphysis pubis: normal and abnormal. *American Journal of Roentgenology*, *112*(3), 517–525.

Walheim, G., & Selvik, G. (1984). Mobility of the pubic symphysis. In vivo measurements with an electromechanic method and a roentgen stereophotogrammetric method. *Europepmc.Org*.

Walker, A., & Leakey, R. E. (1993). *The Nariokotome Homo erectus skeleton*. Harvard University Press.

Wall-Scheffler, C. M., & Myers, M. J. (2013). Reproductive costs for everyone: How female loads impact human mobility strategies. *Journal of Human Evolution*, *64*(5), 448–456. https://doi.org/10.1016/j.jhevol.2013.01.014

Walrath, D. (2003). Rethinking pelvic typologies and the human birth mechanism. In *Current Anthropology* (Vol. 44, Issue 1, pp. 5–31). University of Chicago Press. https://doi.org/10.1086/344489

Walrath, D. E., & Glantz, M. M. (1996). Sexual dimorphism in the pelvic midplane and its relationship to neandertal reproductive patterns. *American Journal of Physical Anthropology*, *100*(1), 89–100. https://doi.org/10.1002/(sici)1096-8644(199605)100:1<89::aid-ajpa9>3.0.co;2-8

Ward, C. V. (2002). Interpreting the posture and locomotion of Australopithecus afarensis: Where do we stand? *American Journal of Physical Anthropology*, *119*(S35), 185–215. https://doi.org/10.1002/AJPA.10185

Washburn, S. L. (1959). Speculations on the interrelations of the history of tools and biological evolution. *Human Biology*, *31*(1), 21–31.

Weaver, T. D., & Hublin, J.-J. (2009). Neandertal birth canal shape and the evolution of human childbirth. *Proceedings of the National Academy of Sciences*, *106*(20), 8151–8156. https://doi.org/10.1073/pnas.0812554106

Weber, G. W. (2015). Virtual anthropology. *American Journal of Physical Anthropology*, 156(S59), 22–42. https://doi.org/10.1002/ajpa.22658

Weber, G. W., & Bookstein, F. L. (2011). *Virtual anthropology : a guide to a new interdisciplinary field*. Springer, Vienna.

Weber, K., Mahlfeld, A., Sekulla, C., & Otto, W. (1997). The benefit of ultrasound in lesions of the pubic symphysis. *European Journal of Ultrasound*, *6*(2), 111–116. https://doi.org/10.1016/s0929-8266(97)10005-2

Wells, J. C. K., DeSilva, J. M., & Stock, J. T. (2012). The obstetric dilemma: An ancient game of Russian roulette, or a variable dilemma sensitive to ecology? *American Journal of Physical Anthropology*, *149*(S55), 40–71. https://doi.org/10.1002/ajpa.22160

White, T.D., & Folkens, P. (2005). The skeletal biology of individuals & populations. In *The human bone manual*. (pp. 374–379). Elsevier.

White, T. D., Lovejoy, C. O., Asfaw, B., Carlson, J. P., & Suwa, G. (2015). Neither chimpanzee nor human, *Ardipithecus* reveals the surprising ancestry of both. *Proceedings of the National Academy of Sciences,* 112(16), 4877-4884. https://doi.org/10.1073/pnas.1403659111

Wright, J. L. (1952). Relaxation of the pelvic joints in pregnancy; a report of three cases. *The New Zealand Medical Journal*, *51*(286), 377–380.

Wurdinger, S., Humbsch, K., Reichenbach, J. R., Peiker, G., Seewald, H.-J., & Kaiser, W. A. (2002). MRI of the pelvic ring joints postpartum: Normal and pathological findings. *Journal of Magnetic Resonance Imaging*, *15*(3), 324–329. https://doi.org/10.1002/jmri.10073

Zelditch, M. L., Swiderski, D. L., Sheets, H. D., & Fink, W. L. (2012). Simple Size and Shape Variables: Shape Coordinates. In *Geometric morphometrics for biologists: a primer*. (pp. 62) Academic Press

Zollikofer, C. P. E., de León, M. S. P., Lieberman, D. E., Guy, F., Pilbeam, D., Likius, A., Mackaye, H. T., Vignaud, P., & Brunet, M. (2005). Virtual cranial reconstruction of *Sahelanthropus tchadensis*. *Nature*, *434*(7034), 755–759.